

PREDICTION OF LOCAL SCOUR AROUND BRIDGE PIER USING SOFT COMPUTING TECHNIQUES

Thesis

**Submitted in partial fulfillment of the requirements for the degree of
DOCTOR OF PHILOSOPHY**

by

SREEDHARA B M

(Reg. No: 138007 AM13F07)



**DEPARTMENT OF APPLIED MECHANICS AND HYDRAULICS
NATIONAL INSTITUTE OF TECHNOLOGY KARNATAKA,
SURATHKAL, MANGALURU – 575 025**

MARCH 2019

**PREDICTION OF LOCAL SCOUR AROUND
BRIDGE PIER USING SOFT COMPUTING
TECHNIQUES**

Thesis

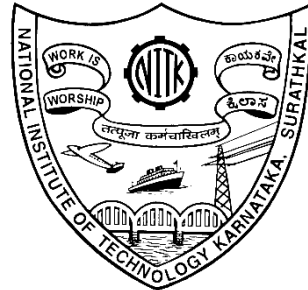
Submitted in partial fulfilment of the requirements for the degree of

DOCTOR OF PHILOSOPHY

by

SREEDHARA B M

(Reg. No: 138007 AM13F07)



DEPARTMENT OF APPLIED MECHANICS AND HYDRAULICS

NATIONAL INSTITUTE OF TECHNOLOGY KARNATAKA

SURATHKAL, MANGALORE - 575025

March - 2019

D E C L A R A T I O N

I hereby *declare* that the Research Thesis entitled “Prediction of Local scour around bridge pier using Soft Computing Techniques”, which is being submitted to the National Institute of Technology Karnataka, Surathkal in partial fulfilment of the requirements for the award of the Degree of Doctor of Philosophy in Department of Applied Mechanics and Hydraulics is a *bonafide report of the research work carried out by me*. The material contained in this Research Thesis has not been submitted to any University or Institution for the award of any degree.

138007 AM13F07, SREEDHARA B M

Department of Applied Mechanics and Hydraulics

National Institute of Technology Karnataka, Surathkal

Place: NITK-Surathkal

Date:

C E R T I F I C A T E

This is to certify that the Research Thesis entitled “Prediction of Local scour around bridge pier using Soft Computing Techniques” submitted by Sreedhara B M (Register Number: 138007 AM13F07) as the record of the research work carried out by him, is *accepted as the Research Thesis submission* in partial fulfilment of the requirements for the award of degree of **Doctor of Philosophy**.

Dr. Manu
(Research Guide)

Dr. S Mandal
(Research Guide)

Prof. Amba Shetty
(Chairman - DRPC)

ACKNOWLEDGEMENTS

I express my deep sense of gratitude to my research supervisors Dr. Manu, Assistant Professor Department Applied Mechanics and Hydraulics, NITK and Dr. S Mandal, Professor Department of Civil Engineering, Presidency University, Bengaluru for their encouraging, logical and critical suggestions during this work. The interaction and the time spent in discussions are imprinted in my memory permanently. Only with their moral support and guidance, this research work could be completed and I could publish my work in many international journals and conferences.

I express my deep sense of gratitude to the Director of National Institute of Technology Karnataka, Surathkal, for permitting me to carry out my research work and to make use of institutional infrastructure facilities.

I am greatly indebted to Research Progress Appraisal Committee members, Prof. Sitaram Nayak and Prof. Subba Rao, for their useful suggestions during the progress of the work.

I sincerely acknowledge the help and support of Prof. Subba Rao, Prof. G. S. Dwarakish and Prof. Amai Mahesha former Heads of the Department and Prof. Amba Shetty, present Head of the Department of Applied Mechanics and Hydraulics, NITK, Surathkal, for permitting me to use the departmental computing and laboratory facilities and his continuous support in completing the work.

I express my deep sense of gratitude to my sister Dr. Geetha Kuntoji and brothers Shreekantha B M and Mohith Babu, Who helped me in every manner and to successfully complete my research work.

I sincerely acknowledge the help and support of all the Professors, Associate Professors, Assistant Professors and Teaching and non-teaching staff of Department of Applied Mechanics and Hydraulics, NITK, Surathkal, in completing the work.

I sincerely acknowledge the invaluable help rendered by all the research scholars of our own department and other departments, RPL organizers, Badminton partners, B.E and M.Tech Friends. I express my special thanks to Sujay Raghavendra, Siddanth K, Harish B C for their valuable support to successfully complete my research work.

I sincerely acknowledge all the non-teaching staff of our department for their support and help during the research work.

I express my heartfelt gratitude to the authors of all those research publications which have been referred to in preparing this thesis.

Finally, I wish to express love and affection to my beloved family members for their continuous support and all the sacrifices they had to make.

Sreedhara B M

ABSTRACT

Bridges play an essential role in the society since they enable quick access across a river or any water body. Bridges facilitate transportation of goods and people and hence play a leading role in the development of a province. The safety of the bridge is the important factor with respect to scour failure which is the leading failure factor in river bridges. Scour is the removal of sediment near or around the structure which is located in the flowing water. There are different factors which affects scour mainly on the scour depth are flow depth, discharge, velocity, sediment size, porosity, pier shape and size etc. There are two types of scour conditions on which scour is classified and studied namely, clear water and live bed scour. The scour is the complex phenomenon and there is no common or general simple method to predict the scour depth around the bridge pier. There are several researchers who studied the scour mechanism using laboratory experiments. In the present days the artificial intelligence is the focal point for several researchers. Soft computing techniques, such as, Artificial Neural Network (ANN), Support Vector Machine (SVM), Adaptive Neuro-Fuzzy Inference System (ANFIS) and Particle Swarm Optimization (PSO) have been efficiently used for modeling scour related problems.

The study used the data for developing the soft computing models, is obtained from a physical model study on scour depth around bridge pier, carried out by Goswami Pankaj in 2013 in a 2-D wave flume. The input parameters, namely, sediment size (d_{50}), velocity (U), time (t) and sediment quantity (ppm) are used to predict the scour depth of different pier shapes such as circular, rectangular, round nosed and sharp nosed pier for both clear water and live bed scour condition. The complete original data is divided into training and testing. In the study, the soft computing techniques such as ANN, SVM, ANFIS, PSO-SVM and PSO-ANN are developed. The ANN model with feed-forward backpropagation network is developed with different hidden neurons. The RBF, Linear and Polynomial kernel functions are used in the SVM model. the ANFIS model is also developed with Trapezoidal, Gbell and Triangular membership function. The evolutionary optimization technique, particle swarm optimization is used to tune the SVM and ANN parameters to improve the efficiency of models prediction.

The performance of individual and hybrid soft computing models are compared using statistical parameters such as, Correlation Coefficient (CC), Normalized Root Mean Square Error (NRMSE), Nash–Sutcliffe coefficient (NSE) and Normalized Mean Bias (NMB). Scatter plots are used to evaluate the accuracies of the models and box plots were used to analyze the spread or distribution of the data points estimated by the models. The validation of the developed models is done using the experimental values. The validation results shows that the proposed models are well correlated and in good agreement with experimental results. The hybrid models displayed a better performance compared to individual models. It is found that the hybrid PSO-SVM model is the best and efficient model in estimating the scour depth effectively around bridge pier for both live bed and clear water scour condition when compared to all the other models developed.

Keywords: Bridge pier, Scour depth, Pier shapes, ANN, SVM, ANFIS, PSO, Clear water scour, Live bed scour

CONTENTS

DESCRIPTION	PAGE NO
ABSTRACT	i
CONTENTS	iii
LIST OF FIGURES	vi
LIST OF TABLES	xii
NOMENCLATURE	xiii
ABBREVIATIONS	xiv
1. INTRODUCTION	1
1.1 General	1
1.2 Types of Scour at Bridges	2
1.2.1 General scour	3
1.2.2 Contraction scour	3
1.2.3 Local scour	4
1.3 Mechanism of Local Scour	4
1.4 Factors Affecting Local Scour	5
1.4.1 Size and Shape of the obstruction	6
1.4.2 Velocity of flow	7
1.4.3 Sediment size	7
1.4.4 Types of scour condition	7
1.5 Need for Present Work	8
1.6 Organization of Thesis	9
2. LITERATURE REVIEW	10
2.1 General	10
2.2 Studies on Scour	10
2.3 Studies on Soft Computing Techniques	12
2.3.1 Artificial Neural Network	12
2.3.2 Support Vector Machine	14
2.3.3 Adaptive Neuro Fuzzy Inference System	15

2.3.4 Hybrid soft computing models	16
2.4 Summary of Literatures	18
2.5 Problem Formulation	19
2.6 Research Objectives	20
3. EXPERIMENTAL DATA AND METHODOLOGY	21
3.1 General	21
3.2 Experimental Data Analysis	21
3.3 Theoretical Overview of Soft Computing Techniques	23
3.3.1 Artificial Neural Network (ANN)	23
3.3.2 Support Vector Machines (SVM)	24
3.3.3 Adaptive Neuro Fuzzy Inference System (ANFIS)	25
3.3.4 Particle Swarm Optimization (PSO)	28
3.4 Development of Soft Computing Models	29
3.4.1 Development of ANN model	29
3.4.2 Development of SVM model	29
3.4.3 Development of ANFIS model	30
3.4.4 Development of Particle swarm optimization based support vector machine (PSO-SVM)	31
3.4.4 Development of Particle swarm optimization based artificial neural network (PSO-ANN)	32
3.5 Methodology Used in the Study	32
3.5 Performance Analysis	36
3.6 Summary	37
4. RESULTS AND DISCUSSION	39
4.1 General	39
4.2 Prediction of Scour Depth around Bridge Pier under Clear Water Scour Condition	39
4.2.1 Performance of Support Vector Machine (SVM) model in the prediction of scour depth.	40
4.2.2 Performance of Adaptive Neuro Fuzzy Inference System (ANFIS) model in the prediction of scour depth.	46

4.2.3 Performance of a hybrid Particle Swarm Optimized Support Vector Machine (PSO-SVM) in the prediction of scour depth.	52
4.2.4 Performance of Artificial Neural Network (ANN) and Particle Swarm Optimized Artificial Neural Network (PSO-ANN) model for the prediction of scour depth.	59
4.2.5 Comparative Study	65
4.3 Prediction of Scour Depth around Bridge Pier for Live Bed Scour Condition	69
4.3.1 Performance of Support Vector Machine (SVM) model in the prediction of scour depth.	70
4.3.2 Performance of Adaptive Neuro Fuzzy Inference System (ANFIS) model in the prediction of scour depth.	75
4.3.3 Performance of Particle Swarm Optimized Support Vector Machine (PSO-SVM) model in the prediction of scour depth.	81
4.3.4 Performance of Artificial Neural Network (ANN) and Particle Swarm Optimized Artificial Neural Network (PSO-ANN) model in the prediction of scour depth.	87
4.3.5 Comparative study	92
4.4 Comparison of the Model Results with Standard Empirical Equations	96
5. SUMMARY AND CONCLUSIONS	97
5.1 Summary	97
5.2 Conclusions	97
5.3 Limitations of the Study	98
5.4 Scope for Future Work from the Study	98
REFERENCES	99
PUBLICATIONS	105
APPENDIX	106
CURRICULUM VITAE	113

LIST OF FIGURES

Figure. No:	Figure caption	Page No:
1.1	Formation of scour around the bridge pier and abutments	2
1.2	Types of scour that can occur at a bridge (Richardson et al. 1993)	3
1.3	Mechanism of local scour	4
1.4	Different pier shapes considered in the study	6
1.5	Equilibrium scour depth for clear water and live bed scour condition (Richardson et al. 1993)	8
3.1	Feed forward back propagation neural network used in study	23
3.2	Maximum separation hyperplane	25
3.3	SVM architecture adopted in the study	25
3.4	ANFIS architecture used in the study	27
3.5	Flowchart for PSO-SVM and PSO-ANN model	34
3.6	Flowchart for the overall methodology used in the study	35
4.1	Scatter plots of SVM models in testing phase for circular pier in clear water scour condition	41
4.2	comparison of measured and SVM model results in testing phase for circular pier in clear water scour condition	42
4.3	Scatter plots of SVM models in testing phase for rectangular pier in clear water scour condition	42
4.4	Comparison of measured and SVM model results in testing phase for rectangular pier in clear water scour condition	43
4.5	Scatter plots of SVM models in testing phase for round nosed pier in clear water scour condition	43
4.6	Comparison of measured and SVM model results in testing phase for	44

	round nosed pier in clear water scour condition	
4.7	Scatter plots of SVM models in testing phase for sharp nosed pier in clear water scour condition	45
4.8	Comparison of measured and SVM model results in testing phase for sharp nosed pier in clear water scour condition	45
4.9	Scatter plots of ANFIS models in testing phase for circular pier in clear water scour condition	47
4.10	Comparison of measured and ANFIS model results in testing phase for circular pier in clear water scour condition	48
4.11	Scatter plots of ANFIS models in testing phase for rectangular pier in clear water scour condition	48
4.12	Comparison of measured and ANFIS model results in testing phase for rectangular pier in clear water scour condition	49
4.13	Scatter plots of ANFIS models in testing phase for round nosed pier in clear water scour condition	50
4.14	Comparison of measured and ANFIS model results in testing phase for round nosed pier in clear water scour condition	50
4.15	Scatter plots of ANFIS models in testing phase for sharp nosed pier in clear water scour condition	51
4.16	Comparison of measured and ANFIS model results in testing phase for sharp nosed pier in clear water scour condition	51
4.17	Scatter plots of PSO-SVM models in testing phase for circular pier in clear water scour condition	53
4.18	Comparison of measured and PSO-SVM model results in testing phase for circular pier in clear water scour condition	54
4.19	Scatter plots of PSO-SVM models in testing phase for rectangular pier in clear water scour condition	55
4.20	Comparison of measured and PSO-SVM model results in testing phase for rectangular pier in clear water scour condition	55
4.21	Scatter plots of PSO-SVM models in testing phase for round nosed pier in clear water scour condition	56

4.22	Comparison of measured and PSO-SVM model results in testing phase for round nosed pier in clear water scour condition	57
4.23	Scatter plots of PSO-SVM models in testing phase for sharp nosed pier in clear water scour condition	58
4.24	Comparison of measured and PSO-SVM model results in testing phase for sharp nosed pier in clear water scour condition	58
4.25	Scatter and line plots of ANN and PSO-ANN models in testing phase for circular pier in clear water scour condition	61
4.26	Comparison of measured, ANN and PSO-ANN model results in testing phase for circular pier in clear water scour condition	61
4.27	Scatter and line plots of ANN and PSO-ANN models in testing phase for rectangular pier in clear water scour condition	62
4.28	Figure 4.28: Comparison of measured, ANN and PSO-ANN model results in testing phase for rectangular pier in clear water scour condition	62
4.29	Scatter and line plots of ANN and PSO-ANN models in testing phase for round nosed pier in clear water scour condition	63
4.30	Comparison of measured, ANN and PSO-ANN model results in testing phase for round nosed pier in clear water scour condition	63
4.31	Scatter and line plots of PSO-ANN models in testing phase for sharp nosed pier in clear water scour condition	64
4.32	Comparison of measured, ANN and PSO-ANN model results in testing phase for sharp nosed pier in clear water scour condition	64
4.33	Comparison plots in testing phase for clear water scour condition	66
4.34	Box plots in testing phase for clear water scour condition	67
4.35	NRMSE of all the models for clear water scour condition.	68
4.36	NSE of all the models for clear water scour condition.	68
4.37	NMB of all the models for clear water scour condition.	69
4.38	Scatter plots of SVM models in testing phase for circular pier in live bed scour condition	71
4.39	Comparison of measured and SVM model results in testing phase for	71

	circular pier in live bed scour condition	
4.40	Scatter plots of SVM models in testing phase for rectangular pier in live bed scour condition	72
4.41	Comparison of measured and SVM model results in testing phase for rectangular pier in live bed scour condition	72
4.42	Scatter plots of SVM models in testing phase for round nosed pier in live bed scour condition	73
4.43	Comparison of measured and SVM model results in testing phase for round nosed pier in live bed scour condition	73
4.44	Scatter plots of SVM models in testing phase for sharp nosed pier in live bed scour condition	74
4.45	Comparison of measured and SVM model results in testing phase for sharp nosed pier in live bed scour condition	74
4.46	Scatter plots of ANFIS models in testing phase for circular pier in live bed scour condition	76
4.47	Comparison of measured and ANFIS model results in testing phase for circular pier in live bed scour condition	77
4.48	Scatter plots of ANFIS models in testing phase for rectangular pier in live bed scour condition	78
4.49	Comparison of measured and ANFIS model results in testing phase for rectangular pier in live bed scour condition	78
4.50	Scatter plots of ANFIS models in testing phase for round nosed pier in live bed scour condition	79
4.51	Comparison of measured and ANFIS model results in testing phase for round nosed pier in live bed scour condition	79
4.52	Scatter plots of ANFIS models in testing phase for sharp nosed pier in live bed scour condition	80
4.53	Comparison of measured and ANFIS model results in testing phase for sharp nosed pier in live bed scour condition	80
4.54	Scatter plots of PSO-SVM models in testing phase for circular pier in live bed scour condition	82

4.55	Comparison of measured and PSO-SVM model results in testing phase for circular pier in live bed scour condition	83
4.56	Scatter plots of PSO-SVM models in testing phase for rectangular pier in live bed scour condition	84
4.57	Comparison of measured and PSO-SVM model results in testing phase for rectangular pier in live bed scour condition	84
4.58	Scatter plots of PSO-SVM models in testing phase for round nosed pier in live bed scour condition	85
4.59	Comparison of measured and PSO-SVM model results in testing phase for round nosed pier in live bed scour condition	85
4.60	Scatter plots of PSO-SVM models in testing phase for sharp nosed pier in live bed scour condition	86
4.61	Comparison of measured and PSO-SVM model results in testing phase for sharp nosed pier in live bed scour condition	86
4.62	Scatter and line plots of ANN and PSO-ANN models in testing phase for circular pier in live bed scour condition	88
4.63	Comparison of measured, ANN and PSO-ANN model results in testing phase for circular pier in clear water scour condition	89
4.64	Scatter and line plots of ANN and PSO-ANN models in testing phase for rectangular pier in live bed scour condition	89
4.65	Comparison of measured, ANN and PSO-ANN model results in testing phase for rectangular pier in clear water scour condition	90
4.66	Scatter and line plots of ANN and PSO-ANN models in testing phase for round nosed pier in live bed scour condition	90
4.67	Comparison of measured, ANN and PSO-ANN model results in testing phase for round nosed pier in clear water scour condition	91
4.68	Scatter and line plots of ANN and PSO-ANN models in testing phase for sharp nosed pier in live bed scour condition	91
4.69	Comparison of measured, ANN and PSO-ANN model results in testing phase for sharp nosed pier in clear water scour condition	92
4.70	Comparison plots in testing phase for live bed scour condition	93

4.71	Box plots for all the models in testing phase for live bed scour condition	94
4.72	NRMSE of all the models for live bed scour condition.	95
4.73	NSE of all the models for live bed scour condition.	95
4.74	NMB of all the models for live bed scour condition	96

LIST OF TABLES

Table No:	Table caption	Page No:
3.1	Statistical parameters in clear water scour condition	22
3.2	Statistical parameters in live bed scour condition	22
3.3	Optimal SVM parameters	30
3.4	Details of ANFIS model	30
3.5	Optimal PSO-SVM parameters	31
4.1	Results of SVM model for clear water scour condition	40
4.2	Results of ANFIS model for clear water scour condition	46
4.3	Results of PSO-SVM model for clear water scour condition	52
4.4	Results of ANN and PSO-ANN model for clear water scour condition	59
4.5	Results of SVM models for live bed scour condition	70
4.6	Results of ANFIS models for live bed scour condition	75
4.7	Results of PSO-SVM models for live bed scour condition	81
4.8	Results of ANN and PSO-ANN models for live bed scour condition	87
4.9	Comparison of PSO-SVM results with empirical equations	96

NOMENCLATURE

- d_{se} : Scour depth
 q : Discharge
 v : Velocity
 D : flow depth
 d_{50} : Sediment size
 σ : Standard deviation
 f : Lacey's silt factor
 b : Pier thickness
 K_s : Pier shape factor
 K : Pier alignment factor
 α : Center to center spacing of the pier

ABBREVIATIONS

AI	:	Artificial Intelligence
ANFIS	:	Adaptive Neuro-Fuzzy Inference System
ANN	:	Artificial Neural Network
BP	:	Back-Propagation
CC	:	Correlation Coefficient
FFBP	:	Feed-Forward Back propagation Network
GP	:	Genetic Programming
NN	:	Neural Network
NMB	:	Normalized Mean Bias
NRMSE	:	Normalized Root Mean Square Error
MF	:	Membership Function
MSE	:	Mean Square Error
PSO	:	Particle Swarm Optimization
RBF	:	Radial Bias Function
RMSE	:	Root Mean Square Error
SI	:	Scatter Index
SVM	:	Support Vector Machine
SVR	:	Support Vector Regression

CHAPTER 1

INTRODUCTION

1.1 General

Bridges play an essential role in the society since they enable quick access across a river or any water body. Bridges facilitate transportation of goods and people and hence play a leading role in the development of a province. The bridge piers and highway embankments leading to the bridge are the main obstructs for the flow of flood waters, increasing velocity and development of vortices leads to the formation of scour near the bridge foundations. The failure of bridges is a severe problem because of the high investment costs, safety problems in the event of a failure and adverse effects on the economy of the region. Scour related to bridge hydraulics, its relation to flood hydrology and hydraulic processes received much attention in the past decade.

“Men who overlook water under the bridge will find bridge underwater” to the provisions in the existing codes of practice for determination of design scour depth require immediate review (Kothyari 2007). This situation highlights the important effect of flowing water on the stability of the bridge and in particular, its impact on a bridge pier. The mechanism of flow around a pier structure is so complicated to the point that it is hard to set up a general observational model to give exact estimates for scouring. The Bridge scour is the removal of sediments such as sand and rocks from around bridge abutments or piers. During the flow of water through an opening of a bridge with acceptable velocity, in general, the bed elevation will be changed. The significance of this change in elevation is more important near the abutments and piers. Figure 1.1 shows some examples of formation of scouring around the bridge pier and abutments.



Figure 1.1 Formation of scour around the bridge pier and abutments

1.2 Types of Scour at Bridges

Scour is a phenomenon of sediment removal from around a hydraulic structure due to the interaction between flow and the hydraulic structure such as bridge piers placed in flowing water. The different types of scour are clearly shown in Figure 1.2. The total scour at a bridge crossing is comprised of three components namely; general scour, contraction scour and local scour.

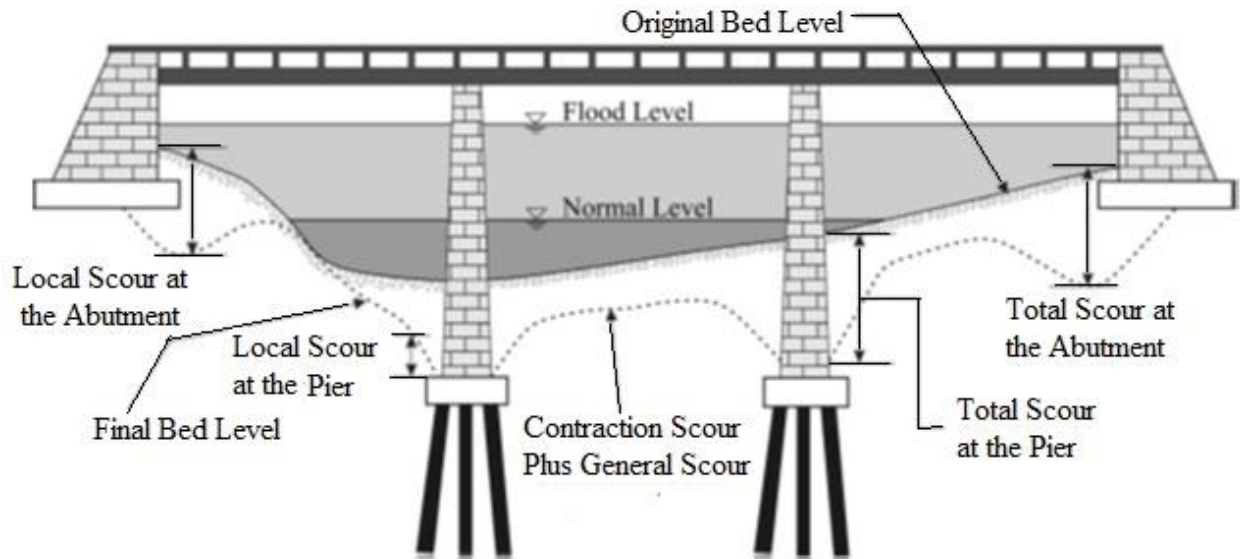


Figure 1.2 Types of scour that can occur at a bridge (Richardson et al. 1993)

1.2.1 General scour

General scour is the overall lowering of the river bed irrespective of the bridge location due to natural and human-induced causes. General scour is further divided as long term or short term scour. As the name itself suggests, long-term general scour takes sufficiently long time in the order of several years to lower the river bed. It may be the natural trend of the river or some modification made to the stream or watershed. The long-term general scour may not be significant during the design life of a bridge if the rate of scour development is relatively low. Similarly, short-term local scour results in a very quick time compared to the previous one, probably in a single or couple of closely spaced flood events.

1.2.2 Contraction scour

Contraction scour occurs when the flow area of the stream is reduced, either by a natural contraction of the stream channel or by a bridge. From continuity, when area decreases, flow velocity increases and consequently bed shear increases. This increases the erosive force and more bed material is removed. But later on, contraction scour comes to rest because the flow area goes on increasing due to increase in depth and also due to a simultaneous decrease in the bed shear stress.

1.2.3 Local scour

Local scour can be defined as the degradation of river banks and/or bed that is localized to a specific area due to a sudden change in the parameters associated with the river. Local scour involves the removal of bed material around a structure located in moving water. It is the result of flow field changes due to the presence of a structure. Scour at the surrounding of the bridge pier, abutment spur dikes and river training works are some examples of local scour.

1.3 Mechanism of Local Scour

The flowing pattern of a normal flow comes to sudden change when it encounters a pier on its path. Large-scale eddy structures or the system of vortices develop at the base of the pier. This vortex system as a basic mechanism of local scouring around bridge pier has been long recognized by Melville 1975. The eddy structure is normally composed of two components:

- The horseshoe vortex
- The wake vortex system

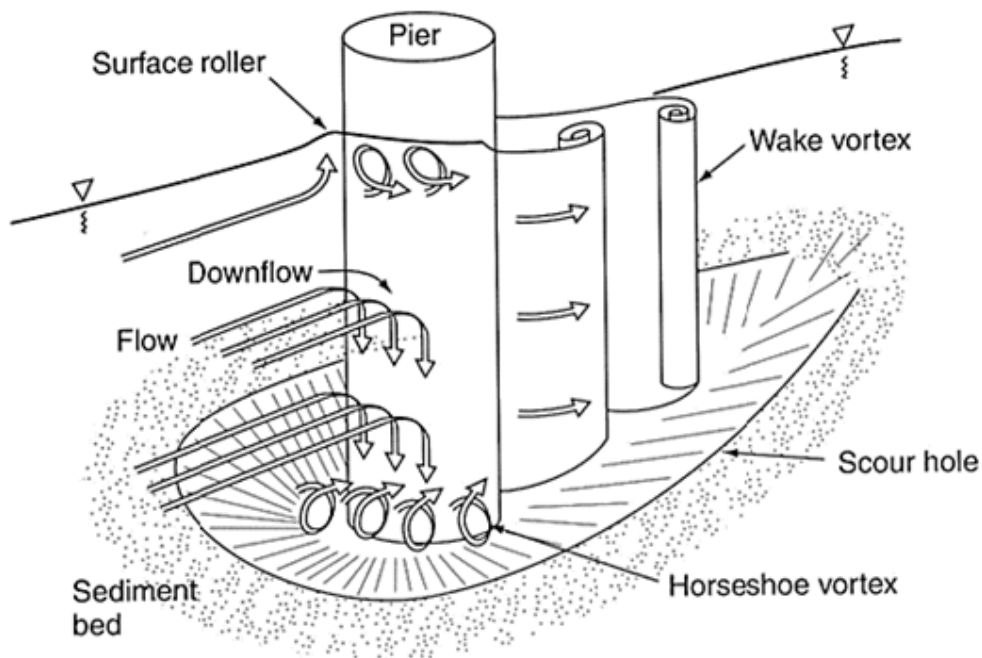


Figure 1.3 Mechanism of local scour

A flow running at a particular velocity, when approaches to the pier come to complete rest which results in, an increase of pressure at the water surface near the pier. The velocity of the flow gradually decreases from top to bottom and consequently, the pressure also decreases from top to bottom. This creates a downward pressure gradient that forces the flow to move downward like a jet of water. This vertical jet when strikes the bed, it makes a hole in the immediate vicinity of a pier base. The downflow impinging on the bed is the main scouring agent. The strength of the downflow reaches a maximum just below the bed level. The downflow rolls up as it continuous to create a hole and through the interaction with incoming flow converts into a complex vortex system of horseshoe shape and hence is called a horseshoe vortex. The horseshoe vortex then extends downstream along pier sides. The horseshoe vortex is very effective in transporting the dislodged particles away past the pier. the strength of the horseshoe vortex reduces as the scour depth increases, thereby reducing the transport rate from the base region and ultimately ceases in clear water scour. For live bed scour, equilibrium is established between bed material inflow and outflow and the scouring process ceases. The separation of flow at the pier sides produces so-called wake vortex. These vortices are not stable and shed alternatively from one side of the pier and the other. Wake vortices rotate about a vertical axis (Figure 1.3), and wake vortices also erode sediment from pier base. The wake vortex system somewhat acts like a vacuum cleaner that sucks the material and carries away. The intensity of wake vortices drastically reduces with distance downstream, such that sediment deposition is immediately downstream of the pier. The horseshoe and wake both the vortices work at the same time to scour around the pier.

1.4 Factors Affecting Local Scour

Local scour around bridge pier depends upon several factors, most of which are interrelated. As justified by the several researchers, amongst Richardson et al. 1993, Ansari et al. 2002 and Raudkivi and Ettema 1983, the factors affecting the local scour at the pier are; 1) approach flow velocity 2) flow depth 3) pier width 4) pier length if skewed to main stream 5) size and gradation of the bed material 6) angle of attack of approach flow 7) pier shape 8) ice and debris jam.

Melville 1975 has arranged the factors affecting the depth of scouring in probable order of importance as below.

- Size and Shape of the obstruction
- Velocity of flow
- Sediment Size
- Types of scour condition

1.4.1 Size and Shape of the obstruction

The pier size primarily affects the time required for local scour to reach equilibrium scour depth. The scour depth depends on the horseshoe vortex one which is proportional to the pier Reynolds number, which is a function of pier diameter. So obviously, larger the pier, larger the scour volume and longer the time required to erode the sediment at given bed shear stress.

The effect of the pier shape is investigated by several researchers and concluded that the experimental results, minimum scour on six pier shapes, achieved at a pier of lenticular shape. Front nose of the pier plays an important role in the scouring phenomena, whereas the rear nose has no effect. According to Richardson et al. 1993, the nose of the pier or abutment has 20% influences on scouring. The length of the pier has a negligible effect unless the flow is skewed. The study conducted from Breusres et al. 1977 concluded that a rectangular pier gives 20 to 40% more scour than the circular pier. A square nose pier possesses 20% more scour than sharp nose pier and 10% more than cylindrical or round nose pier. Figure 1.4 shows the different types of pier shapes used in the present study.

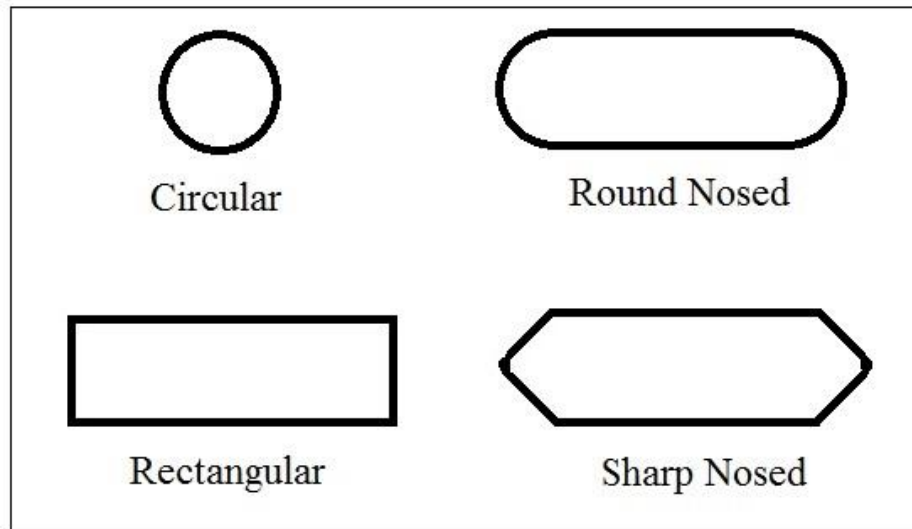


Figure 1.4 Different pier shapes considered in the study

1.4.2 Velocity of flow

The velocity of flow varies with depth and shear stress. In case of flow over a sediment bed, the flow velocity depends on the shear stress offered by the sediment particles to the water flow. The resistance offered by the sediment material to the water flow reduces the flow velocity as the flow depth decreases. The velocity distribution may sometimes differ from the typical velocity distribution due to various factors such as flow turbulence, properties of bed material, and flow obstructions. The scour is typically most profound close to the peak of flood, but barely visible and also as the flood retreats the scour opening which may be filled up to some degree. The rate of scouring depends upon the bed material and the hydraulic parameters of the flow.

1.4.3 Sediment size

Based on recent literature, it is observed that a sediment size of $d_{50} \leq 0.7\text{mm}$ leads to the formation of ripples whereas sediment of size $d_{50} \geq 0.7\text{mm}$ does not cause ripple (Laursen and Toch 1956). In the early days of investigation, the investigators failed to give a clear picture of scour depth due to sediment size. Laursen and Toch 1956 said the secondary effect of velocity and sediment can't be determined at the laboratory range and are rather more important at large scale.

1.4.4 Types of scour condition

The clear water scour occurs when there is no movement of bed material in the flow upstream of the crossing. This condition of scour is just because of the obstructions (piers, abutments) in the flow. The rate of sediment supply to the scour hole is equal to zero for clear water scour condition and the depth of scour hole continues to grow until the equilibrium scour depth is reached. Once the transport of bed material reaches the crossing from upstream scours of the live-bed occurs. The scour opening of the live-bed is continuously supplied with the sediment transported from upstream reach. The supply of sediment rate to the scour hole is equal to the sediment transported rate out of the scour hole due to which equilibrium of scour depth is achieved. Figure.1.5 shows the two types of scour and equilibrium scour depth, in which depth of the scour is presented as a function of time.

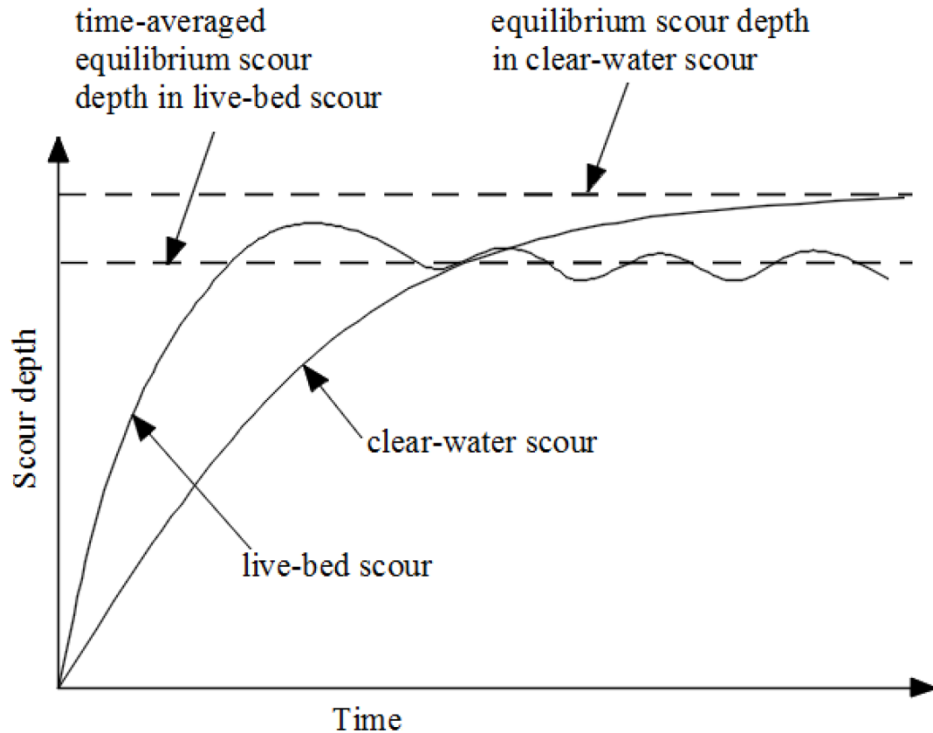


Figure 1.5 Equilibrium scour depth for clear water and live bed scour condition (Richardson et al. 1993)

Time is one among the primary factor that can effect the scour depth and the time development trend of scour depth is presented in Figure 1.5. It can be noted that the local scour rate and equilibrium scour depth under clear water and live bed conditions are different. Additionally, from the figure, it can be observed that the scour rate decreases and scour depth increases with time.

1.5 Need for Present Work

In earlier decades, most of the researchers carried out experimental, theoretical and numerical studies on scour phenomenon. Experimental studies on scour depth investigation involve several common assumptions made in hydrodynamics which may not be accurate. In physical modeling, there are large numbers of factors which are influencing the scour depth to be considered. Thus, complexity is also an inherent feature of these problems. Because of these characteristics, conventional mathematical modeling for predicting the scour depth around the bridge pier tends to become very difficult and often the prediction is quite unreliable. Further, a simple mathematical model is not available to predict the scour depth

because of these complexities. Hence, there is no common method to predict scour depth around the bridge pier.

In recent years, application of soft computing techniques in modeling hydraulic processes such as prediction of scour depth and other scour related problems has received as much attention from the researchers. The soft computing models are developed using experimental data and provide an explanation of an externally driven process without a need for complex physical models. In the study, the soft computing models such as an Artificial Neural Network (ANN), Support Vector Machine (SVM), Adaptive Neuro-Fuzzy Inference System (ANFIS) and Particle Swarm Optimization technique (PSO) used as an evolutionary optimization technique to predict scour depth. The prediction performance of soft computing models is analyzed by using different statistical indices. The predicted results from these models are compared and validated with the experimentally collected results for the model efficiency.

1.6 Organization of Thesis

This thesis contains six chapters and the brief outline of the thesis is as follows.

In chapter 1, the background of scour, types and mechanism of the scour and factors affecting local scour are presented. Also, the chapter presents the need for the study.

Chapter 2 focused on the review of past literature on experimental studies, soft computing and other applications in the prediction of scour depth around the pier. This chapter also presents the literature gap, problem formulation, and objective of the present study.

Chapter 3 gives the details of experimental data collection and analysis. The methodology used in the study, development and performance analysis of the models is explained in detail.

Chapter 4 provides the results obtained from the soft computing models, developed and the comparisons of soft computing model results with experimental values are discussed.

Finally, the conclusions from the study, limitations of the present study and recommendations, and scope of future work are presented in chapter 5, followed by references to the present study.

CHAPTER 2

LITERATURE REVIEW

2.1 General

Considering the importance of estimating accurate scour depth, several researchers have mainly focused on the development of accurate and reliable methods. In this chapter, the various techniques used by the researchers to estimate the scour depth under conditions are discussed. In the first section, the applications of experimental based methods and numerical studies are presented. In the other sections the reviews of soft computing techniques used to predict the scour depth around pier and scour formation around other hydraulics structures are presented.

2.2 Studies on Scour

Many researchers have carried out experimental and numerical studies on scour depth in the past and important out of them are discussed below:

Sturm and Janjua (1994) investigated the scour around bridge abutment in flood plains of compound channel in clear water scour condition. The experiments were conducted in a flume with fixed bed main channel and moveable bed flood plain. The scour depth and velocity distributions were measured by varying discharge, flow depth, abutment length and channel geometry.

Coleman et al. (2003) investigated the development of scour depth near vertical-wall bridge abutment with uniform sediments in clear water scour condition. The different flow-sediment-abutment length combinations were considered and analyzed. The results of similar earlier abutment-scour experimental studies were also incorporated in analyses of scour development. Variations in scour rates and depths with flow and sediment parameters are found to be different for short and long abutments.

Debnath and Chaudhuri (2010) described the scour mechanism around the cylinders embedded in clay sand mixed beds. The effects of clay-content, water content, bed shear strength and pier Froude number on maximum equilibrium scour depth, equilibrium scour hole geometry, scouring process, and time variation of scour were investigated. Further,

equations for estimation of non-dimensional maximum scour depth for cylinders embedded in clay–sand mixtures were proposed as functions of pier Froude number, clay content, water content, and bed shear strength.

Oben and Ettema (2011) evaluated the interactions between pier-scour and abutment-scour by conducting series of flume experiments in a non-cohesive boundary. The scour depth, scour location, and bathymetry data were recorded for spill-through and wing-wall abutments during the study. The results from the study indicates that pier presence does not lead to substantial increase in abutment scour, although it may reduce abutment-scour depth when the pier is close to the spill-slope toe of a spill-through type abutment. In case of wing-wall abutment, the abutment scour increases with decreasing pier abutment distance.

Lanca et al. (2013) conducted the 75 long-duration laboratory tests under steady, clear-water flow close to the threshold for initiation of sediment motion, to address the effect of time, pile spacing, skew-angle and number of pile group columns on the equilibrium scour depth. Pile groups consisted of matrical arrangements of one, two, or three columns of four rows, with spacings of 1, 2, 3, 4.5, and 6 pile diameters; the tested skew-angles were 0, 15, 30, 45, and 90°.

Barbhuiya and Mazumder (2014) performed the experimental study with four different uniform cohesion less sediment diameters and five vertical-wall abutments with projected lengths perpendicular to the flow. These tests were conducted under varying flow velocity characteristics. It was observed that the scour depth increases with the increase of sediment sizes and abutment lengths. Further, the scour depth decreases with the increases of non-uniformity under all flow conditions. They proposed a design equation based on the obtained experimental data and existing live bed scour data. The measured values of scour depth are compared with the calculated values using proposed equation and also with three different live-bed local scour equations for the conditions of the tests.

Qi and Gao (2014) conducted the experiments on local scour around large diameter monopile considering both waves and current. The time development scour depth was measured in series of experiments. The study concluded that, the equilibrium scour depth in combined waves and current is greater than the linear sum of those in waves and current separately. It was observed that the maximum flow velocity at the boundary layer for the following-current

case is larger than that for the opposing-current case, which further results in faster time development of scour depth and greater equilibrium scour depth for the following-current case.

Mohamed et al. (2015) carried out the numerical and experimental investigations to study the effect of abutment providing with collar on local scour depth. The scour depth is simulated by using a 3D Navier Stokes equation based model. The study concluded that, the curvature shape of bridge abutment with collar could share to reduce the local scour depth by more 95%. Also, the results showed that, simulation models agree well with the experimental data.

Ghani and Mohammadpour (2016) carried out the experiments to investigate the temporal variation of local scour around compound abutments under clear water scour condition. The study showed that, a suitable level of foundation is able to decrease the scour depth and increase scour time during the flood events. The trend of temporal scour depth at compound pier and abutment is similar, and duration of scour development depends on the foundation level, velocity ratio and foundation dimension. The study concluded that, proper design of foundation level increases duration of scouring and provides enough time to treat bridge foundation after the flood events.

Mohamed et al. (2016) investigated the effect of different contraction ratio and entrance angle of abutments on scour depth using experimental and theoretical studies. The Navier Stokes equation based 3D model was used in simulation and the computed results are compared with experimental results. The results show the ability of the numerical model to simulate local scouring at abutments for different contraction ratios and entrance angles of abutment with high accuracy. The obtained determination coefficient and mean relative absolute error, in average, are 0.95 and, 0.12, respectively.

2.3 Studies on Soft Computing Techniques

In recent years, the soft computing techniques are widely used to solve the scour mechanism around the pier and other hydraulic structures, and some of them are discussed below:

2.3.1 Artificial Neural Network

Bateni et al. (2007) applied the ANN and ANFIS approach to estimate the equilibrium and time development scour depth. The BP (Back Propagation) based MLP (Multilayer

Perception) neural network and RBF (Radial Basis Function) based ANFIS model was used. Five different variables were used to predict the equilibrium scour depth and the results showed that ANFIS model have good prediction accuracy. The study concluded from the sensitivity analysis that, pier diameter has a greater influence on equilibrium scour depth than the other independent parameters.

Soliman (2007) formulated the back propagation based neural network to predict the maximum scour depth at the downstream of hydraulic structures. The physical study data were used to train and test the model. The discharge, gate opening, bed material and length of apron were used as input variables. The results of ANN models were compared with experimental results and showed good correlation.

Azamathulla et al. (2008) used the ANN to estimate the scour depth below ski-jump type spillways. The FFBP neural network architecture was used. The characteristics head and discharge intensity over the spillway were used to predict the scour depth at downstream of the bucket. The performance of the model was analyzed using MSE, CC, average error and average absolute deviation. The ANN model was compared with RBF based ANFIS model and concluded that Neuro-Fuzzy model was most satisfactory model for the under considered problem.

Firat and Gungor (2009) used Generalized Regression Neural Networks (GRNN) and Feed Forward Neural Networks (FFNN) approaches to predict the scour depth around circular bridge piers. The performance of the models in training and testing sets are compared with observations. Also, models were tested by Multiple Linear Regression (MLR) and empirical formula. The results of all approaches are compared in order to get more reliable comparison. The results indicated that GRNN can be applied successfully for prediction of scour depth around circular bridge piers.

Kaya (2010) developed the ANN model to study the pattern of scour depth around bridge pier using FHWA data set. The data set composed of 380 measurements considered at 56 bridges in 13 different states. The ANN models were developed for different input combinations by reducing number of variables from 14 to 9 and it showed that, there is negligible change in the coefficient of determination. The pier shapes, skew, flow depth and

velocity are selected by conducting sensitivity analysis and estimated the scour depth. The study suggested that, addition of some of variables actually decreases the quality of ANN prediction of scour pattern.

Begum et al. (2012) applied the artificial neural network to the problem of scour around semicircular bridge abutments. Multilayer Perceptron (MLP) with single hidden layer and Radial Basis Function (RBF) network have been trained with the experimental data from literature and an appropriate model of each of the network is identified. The model performances were analyzed with the statistical measures like CC and RMSE. The ANN model result was compared with empirical equations.

Kiziloz et al. (2015) presented the ANN model to predict the scour depth beneath the pipelines under different storm conditions. The regular and irregular waves were considered in the storm conditions. The FFBP neural network was developed for different inputs and neuron numbers using a trial and error approach.

Raikar et al. (2016) applied the soft computing tools such as artificial neural network (ANN) and genetic algorithm (GA) in the prediction of scour depth within channel contractions. The experimental data of earlier investigators were used in developing the models and ANN and GA Toolboxes of MATLAB software were utilized. The multilayered perceptron (MLP) neural networks with feed-forward back-propagation training algorithms were designed to predict the scour depth. The mean squared error and correlation coefficient are used to check the performance of networks. It was found that both ANN and GA models can be satisfactorily used to predict the scour depth within channel contractions.

2.3.2 Support Vector Machine

Ghazanfari H et al. (2011) applied the SVM and ANN approaches to estimate the scour depth around pile groups under wave condition. The non-dimensional controlling parameters, including the Keulegan–Carpenter number, pile Reynolds number, Shield's parameter, sediment number, gap to diameter ratio and number of piles was used as the inputs. The performance of both the models were compared with existing empirical equations and concluded that, SVM model provides the good prediction of scour depth than other ANN and other empirical equations.

Pal et al. (2011) investigated the potential of support vector machines in the prediction of scour around bridge pier using field data. The dataset of 232 measurements were collected from BSDMS for the analysis. The SVM with RBF and polynomial kernel functions were modeled and the results were compared with empirical relations and artificial neural network. The SVM showed good performance with coefficient of determination of 0.891 compared to BP neural network with 0.880.

Hong et al. (2012) used an alternative approach SVM to estimate the temporal variation of pier scour depth under clear water condition with non-uniform sediments. The dimensionless parameters such as, flow shallowness, sediment coarseness, dens metric Froude number, pier Froude number, Geometric standard deviation for sediment particle size distribution were used in the study. The results of SVR models were compared with other conventional regression models and experimental results.

Goel (2008 and 2015) considered the SVM model to predict the scour depth around pier and downstream of spillways. The SVM with PBF and Polynomial kernel functions models were developed and evaluated using statistical parameters such as, CC and RMSE. The study concluded that, the SVM with RBF kernel function showed good performance in scour depth prediction.

Najafzadeh et al. (2016) investigated the scour depth in contraction of rectangular channel using ANFIS and SVM approach. The flow velocity, critical threshold velocity of sediment movement, flow depth, particle diameter, un-contracted and contracted channel widths were used as input parameters. The training and testing of the models were carried out using experimental data and compared with existing equations. The results showed that, the ANFIS model can predict the scour depth compared to SVM and other equations.

2.3.3 Adaptive Neuro Fuzzy Inference System

Azamathulla and Ghani (2010) described the use of ANFIS in the prediction of scour depth near culvert outlets. The laboratory data sets from the past published literatures were used to train the model. The performance of the ANFIS model was found to be more effective with CC=0.94 compared to regression models and ANN model of CC=0.78.

Akib et al. (2014) predicted the scour depth at bridges using ANFIS as a modeling tool. The different sediment sizes, flow rates and time evolution used as input parameters for predicting the scouring on integral bridge piers. The integral bridges with single row and double row piers with pile groups were embedded in the two floodplains. The results of ANFIS models were compared with linear regression and that showed a reasonable good degree of accuracy.

Bonakdari and Ebtehaj (2017) estimated the scour depth around bridge piers using ANFIS and ANN models. The model performances were compared with nonlinear regression methods. The study concluded that, both methods were out performed compared to other existing methods. Also, study showed that, using ratio of pier length to flow depth, ratio of pier width to flow depth, Froude number and standard deviation of bed grain size parameters leads to optimal performance in scour depth estimation.

Choi et al. (2017) proposed the use of ANFIS method in the prediction of scour depth around bridge pier. The mean velocity, flow depth, sediment size, critical velocity and pier width were used as input parameters to predict the scour depth. The ANN model was also developed using field scale data set to compare ANFIS model performance. The results indicated that, the modeling with dimensional variables yields better predictions than when normalized variables are used. Prediction results indicated that the errors are much larger compared to the case of a laboratory-scale dataset. The five selected empirical equations were also applied for the same data set and Sheppard and Melville's formula was found to provide the best prediction. The study concluded that, ANFIS method predicts much better if the range of the training dataset is sufficiently wide to cover the range of the application dataset.

Varaki et al. (2017) predicted the scour depth around the inclined bridge pier located on rectangular foundation using optimized ANFIS parameters with GA. 48 data sets of experimental results for various flow conditions were used. The model results were evaluated based on CC and RMSE values. The results were compared and indicated that, the optimization of ANFIS parameters improved the accuracy of prediction.

2.3.4 Hybrid soft computing models

Najafzadeh and Barani (2011) introduced a new application of GMDH in the prediction of scour depth around pier. Two models of the GMDH network were developed using genetic programming and a back propagation algorithm. Genetic programming was performed in each neuron of the GMDH instead of performing the quadratic polynomial. In the second model of the GMDH, the quadratic polynomial was used in each neuron of the network as a transfer function, and a back propagation algorithm was used for training of the network. Six effective input parameters were considered to predict scour depth. The results showed that, the GMDH-GP performs better than the GMDH-BP in both training and testing phases.

Chou and Pham (2014) investigated the potential use of genetic algorithm (GA)-based support vector regression (SVR) model to predict bridge scour depth near piers and abutments. An SVR model developed by using MATLAB® was optimized using a GA, maximizing generalization performance. Data collected from the literature were used to evaluate the bridge scour depth prediction accuracy of the hybrid model. To demonstrate the capability of the computational model, the GA–SVR modeling results were compared with those obtained using numeric predictive models and empirical methods. The results showed that, the GA–SVR model effectively outperformed existing methods and can be used by civil engineers to efficiently design safer and more cost-effective bridge substructures.

Basser et al. (2015) proposed a new approach ANFIS-PSO to determine the optimum parameters of a protective spur dike. The angle of the protective spur dike relative to the flume wall, its length, and its distance from the main spur dikes, flow intensity, and the diameters of the sediment particles were used to find the optimum parameters. The results from the study indicated that, the accuracy of the proposed method has increased significantly compared to other approaches. The performance of the ANFIS-PSO method was confirmed using the available data.

Harish et al. (2015) presented the SVM and hybrid of Particle Swarm Optimization (PSO) with SVM (PSO–SVM) is developed to predict damage level of non-reshaped berm breakwaters. Optimal kernel parameters of PSO–SVM are determined by PSO algorithm. Both the models were trained on the data set obtained from experiments. Results of both models were compared in terms of statistical indices, such as correlation coefficient, root

mean square error and scatter index. The PSO–SVM model with polynomial kernel function outperformed other SVM models.

Jannaty et al. (2015) implemented the Particle Swarm Optimization (PSO) technique to predict scour depths by obtaining appropriate parameters for the neural network model and fuzzy inference system. The test was conducted based on samples obtained from 188 pier scour depths presented by the United States Geological Survey (USGS). The empirical results showed that, due to its minimum Root Mean Square Error (RMSE), the presented model was preferable to the ANFIS model. Moreover, the proposed model produced better solutions than FDOT and HEC-18 equations. The momentum method was implemented to accelerate the teaching process for increasing the accuracy of short term predictions.

Najafzadeh (2015) utilized Neuro-Fuzzy based GMDH as an adaptive learning network to predict the scour depth at downstream of grade control structures. The NF-GMDH was developed using PSO. The model training and testing were carried out using non-dimensional variables. The testing results were compared with genetic programming and evolutionary polynomial regression models. The study concluded that, the NF-GMDH-PSO network produced lower error of the scour depth prediction than those obtained using the other models.

Hasanipanah et al (2016) presented the new hybrid model of artificial neural network (ANN) optimized by particle swarm optimization (PSO) for prediction of maximum surface settlement (MSS). The PSO-ANN model were constructed using, horizontal to vertical stress ratio, cohesion and Young's modulus were set as input parameters and maximum surface settlement predicted as output. The model performances were analyzed using CC, RMSE and MSE. The results from the study showed that, the proposed PSO-ANN model was able to predict MSS better than ANN.

2.4 Summary of Literatures

From the literature review, the soft computing techniques can be successfully used for modeling the scour related problems. Several studies are carried out to estimate the scour depth. The soft computing models have performed better than other existing empirical equations. The hybrid models combining the advantages of different individual techniques

have performed better in the prediction. However, there is a need for further investigation on the behavior of these models under different types of scour condition.

AI models are data driven models and limited datasets availability has been always a concern while using these models. There is a need to address this issue by testing different input combinations.

2.5 Problem Formulation

- Accurate estimation of scour depth around the pier is very important for the safety and stability of the bridge structures. From the literature it is clear that, there is no common method to estimate the scour depth.
- There are various factors which affect the scour depth and considering of different factors in a single study is essential to understand the scour pattern and scour mechanism.
- Scour mechanism is different in both clear water condition and live bed condition. There is a necessity to understand the scour pattern in both conditions with different input parameters.
- Number of studies has reported on soft computing models such as ANN, ANFIS, SVM etc., in the prediction of scour depth around the bridge pier and other scour related problems.
- It is observed from the literature that, a few studies are carried out using hybrid soft computing models for the prediction of scour depth.
- Recently, the particle swarm optimization (PSO) becomes an efficient tool to optimize the other soft computing model parameters to improve the prediction accuracy.
- There is no literature available for the application of PSO-SVM and PSO-ANN in the prediction of scour depth around the bridge pier under different scour conditions.
- In the view of above aspects, there is a need to take up a study on application of hybrid PSO based soft computing models for modeling to predict the scour depth around different shapes of bridge pier under both clear water and live bed scour condition.

2.6 Research Objectives

The objective of the present research is to check the applicability of soft computing techniques in the prediction of scour depth:

- To develop Soft Computing models (ANN, SVM and ANFIS) to predict the scour depth around different pier shapes under clear water and live bed scour condition.
- To develop hybrid soft computing models by combining Particle Swarm Optimization SVM and ANN individual models (PSO-SVM and PSO-ANN).
- To analyze and recommend the most reliable soft computing model in predicting scour depth around bridge pier.

EXPERIMENTAL DATA AND METHODOLOGY

3.1 General

A physical model study on scour depth around bridge pier was carried out by Goswami Pankaj in 2013 in two-dimensional wave flume. In the present work, experimental data obtained from the physical model study is used for developing soft computing models to predict the scour depth around bridge pier. Experimental data are collected and organized in a systematic data base. These data are divided into two sets, about 50% of the data for training and remaining data for testing models.

In this chapter details of the experiments are explained along with the methodology adopted for the present study. Also, details about Artificial Neural Network (ANN), Support Vector Machines (SVM), Adaptive Neuro-Fuzzy Inference System (ANFIS) and Particle Swarm Optimization (PSO) are described in detail.

3.2 Experimental Data Analysis

The depth of scour is generally influenced by flow, sediment, and geometry of the pier . The functional interdependency between the input and output parameters is expressed in the form of equation below,

$$d_{se} = f[\text{flow}(q, u, y), \text{sediment}(d_{50}, \sigma), \text{pier geometry}(b, \alpha, \beta)] \quad (3.1)$$

The experimental data are collected from Goswami P (2013). The laboratory data sets are taken with a 1000 mm wide, 1300 mm depth and 19.25 m length of flume dimensions. The bed material used in the study is sand gravel of $d_{50}= 4.2$ mm and uniformly graded sand of $d_{50}= 0.42$ mm. The experiment was conducted for clear water scour condition with velocities of 0.215 m/Sec, 0.226 m/Sec, 0.278 m/Sec for sand gravel and 0.184 m/Sec, 0.278 m/Sec, 0.351 m/Sec for uniformly graded sand. The data were collected for 0-6 hours with 1 hour interval. Similarly, the experiment was conducted for live bed scour condition with sediment flow of 747.78 ppm and 1066.67 ppm. The velocities of flow considered in this case were 0.215 m/Sec and 0.226 m/Sec and the data were collected from 0-4 hours with 1-

hour interval. The pier of circular, rectangular, round nosed and sharp nosed shapes were used in the experiment in both scour conditions.

The input parameters, namely, sediment size (d_{50}), velocity (U), time (t) and sediment quantity (ppm) are used to predict the scour depth for different pier shapes such as circular, rectangular, round nosed and sharp nosed pier. The whole data set is divided randomly into training data (50%) and testing data (50%). The statistical parameters such as most extreme (maximum), least (minimum), mean, standard deviation and kurtosis of each factor for different pier shapes are listed in the Table 3.1 and 3.2. The negative value for kurtosis indicates that the distribution of data has lighter tails and flatter peaks. The training and testing data are applied to the models and the predicted scour values are compared to the measured values.

Table 3.1 Statistical parameters in clear water scour condition

Data set	Statistical Parameters	Variables						
		Sediment size, d_{50} (mm)	Velocity (m/Sec)	Time (hrs)	Scour depth (mm)			
					Circular	Rectangular	Round Nosed	Sharp Nosed
Training	Max	4.2	0.351	6	118	122	113	120
	Min	0.42	0.184	0	55	55	53	53
	Mean	2.31	0.261	3	84.26	87.89	82.512	84.77
	SD	1.89	0.0515	2	14.17	14.99	13.06	13.8
	Kurtosis	-2.049	-0.547	-1.253	-0.139	-0.222	0.064	0.472
Testing	Max	4.2	0.351	6	115	121	111	120
	Min	0.42	0.184	0	54	55	54	55
	Mean	2.31	0.261	3	84.512	88.345	83.32	84.14
	SD	1.89	0.0515	2	14.206	14.58	13.23	13.33
	Kurtosis	-2.049	-0.547	-1.253	-0.155	-0.225	-0.143	0.633

Table 3.2: Statistical parameters in live bed scour condition

Data set	Statistical Parameters	Variables						
		Sediment Quantity (ppm)	Velocity (m/Sec)	Time (hours)	Scour depth (mm)			
					Circular	Rectangular	Round nosed	Sharp nosed
Training	Max	1066.67	0.251	4	98	108	98	99
	Min	747.78	0.226	0	71	71	70	68
	Mean	907.225	0.2385	2	83.575	89.213	83.513	84.49
	SD	159.45	0.0125	1.414	7.69	9.907	7.20	8.24
	Kurtosis	-2.052	-2.052	-1.31	-1.134	-1.157	-1.019	-1.039
Testing	Max	1066.67	0.251	4	99	106	97	98
	Min	747.78	0.226	0	70	73	68	68
	Mean	907.225	0.2385	2	83.825	89.633	83.35	85.24
	SD	159.45	0.0125	1.414	7.938	10.024	7.394	8.95
	Kurtosis	-2.052	-2.052	-1.31	-1.190	-1.276	-1.052	-1.40

3.3 Theoretical Overview of Soft Computing Techniques

3.3.1 Artificial Neural Network (ANN)

Artificial Neural network is a group of interconnected artificial neurons that can be used as a computational model for information processing. These are nonlinear statistical data modeling tools, used to develop a relationship between input and output. Mathematically, an ANN can be treated as universal approximations having ability to learn from examples without the need of explicit physics.

Neural Networks are computational models naturally performing a parallel processing of information. Essentially, an ANN can be defined as a pool of simple processing units (neurons) which communicate among themselves by means of sending analogue signals. These signals travel through weighted connections between neurons. Each of these neurons accumulates the inputs it receives, producing an output according to an internal activation function. This output can serve as an input for other neurons, or can be a part of the network output. There is a set of important issues involved in the ANN design process. As a first step, the architecture of the network has to be decided.

In the present research work, feed forward back-propagation neural network is used. The feed forward back-propagation architecture is developed in the early 1970s (Katukam R. 2014). Its greatest strength is in non-linear solutions to ill-defined problems. The typical back-propagation network has an input layer, an output layer, and at least one hidden layer. There is no theoretical limit on the number of hidden layers but typically, there is just one or two. Each layer is fully connected to the succeeding layer, as shown in Figure. 3.1.

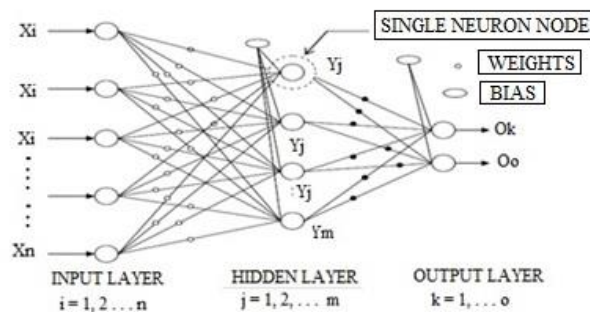


Figure 3.1 Feed forward back propagation neural network used in study

3.3.2 Support Vector Machines (SVM)

A learning tool is derived from the past statistical learning algorithms, which is named as support vector machine (SVM) by Vapnik 1999. SVM acts as training algorithm and regression tool for linear and nonlinear classification respectively. In the high dimensional feature space, simpler and linear hyperplane classifiers that have a maximal margin between the classes are obtained. SVM is a machine learning approach which provides maximized predictive accuracy automatically either by avoiding/minimizing or overwriting of data. SVM depends on SRM (Structural Risk Minimization) principle and convex optimization algorithm wherein the empirical risk and the confidence interval of the learning machine are simultaneously minimized by maximizing the geometric margin.

In case of non-linear data, the SVM has the ability to map the data points of input space to the feature space of D-dimension by using different kernels and is known as “Kernel trick” i.e., the dot product of the data points,

$$\text{Given as: } K(x_i, x_j) = (x_i, x_j)(x_i, x_j), \quad (3.2)$$

$$\text{It can also be written as: } f(x) = \sum_{i=1}^n \alpha y_i K(x_i, x) + b \quad (3.3)$$

Each data point of input space is mapped into a D-dimensional space via kernel function i.e., “Kernel trick”, $K(x_i, x_j) = \phi(x_i, \bar{x})(x_j, \bar{x})$ dot product in the feature space. The role of the kernel function simplifies the learning process by changing the representation of the data in the input space to a linear representation in a higher-dimensional space called a feature space. The kernel functions can convert nonlinear data points into linear ones. The SVM develops a different hyperplane margin between the points in the feature space and amplifies edge between two informational indexes of two input points (Figure 3.2). It makes an effort of constructing a fit curve with a kernel function and used on entire data points such that, data points should lie between two largest marginal hyperplane to minimize the error of regression (Cortes and Vapnik 1995). The predictive capacity and classification error is dealt with learning some basic concept. Firstly, the hyperplane is separated, and then the process involves the selection of proper kernel function and SVM between hard and soft margin. The SVM model architecture adopted in the present work is shown in Figure.3.3.

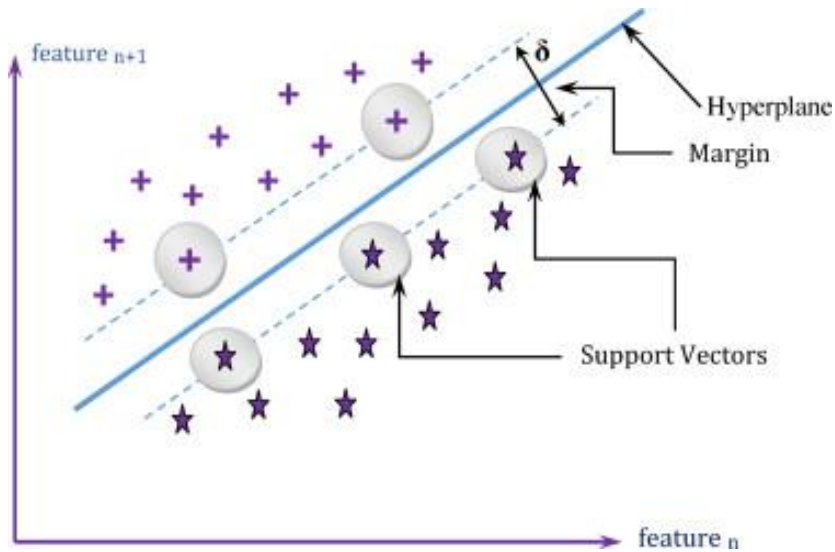


Figure 3.2 Maximum separation hyperplane

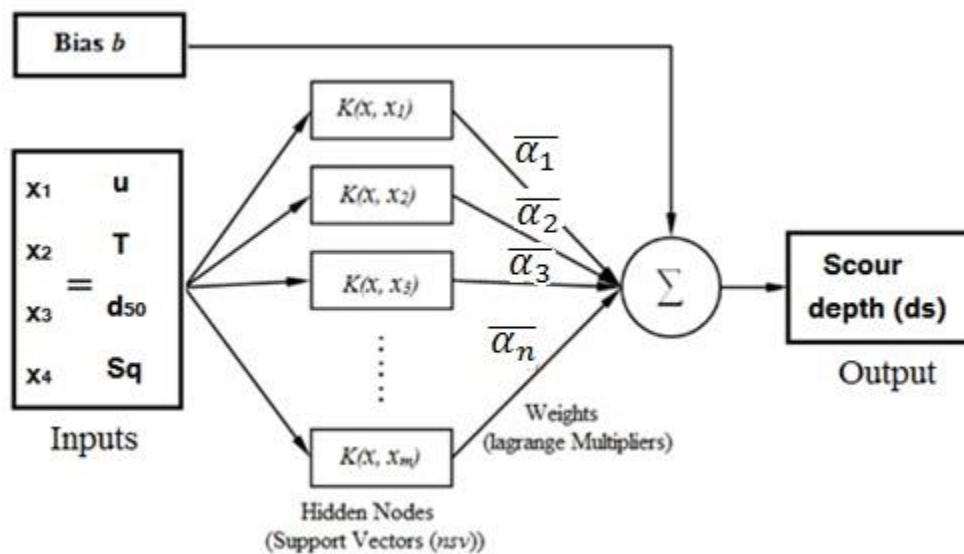


Figure 3.3 SVM architecture adopted in the study

3.3.3 Adaptive Neuro Fuzzy Inference System (ANFIS)

The principle involved behind ANFIS technique says that an artificial intelligence (AI) tool which has a set of networks for adaptation presented by Jang and Sun 1995 and a benefit of the tool is exploited to support in forecasting and to predict desired outputs. This AI tool can be viewed as a structure with the system of neural network induced feed-forward network, in which every layer is taken as Neuro-Fuzzy Structure (NFS) element. It imitates the fuzzy

rule of Sugeno and part by part of the rule is a direct fusion of given input and a constant. Finally, end prediction of the method is the weighted average of each rule's outcome.

The concept of a hybrid technique is adopted here because FIS (Fuzzy Inference System) alone lacks learning capability from the examples. The ANN can overcome this. ANFIS uses the gradient descent method (GDM) and Least Square Method (LSM) and then combined with Feed Forward Back Propagation (FFBP) technique. In which, FIS is used to measure the input and output parameters, and NN is used to define and measure the error regarding the sum squared differences between actual and desired outputs. The ANN can learn the problem and complexity involved in the relationship between the inputs and output, ANN performs the non-linear and uncertainty modeling without any prior knowledge. Hence, FFBP with TS based FIS system used to estimate the depth of the scour. To skip the deficiency of a training algorithm all along the process. NN used in combination with FIS with the introduction of FFBP. The disadvantages of ANN are overcome by training the FIS structure and associated parameters. ANFIS is considered to be transparent technique (Catto et al. 2003). If the amount of the available data is confined, then FIS is regarded as an efficient tool compared to ANN alone (Mahabir et al. 2006). Therefore, it is believed that ANFIS is a very reliable and robust tool to estimate the scour depth around the bridge pier (Wang and Elhag 2008).

The details about the first-order Takagi-Sugeno method of a fuzzy model with Multi-Input and Single Output (MISO) system is presented in Figure 3.4. ANFIS uses linguistic rules for estimation and formulates if-THEN rules from its knowledge to ensure the proper prediction of scour depth.

ANFIS is multilayer feed forward five-layer architecture as illustrated in Figure 3.4. The fixed nodes are represented by circular outline and the square outlines are adaptive nodes presided by parameter settings. Each node performs a particular function on incoming signals. Every node in the layer 1 (adaptive node) is associated with a node function governed by premise parameters. The output of every single node of layer 2 (fixed node) represents the firing strength of a rule which is nothing but the product of all incoming signals. Similarly, the output of every single node of layer 3 (fixed node) represents the normalized firing strength. Every node in the layer 4 is an adaptive node associated with a node function governed by consequent parameters. The final fixed node in layer 5 labeled as

(Σ) computes the overall output as the summation of all incoming signals (Abraham, 2005). The premise and consequent parameters of ANFIS are tuned in the learning process by means of a hybrid technique which involves the gradient descent back propagation method coupled with a least squares optimization algorithm to provide optimal outputs. Soon after the training converges, the values of the premise parameters of membership function are fixed in the search space and the overall output is expressed as a linear combination of the consequent parameters (Jang, 1992). Herein, grid-partitioning (GP) type of the ANFIS model (ANFIS-GP) is employed in the scour depth modeling scheme. The performance of ANFIS-GP model is greatly affected by the type and number of membership functions, which are usually ascertained by trial and error procedure.

The rules generated during inference system operation and is represented in the form of equation as, $R_u : \text{if}(x_1 \text{ is } A_u^1) ((x_2 \text{ is } A_u^2) \text{ and } (x_3 \text{ is } A_u^3))$

$$(3.4)$$

Then, $f = C_1^u x_1 + C_2^u x_2 + C_3^u x_3 + C_4^u$

$$(3.5)$$

Where, $u = 1, 2, 3, \dots, 27$ the number of rules.

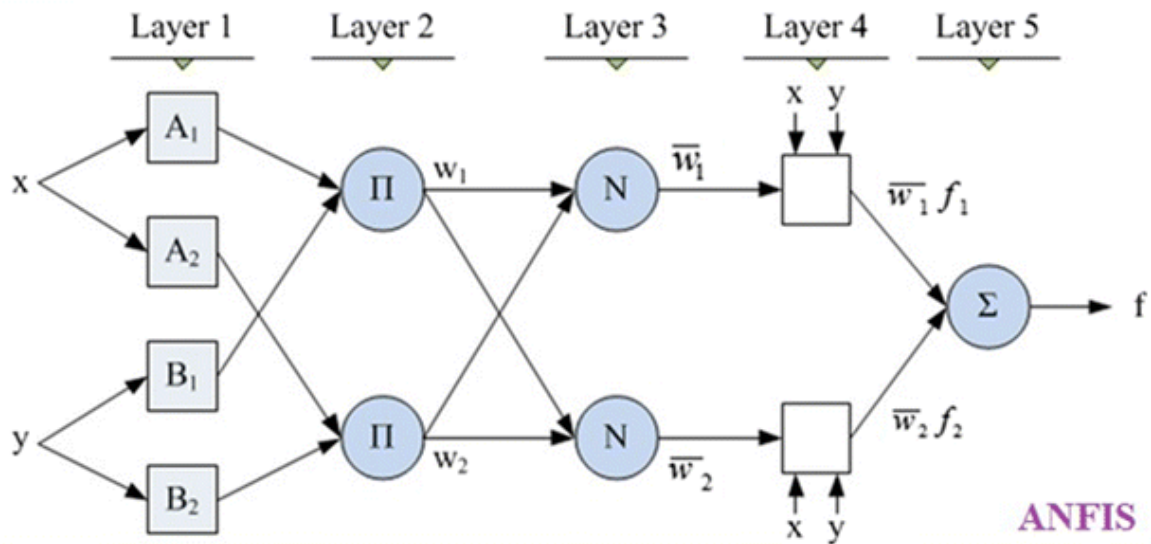


Figure 3.4 ANFIS architecture used in the study

3.3.4 Particle Swarm Optimization (PSO)

Particle swarm optimization (PSO) is a population-based stochastic optimization technique motivated by social behavior, such as bird flocking and fish schooling. PSO was first proposed by Kennedy and Eberhart 1995. In PSO, each particle makes use of its individual memory and knowledge gained by the swarm as a whole to find the best solution. All the particles have fitness values, which are evaluated by fitness function to be optimized and have velocities which direct the movement of the particles. The best position of each particle is chosen from its own and by neighboring particle experience in the process of movement of the particles. For every iteration, each particle is updated by following two ‘best’ values called *pbest* and *gbest* (Kuntoji G et al. 2017).

The PSO algorithm is defined by the direction and movement of each particle through the search space, by updating its velocity and position:

$$Vel_{j+1}^i = W_j Vel_j^i + C_1 rand_1 (pbest_j - pos_j^i) + C_2 rand_2 (gbest_j - pos_j^i) \quad (3.6)$$

$$pos_{j+1}^i = pos_{j+1}^i + Vel_{j+1}^i \quad (3.7)$$

Where pos_j^i is the current position of the particle i with subscript j representing iteration count, Vel_j^i is the search velocity of the i^{th} particle, C_1 and C_2 are the cognitive and social scaling parameters, $rand_1$ and $rand_2$ are the random numbers with interval $[0,1]$ applied to the i^{th} particle, W_j is the particle inertia, $pbest_j$ is the best position found by the i^{th} particle (personal best) and $gbest_j$ is the global best position found among all the particles in the swarm. The particle inertia controls the balance of global and local search abilities, where a larger W_j facilitates a global search. Particle i flutter toward a new position using Eqs. (3.6) and (3.7), which allow all particles in the swarm to update their $pbest_j$ and $gbest_j$.

In order to develop the optimal PSO algorithm the cognitive component and a social component weighted by the constants, C_1 and C_2 , respectively should be optimally balanced. When a C_1 greater than C_2 is used, each particle approaches its previous individual best position. When a C_2 greater than C_1 is used, each particle moves closer to the previous global best position (Zhao, 2016).

3.4 Development of Soft Computing Models

3.4.1 Development of ANN Model

Artificial Neural Network (ANN) is one technique in the broad area of computer intelligence. Since 1960 ANN models inspired by human brains made of a group of neurons as nodes. The typical neural network structure consists of the input layer, hidden layer, and an output layer. The hidden layers and neurons numbers are decided by trial and error technique (Hasanipanah et al. 2016). The neurons used to process the information received by the input layer neurons. The weights are the connectivity element between neurons in adjacent layers. By changing the weights of the training patterns at each process network learning is achieved (Ghasemi et al. 2017). In this study, the feed forward back propagation (FFBP) neural network is considered. The ANN models are developed by varying hidden neurons form 1 to 5. The statistical results of ANN with four hidden neurons are discussed in the next chapter.

3.4.2 Development of SVM model

The SVM algorithm is adopted to predict the scour depth with respect to different pier shape using sediment size, velocity and time as input variables. The SVM models are developed using MATLAB software for linear, polynomial, and radial basis (RBF) kernel functions. The developments of SVM model with linear, RBF kernel functions are explained in detail. The efficiency and accuracy of the SVM model with different kernels functions depends on the model parameters, namely, SVM parameter (C), kernel width parameter-Gamma (γ), and the epsilon parameter (ϵ). The four K-fold Cross-Validation search is used to identify and finalize the optimal parameters. Optimal parameters (c, γ , and ϵ) are chosen for a number of trials with various combinations of C (ranges from 1 to 1000), γ (ranges 1 to 100) and ϵ (ranges 0.001-10). The obtained optimal SVM parameters are shown in Table 3.3. The predicted values from the models are compared with the experimental values.

Table 3.3: Optimal SVM parameters

Optimal SVM parameters	Circular Pier		Rectangular Pier		Round Nosed Pier		Sharp Nosed Pier	
	Clear water scour	Live bed scour	Clear water scour	Live bed scour	Clear water scour	Live bed scour	Clear water scour	Live bed scour
C	388	100	800	500	60	500	221	500
gamma (γ)	2	26	1	26.25	3	26.25	2	25
Epsilon (ϵ)	0.1	7	0.1	10	0.1	10	0.1	10

3.4.3 Development of ANFIS model

In the study, the ANFIS model is developed and tested to predict the scour depth with respect to different pier shapes using various input parameters. The ANFIS model is trained and tested to predict the scour depth concerning different pier shapes using Sediment quantity in the flow, the velocity of flow and time as the input parameters. The ANFIS model is developed in MATLAB software with trapezoidal, triangular, Gbell and Gaussian membership functions. The development of ANFIS with trapezoidal and Gbell MF are explained in this section. The 3 membership functions with 27 fuzzy rules are adopted in the present discussion. The details of the ANFIS model used in the study are developed using the following parameters, as listed in the Table 3.4. The estimated simulations obtained from the ANFIS models are compared with experimental values for validation of the developed models.

Table 3.4: Details of ANFIS model

ANFIS Architecture	
Number of membership functions	3
Algorithm selected	Hybrid
Number of Epoch runs given	400-500
Generated Fuzzy inference system	Grid Partition
Membership function (MF) type	Constant
Number of fuzzy rules generated	27
Type of membership function (MF) used	Trapezoidal, Gbell

3.4.4 Development of Particle Swarm Optimization based Support Vector Machine (PSO-SVM)

It is proved by the previous studies that if the selection of SVM and kernel parameters is done, then there is a chance of over fitting or under fitting. To avoid this over-fitting or under-fitting of the SVM model due to the improper selection of SVM and kernel parameters, PSO is used as optimizer to select suitable parameters of SVM. PSO is an optimization method, which not only has strong global search capability, but also is very easy to implement. So, it is very suitable for proper selection of SVM parameters. In order to develop the optimal PSO algorithm the cognitive component and a social component weighted by the constants, C_1 and C_2 , respectively should be optimally balanced. The importance of algorithm parameters can be explained by the selection of the number of particles usually between 10 and 50, where, C_1 implies the importance of personal best value and C_2 implies the importance of neighbourhood best value. Usually, $C_1 + C_2 = 4$ (empirically chosen value). The linear, RBF and Polynomial kernel functions are used in the model. The optimal parameters for the PSO-SVM with linear and polynomial kernel function are tabulated in Table 3.5. The steps involved in the development of PSO-SVM model is explained in section 3.5. The flowchart for the same is as shown in Figure 3.5.

Table 3.5: Optimal PSO-SVM parameters

Optimal PSO-SVM parameters	Circular Pier		Rectangular Pier		Round Nosed Pier		Sharp Nosed Pier	
	Clear water scour	Live bed scour	Clear water scour	Live bed scour	Clear water scour	Live bed scour	Clear water scour	Live bed scour
C1	0.8	1.4	0.8	1.4	0.8	1.4	0.8	1.4
C2	3.2	2.6	3.2	2.6	3.2	2.6	3.2	2.6
P	25	25	25	25	25	25	25	25
C	680	225	500	450	110	750	48	600
gamma (γ)	1	5	1	4.5	1	4.5	1	4.5
Epsilon (ϵ)	0.5	2	0.5	2.5	0.5	2.5	0.5	2
Degree (d)	3	3	3	3	3	3	3	3

3.4.5 Development of Particle swarm optimization based artificial neural network (PSO-ANN)

The performance of ANN architecture is usually dependent on settings of hyper-parameters (number of layers, layer size, layer type), activation function for each layer, optimization algorithm, learning rate with momentum coefficient, regularization and initialization methods (Ludermir et al., 2006). Hyper-parameters can strongly interact with each other to affect the performance. On these grounds, neural network is known to have some intrinsic disadvantages such as slow convergence speed, less generalizing performance, over-fitting problems, issues of local minima and saddle points, which can trap the optimization algorithm at bad solutions (Lawrence et al., 1996; Lawrence and Giles, 2000). Hence, optimizing ANN using nature-inspired optimization algorithms can elevate the predictability performance of the model.

In the learning process of ANN, the initial weights are randomly selected. This weakness of the ANN model requires a number of iterations to fit optimal weights and is strongly dependent on the initial weights. This study proposed to improve the learning speed of ANN by selecting initial weights by using the PSO algorithm. The points involved in the PSO-ANN algorithm are as shown in flowchart (Figure 3.5). The optimal PSO algorithm depends on the selection of optimal C_1 and C_2 components. In the PSO-ANN model the $C_1=1.5$ and $C_2=2.5$ are used for the development of optimal model. The population size of 25 and 6 hidden neurons are considered in the model. The steps involved in the development of PSO-ANN model is explained in section 3.5. The flowchart for the methodology adopted in the PSO-ANN model is as shown in Figure 3.5.

3.5 Methodology used in the Study

The steps involved in the development of optimal PSO-SVM and PSO-ANN model for the prediction of scour depth around the bridge pier is as explained below.

Step 1: data analysis and preprocessing

- collection of experimental data
- selection of input and output variables
- experimental data, split into two sets (training and testing data)

Step 2: developing hybrid (PSO-ANN) model

- In case of PSO-ANN model- the most important step in the learning ANN algorithm is a selection of network architecture (feed-forward back propagation neural network).
- In case of PSO-SVM model- selection of kernel parameters such as, C , γ , ϵ and d

Step 3: random selection of the position and velocity of particles.

Step 4: After every iteration, position and velocity of each particle keep updated with pbest and gbest values.

Step 6: Particle or swarm position and velocity are updated using the equations (3.6) and (3.7).

Step 7: The iterations will repeat until the target meets.

Step 8: After satisfying the criteria (RMSE), the model will test the SVM/ANN using testing data.

The flowchart for developing the PSO-SVM and PSO-ANN model is as shown in Figure 3.4.

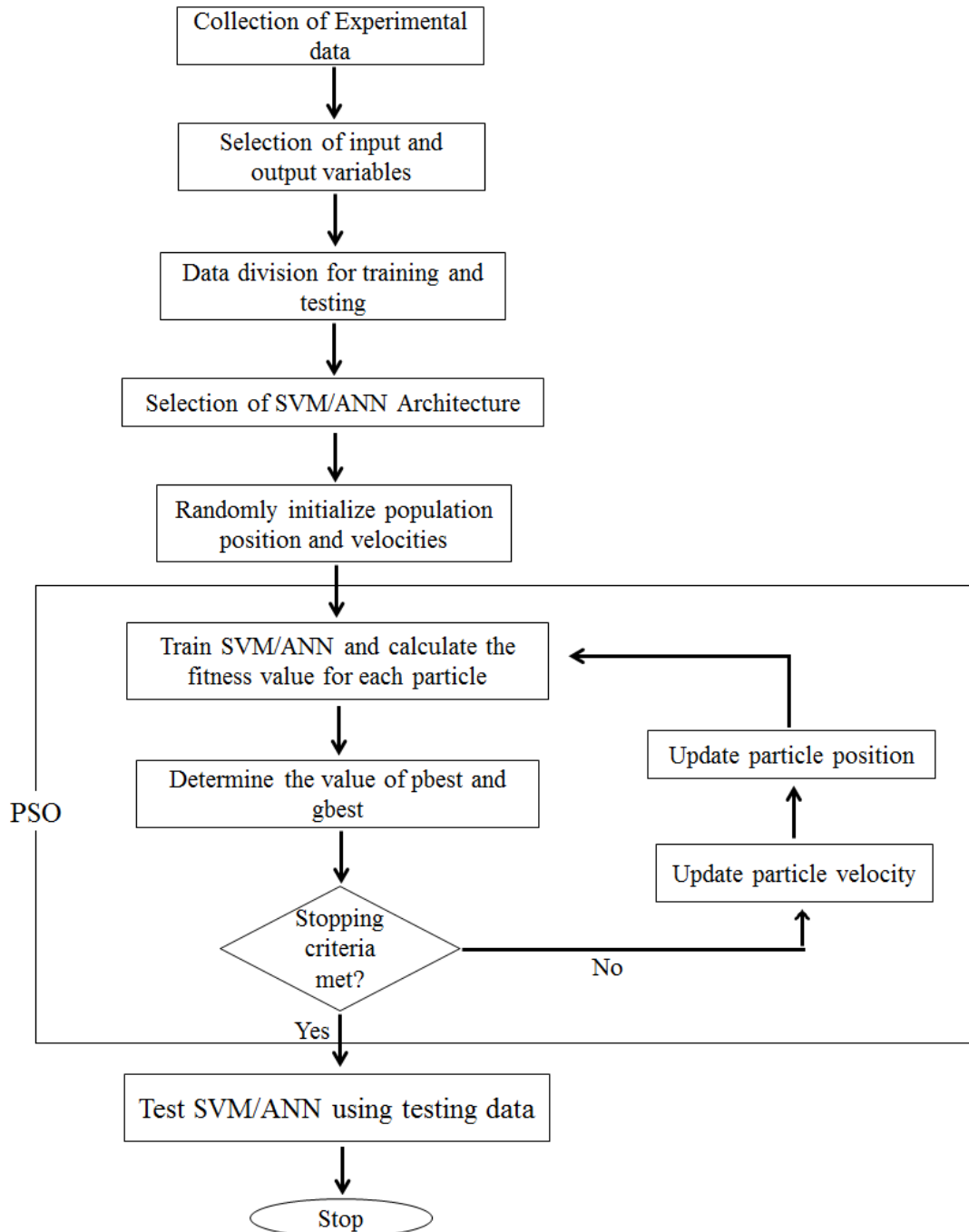


Figure 3.5 Flowchart for PSO-SVM and PSO-ANN model

In the present study, the scour depth around the bridge pier is predicted using soft computing techniques. The scour depth around circular, rectangular, round nosed and sharp nosed pier are predicted under clear water and live bed scour condition. The SVM, ANFIS, PSO-SVM and PSO-ANN techniques are considered. The model performances are analyzed

and the best model is selected using different statistical parameters such as CC, NRMSE, NSE and NMB. The overall methodology used in the study is shown in Figure 3.6.

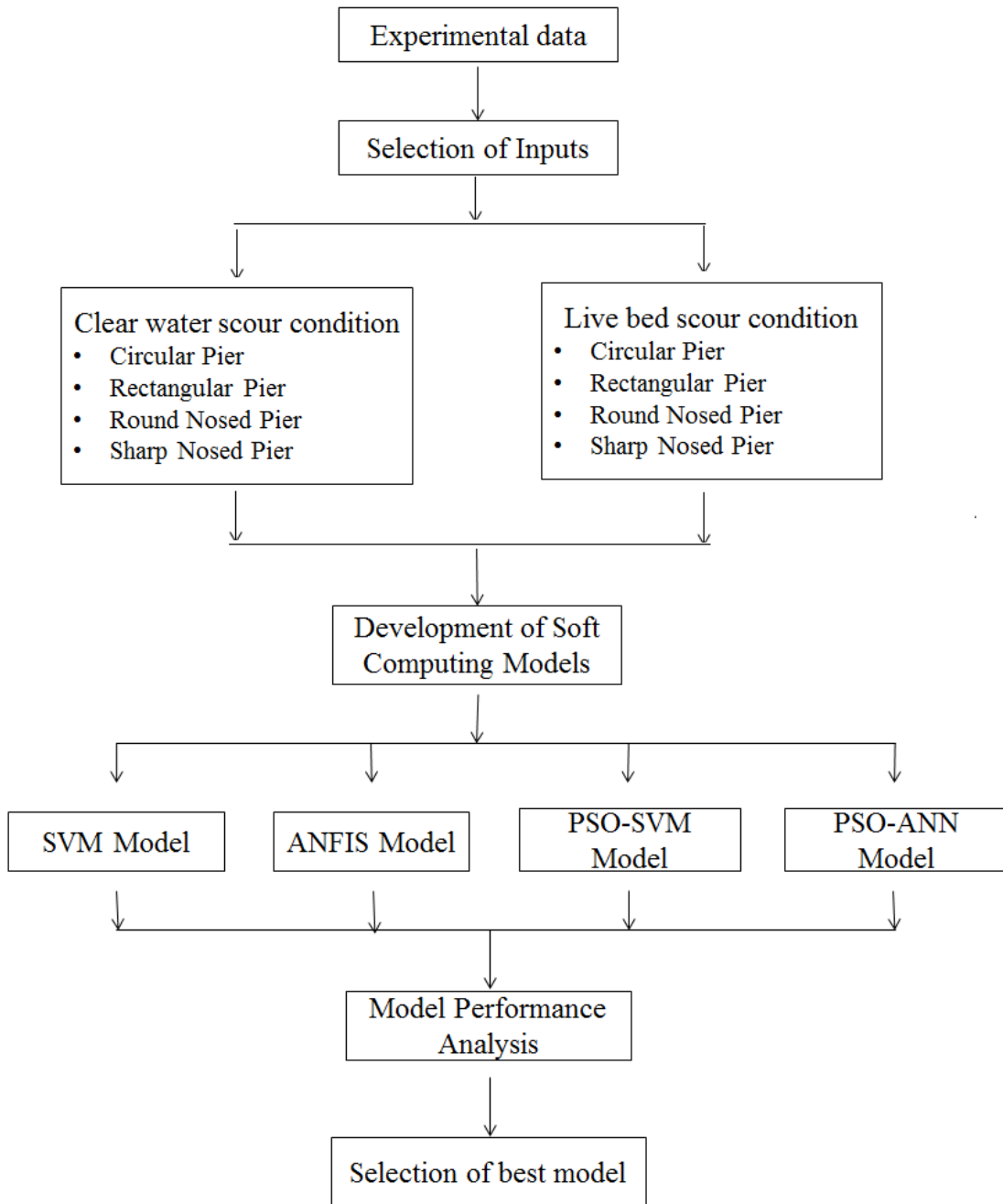


Figure 3.6 Flowchart for the overall methodology used in the study

3.5 Performance Analysis

The performances of soft computing models are evaluated in terms of different statistical measures.

1. NRMSE:

The Normalized Root Mean Square Error (NRMSE) frequently used to measure the difference between experimentally measured values and model predicted values.

$$NRMSE = \left(\frac{RMSE}{X_{max}-X_{min}} \right) \times 100 \quad (3.8)$$

$$\text{Where, } RMSE = \sqrt{\left(\frac{\sum_{i=1}^N (X_i - Y_i)^2}{N} \right)} \quad (3.9)$$

Where, X - Observed/Measured values, Y - Predicted values, N - No. of total data set points. The lowest NRMSE of the model is best predicted model.

2. NSE:

The Nash–Sutcliffe coefficient (NSE) is used to access the predictive power of the model. NSE can be range from -1 to 1 and the efficiency of the model is closer or equal to 1, the model is more accurate.

$$NSE = 1 - \left(\frac{\sum_{i=1}^N (X_i - Y_i)^2}{\sum_{i=1}^N (X_i - \bar{X})^2} \right) \quad (3.10)$$

3. NMB:

In order to know the model prediction, the Normalized Mean Bias (NMB) is used. The positive value of NMB shows that, the model is over predicted and the negative values of NMB shows that, the model is under predicted. For the better prediction the NMB value of the model should be zero.

$$NMB = \sum_{i=1}^N \left(\frac{Y_i - X_i}{X_i} \right) = \left(\frac{\bar{Y}}{\bar{X}} - 1 \right) \quad (3.11)$$

Where, \bar{X} - Mean of actual data and \bar{Y} - Mean of predicted data.

4. CC:

The correlations between the predicted and observed values are measured using Correlation Coefficient (CC). The CC varies from -1 to 1 and if the CC value closer to 1, the model is having good correlation with experimental results.

$$CC = \frac{\sum_{i=1}^N (X_i - \bar{X}) \cdot (Y_i - \bar{Y})}{\sqrt{\sum_{i=1}^N (X_i - \bar{X})^2 \cdot \sum_{i=1}^N (Y_i - \bar{Y})^2}}$$

(3.12)

Scatter plots are also used to evaluate the accuracies of the models, while boxplots are used to learn the distribution of the data points estimated by the models with respect to experimental models.

3.6 Summary

A detailed experimental study on scour depth around the bridge pier was carried out by Goswami in 2013, is described in this chapter. The data analyses in terms of statistical parameters are discussed. The input parameters, namely, sediment size (d_{50}), velocity (U), time (t) and sediment quantity (ppm) are used to predict the scour depth for different pier shapes such as circular, rectangular, round nosed and sharp nosed pier under both clear water and live bed scour conditions are presented. Also the overall research methodology used to develop soft computing tools such as SVM, ANFIS, ANN and PSO are explained. The basic concepts of individual and proposed PSO based hybrid models are discussed in detail.

RESULTS AND DISCUSSION

4.1 General

In this chapter, the performance of the proposed models for estimating the scour depth around different shapes of bridge piers under clear water and live bed scour conditions are discussed. The circular, rectangular, round nosed and sharp nosed shaped piers are considered in the models. The performances of the developed models are analyzed and validated using statistical measures such as CC, NRMSE, NSE and NMB. An attempt is made to identify efficient and reliable models for predicting scour depth using different input combinations. The results for clear water scour condition are discussed first, followed by the live bed scour condition. The result of best model is compared with available empirical equations.

4.2 Prediction of Scour Depth around Bridge Pier under Clear Water Scour Condition

In this case, the scour depth around the bridge pier is carried out under clear water scour conditions. Three inputs namely, velocity, time and sediment size are used to predict scour depth as output. The statistical parameters in terms of maximum, minimum, standard deviation and kurtosis of the data used for the study are shown in Table 3.1. The whole data set is divided into 50% for training purpose and remaining 50% for testing the models after performing many trials. The soft computing techniques such as ANN, SVM, ANFIS, PSO-SVM and PSO-ANN are discussed in the present study. The scour depth around circular, rectangular, round nosed and sharp nosed pier shapes is predicted separately and discussed. The predicted results are analyzed using statistical indices, explained in section 3.5 and validated using experimental results.

4.2.1 Performance of Support Vector Machine (SVM) model in the prediction of scour depth.

The performance of the SVM techniques depends on the proper selection of kernel parameters. The development of SVM model is explained in section 3.4.1 and the optimal kernel parameters used in the study are tabulated in Table 3.3. The linear, RBF and Polynomial kernel functions are used in the SVM model. The results of SVM with linear and RBF kernel functions are presented and discussed in this section. The results in terms of statistical indices obtained from SVM model are tabulated in Table 4.1 for all four pier shapes in both training and testing phase. The predicted results of SVM model are compared by plotted with experimental results.

Table 4.1: Results of SVM model for clear water scour condition

Pier shape	Statistical indices	SVM Model			
		Linear		RBF	
		Train	Test	Train	Test
Circular	CC	0.819	0.815	0.906	0.903
	NRMSE	14.09	14.430	9.88	10.430
	NSE	0.607	0.604	0.807	0.800
	NMB	0.011	-0.004	-0.008	-0.022
Rectangular	CC	0.738	0.737	0.808	0.803
	NRMSE	15.560	15.246	14.00	13.744
	NSE	0.517	0.523	0.609	0.613
	NMB	0.018	0.013	0.016	0.011
Round nosed	CC	0.813	0.832	0.870	0.877
	NRMSE	14.670	15.430	12.46	13.10
	NSE	0.546	0.559	0.672	0.682
	NMB	0.003	-0.006	0.011	0.002
Sharp nosed	CC	0.77	0.760	0.836	0.843
	NRMSE	14.67	14.64	12.44	12.14
	NSE	0.49	0.49	0.635	0.650
	NMB	0.002	0.009	0.002	0.009

The SVM with linear and RBF kernel functions are modeled to predict the scour depth around circular pier shape. Figure 4.1 shows the scatter plots of SVM model in testing phase for circular pier. The model results are compared with measured values and plotted the testing phase results in Figure 4.2. The statistical results are tabulated in the Table 4.1 for both testing and training. SVM with RBF shows good correlation with higher $CC=0.906$ and 0.903 , $NSE=0.807$ and 0.800 , lower $NRMSE=9.88$ and 10.430 for training and testing respectively. It is clear from the table that, SVM with RBF kernel function performed better than SVM with linear kernel function in both training and testing phase for circular pier case. The negative NMB value shows that, the model is performing under prediction, due to the linearity property of a linear kernel function, where it is not accounting for non-linear values of the data set, compared to RBF kernel function.

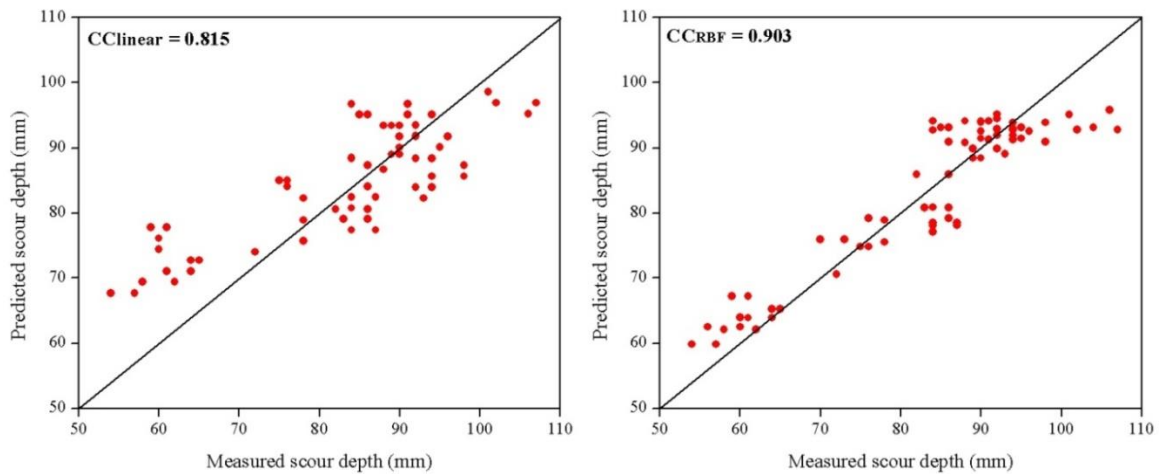


Figure 4.1 Scatter plots of SVM models in testing phase for circular pier in clear water scour condition

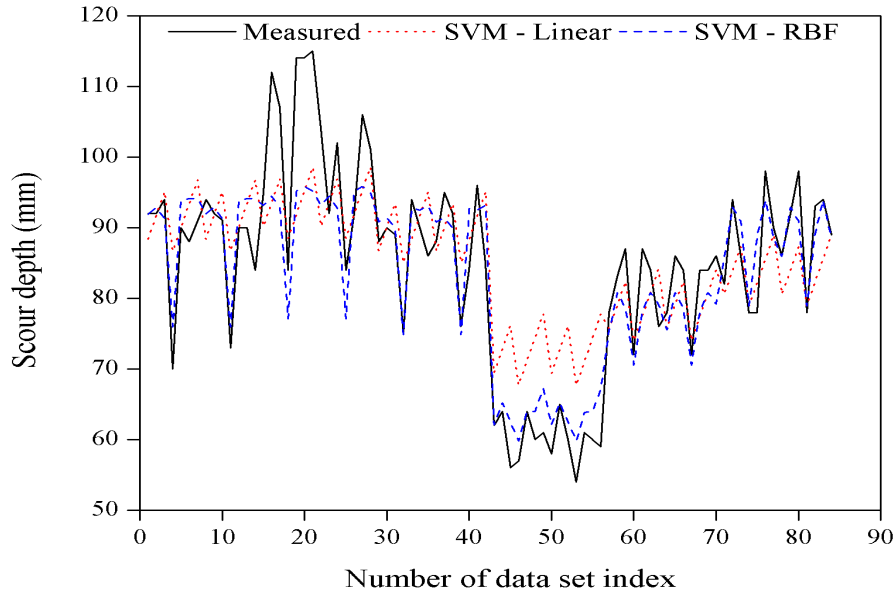


Figure 4.2 Comparison of measured and SVM model results in testing phase for circular pier in clear water scour condition

In the case of the scour depth around rectangular pier is predicted using SVM technique. Figure 4.3 and 4.4 shows the scatter and comparison plots of model for predicted and measured results in testing phase. The SVM results for both linear and RBF kernel functions are tabulated in Table 4.1 in both training and testing condition. The scatter and comparison plots shows that, the SVM with RBF kernel function showing good correlation with measured values compared to SVM with linear kernel function. Positive NMB values from the Table 4.1 clears that, SVM with both kernel functions are performing over prediction.

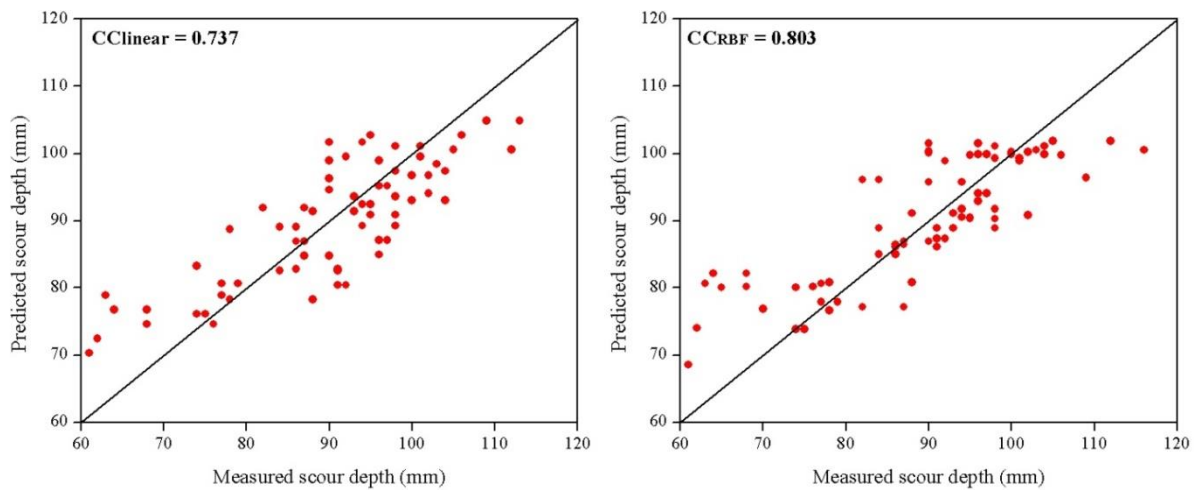


Figure 4.3 Scatter plots of SVM models in testing phase for rectangular pier in clear water scour condition

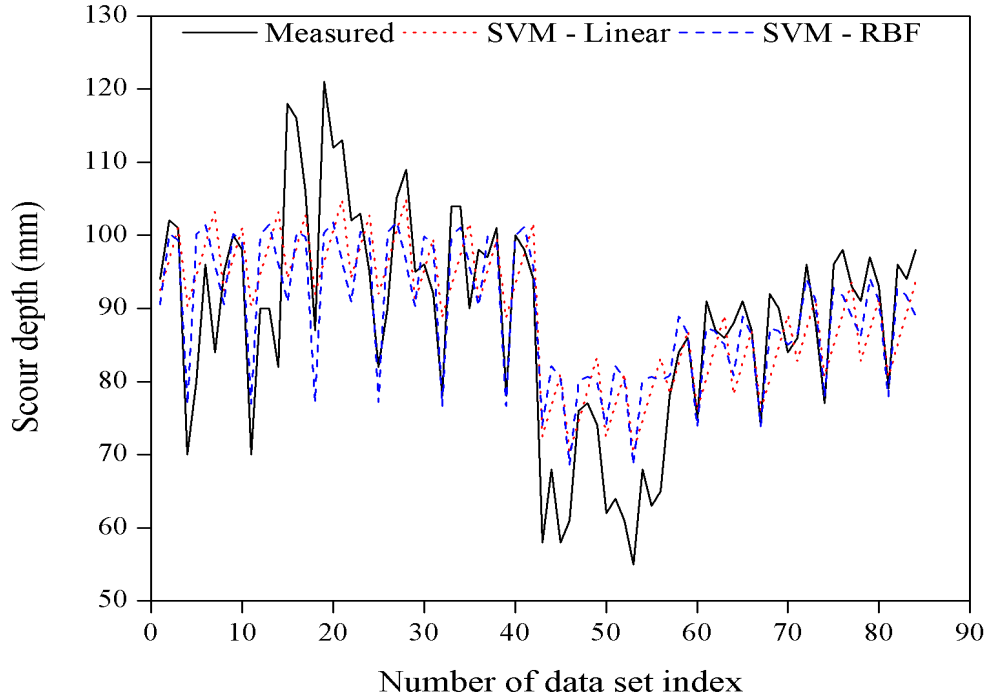


Figure 4.4 Comparison of measured and SVM model results in testing phase for rectangular pier in clear water scour condition

In case of round nosed shaped bridge pier the predicted scour depth results of SVM with both kernel function models are plotted against measured values in Figure 4.5. The statistical measures from the Table 4.1 shows that, SVM with RBF kernel function predicting better for round nosed pier. The comparison plots of measured and SVM model predicted results are plotted in Figure 4.6.

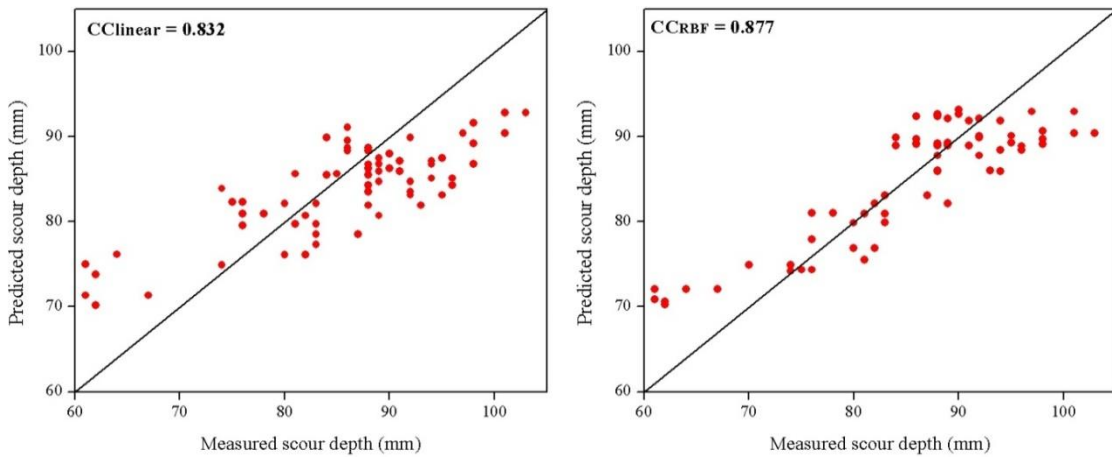


Figure 4.5 Scatter plots of SVM models in testing phase for round nosed pier in clear water scour condition

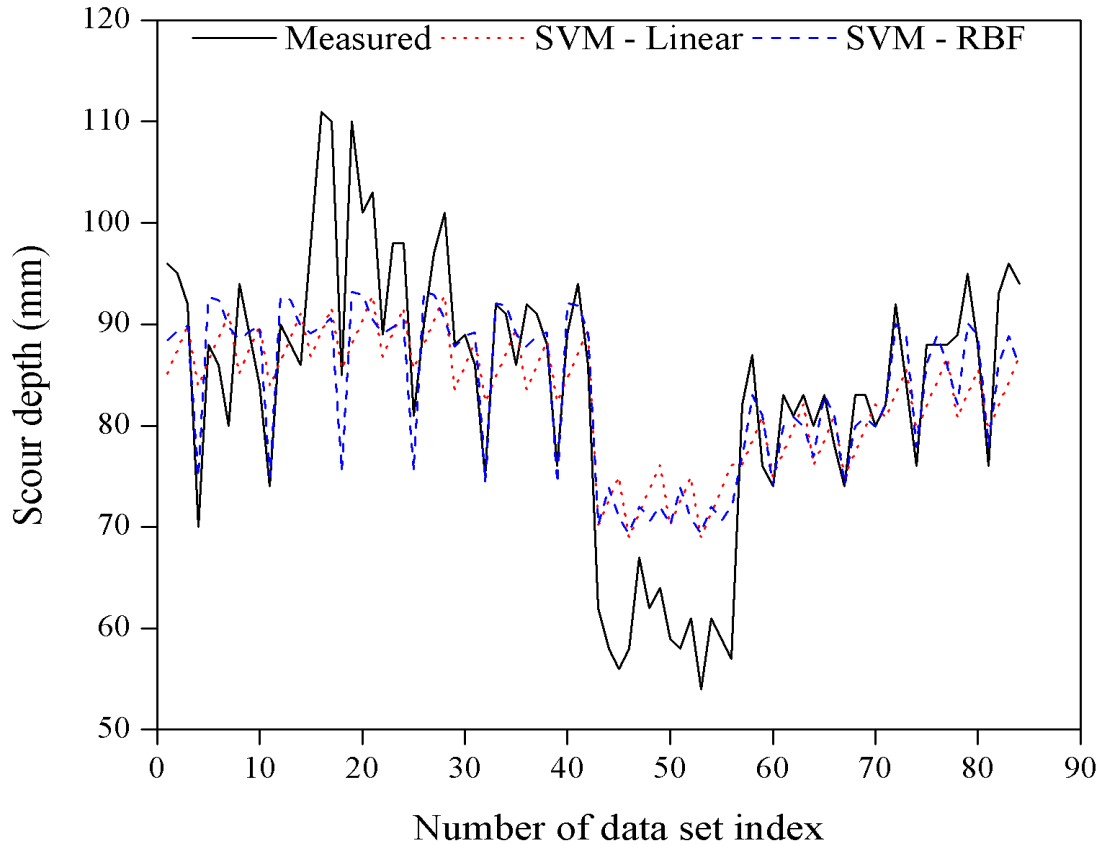


Figure 4.6 Comparison of measured and SVM model results in testing phase for round nosed pier in clear water scour condition

The scour depth around sharp nosed pier is predicted using SVM with linear and RBF kernel functions. The results obtained from the model are tabulated in Table 4.1. the scatter plots from Figure 4.7 shows that, the SVM with RBF kernel function shows good correlation with $CC=0.843$ compared to linear kernel function of $CC=0.760$. Figure 4.8 shows the comparison of measured and predicted values in testing phase. The positive NMB values from the Table 4.1 indicate that, SVM with both the kernel functions are shows over prediction.

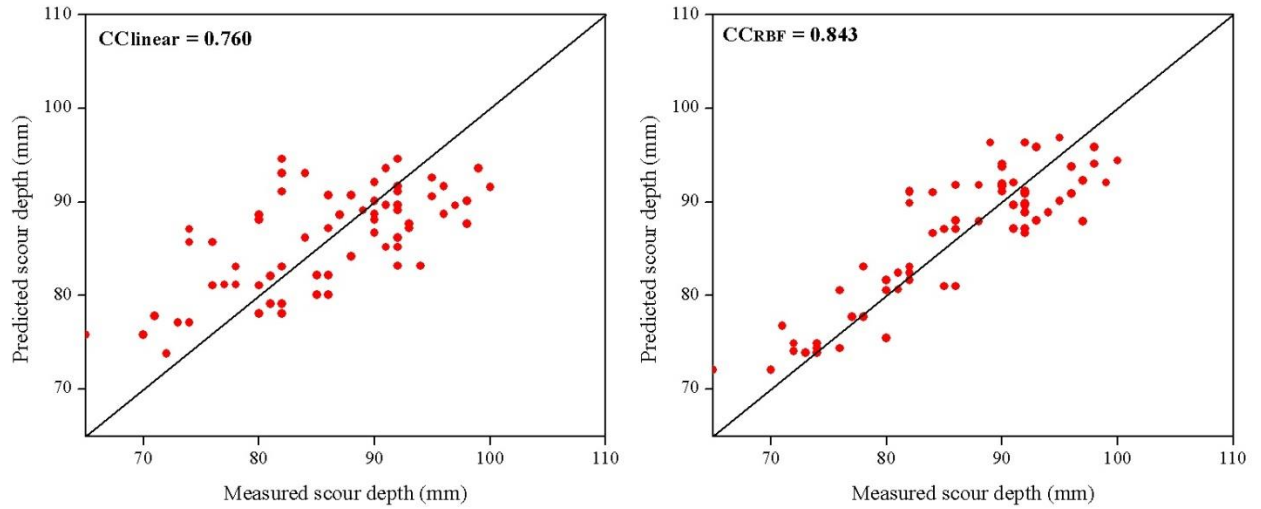


Figure 4.7 Scatter plots of SVM models in testing phase for sharp nosed pier in clear water scour condition

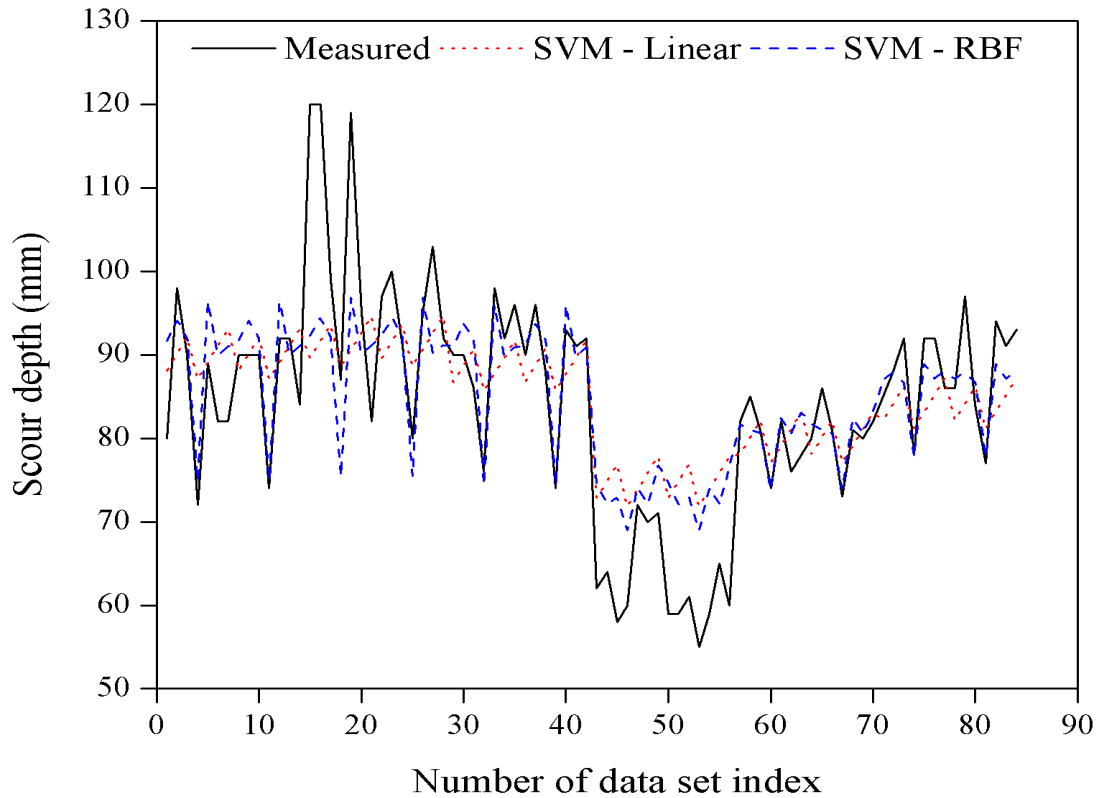


Figure 4.8 Comparison of measured and SVM model results in testing phase for sharp nosed pier in clear water scour condition

The scour depth around different pier shapes in clear water scour condition is predicted using SVM with linear and RBF kernel functions. The scatter and comparison plots are plotted against measured values and predicted results in testing phase. The statistical results from the Table 4.1 indicates that, the SVM with RBF kernel function performs well compared to linear kernel function for all the four pier shapes. However for higher scour depths under-estimation is noticed and over-estimation for lower scour depths using both linear and RBF functions Also, SVM with RBF kernel function shows good prediction for circular pier shape among the other three pier shapes.

4.2.2 Performance of Adaptive Neuro Fuzzy Inference System (ANFIS) model in the prediction of scour depth.

The ANFIS model with three inputs and one output is developed using different membership functions, fuzzy rules and epochs. The various membership functions considered are Triangular-shaped built-in membership function (TRIMF), Trapezoidal-shaped built-in membership function (TRAPMF), Generalized bell-shaped built-in membership function (GBELLMF), and Gaussian curve built-in membership function (GAUSSMF). The results of ANFIS with Trapezoidal and Gbell membership functions are presented and discussed in the below section. The theoretical overview of ANFIS technique is explained in section 3.3.3. The development of architecture of ANFIS model with trapezoidal and gbell membership function are listed in Table 3.4. The results obtained from the different ANFIS model are tabulated in Table 4.2 for both training and testing phase with respect to all four pier shapes.

Table 4.2: Results of ANFIS model for clear water scour condition

Pier shape	Statistical indices	ANFIS Model			
		Trapezoidal		Gbell	
		Train	Test	Train	Test
Circular	CC	0.924	0.913	0.963	0.955
	NRMSE	8.61	9.49	6.05	7.24
	NSE	0.85	0.834	0.928	0.912
	NMB	0.00	-0.003	0.00	-0.003
Rectangular	CC	0.890	0.869	0.931	0.912

	NRMSE	10.30	11.00	8.147	9.156
	NSE	0.790	0.752	0.867	0.828
	NMB	0.00	-0.005	0.00	-0.005
Round nosed	CC	0.906	0.919	0.954	0.951
	NRMSE	9.223	9.277	6.522	7.327
	NSE	0.820	0.840	0.910	0.900
	NMB	0.00	-0.01	0.00	-0.01
Sharp nosed	CC	0.890	0.879	0.931	0.911
	NRMSE	9.478	9.856	7.533	8.589
	NSE	0.790	0.769	0.866	0.825
	NMB	0.00	0.007	0.00	0.007

The ANFIS with trapezoidal and Gbell MF is developed for the prediction of scour depth around circular pier. The results obtained from the models are tabulated in Table 4.2 in terms of different statistical measures. The scatter plots are presented against measured and predicted values for both the membership function (MF) in during testing as shown in Figure 4.9. The comparison plots measured and predicted results are shown in Figure 4.10. From the Table 4.2, it is clear that, ANFIS with Gbell MF performs better with good correlation by higher CC=0.963 and 0.955, NSE=0.928 and 0.912 and lower NRMSE=6.05 and 7.24 during training and testing respectively. The negative NMB from the Table 4.2 indicates that, the model is performed under prediction during testing phase for both the MFs.

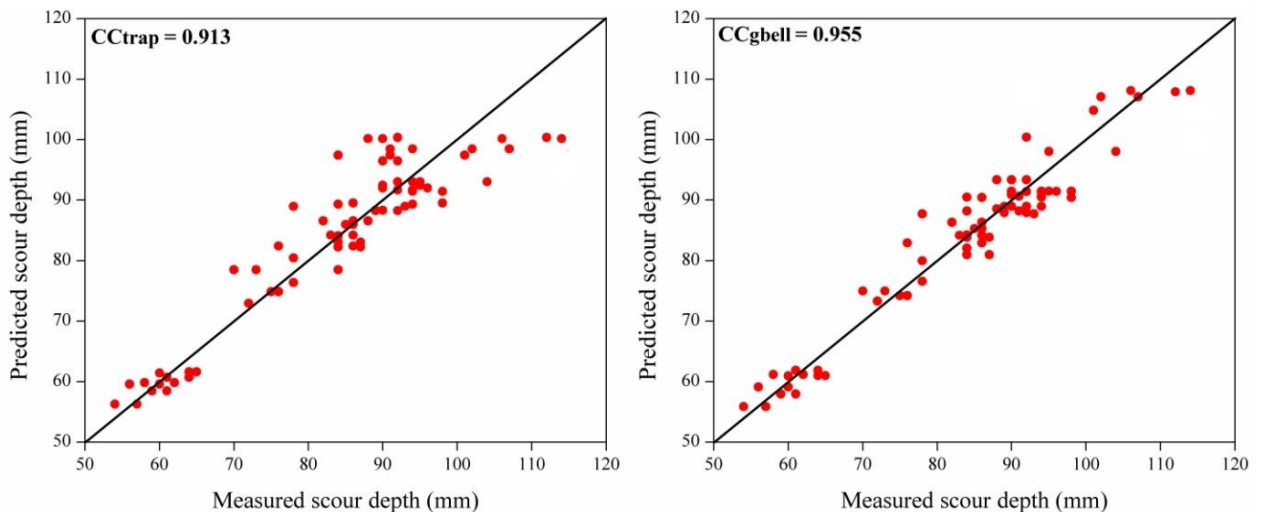


Figure 4.9 Scatter plots of ANFIS models in testing phase for circular pier in clear water scour condition

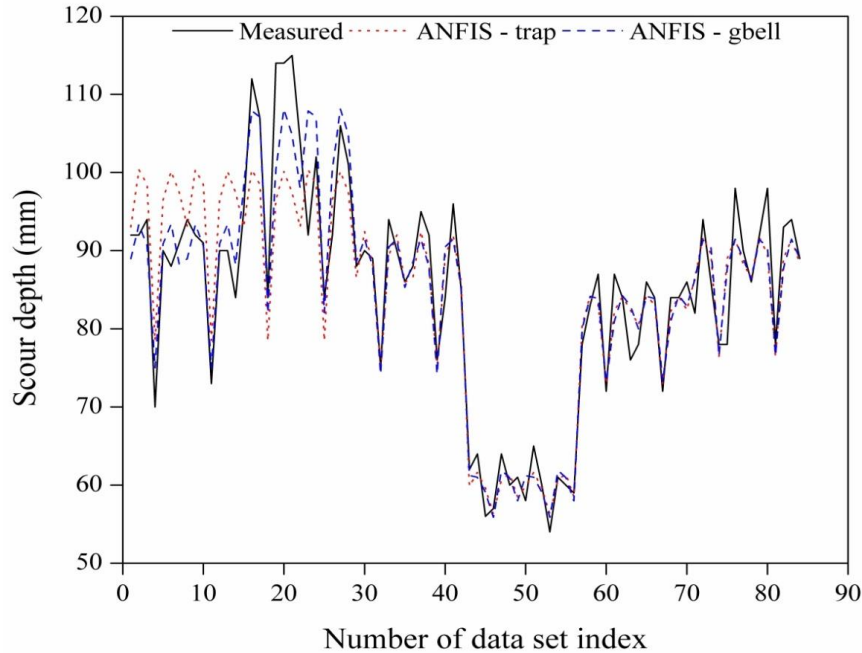


Figure 4.10 Comparison of measured and ANFIS model results in testing phase for circular pier in clear water scour condition

In case of the scour depth around rectangular pier for predicting ANFIS models are developed. The predicted scour depth is compared with measured values. The scatter and comparison plots are presented for measured and ANFIS model results as shown in Figure 4.11 and 4.12 respectively. From the Table 4.2, ANFIS with gbell MF performs better with $CC=0.912$ compared to trapezoidal MF with $CC=0.869$.

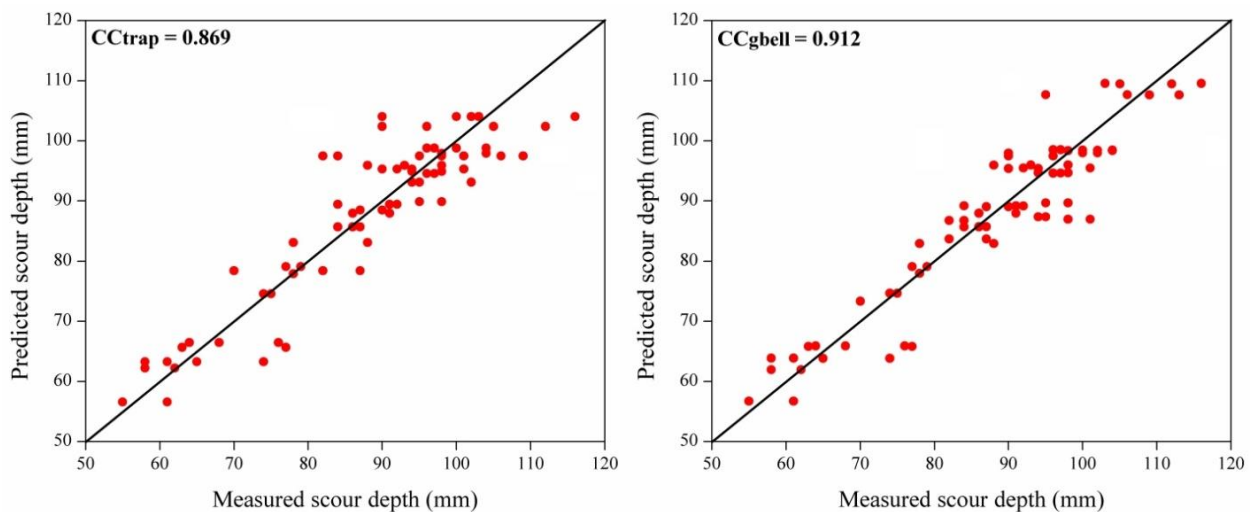


Figure 4.11 Scatter plots of ANFIS models in testing phase for rectangular pier in clear water scour condition

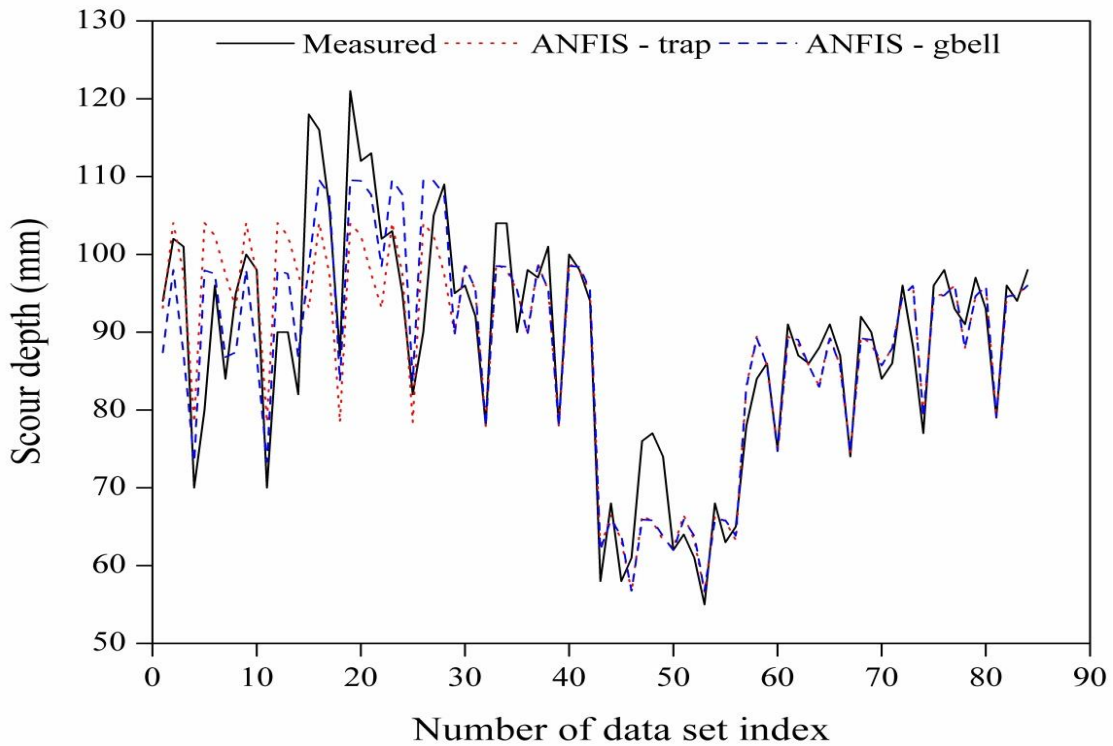


Figure 4.12 Comparison of measured and ANFIS model results in testing phase for rectangular pier in clear water scour condition

In this case, the ANFIS with trapezoidal and gbell MF are used to predict the scour depth around round nosed pier. The obtained results are tabulated in terms of statistical measures in Table 4.2. The scatter plots are presented against measured and predicted values of scour depth in Figure 4.13 and shows that, ANFIS Gbell MF performs well with $CC=0.915$ compared to ANFIS Trapezoidal MF with $CC=0.919$ during testing phase. Figure 4.14, shows the comparison plot for measured and predicted values.

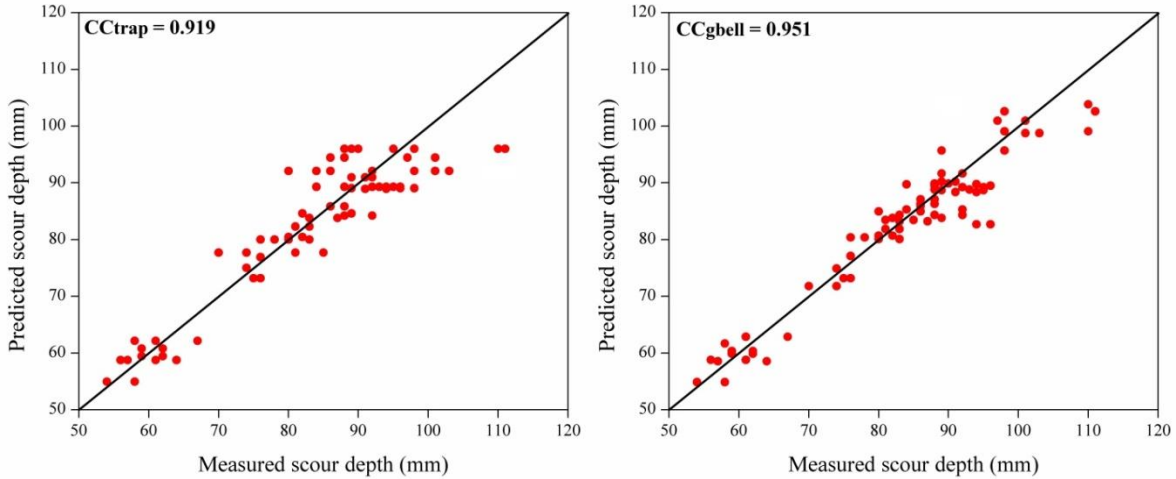


Figure 4.13 Scatter plots of ANFIS models in testing phase for round nosed pier in clear water scour condition

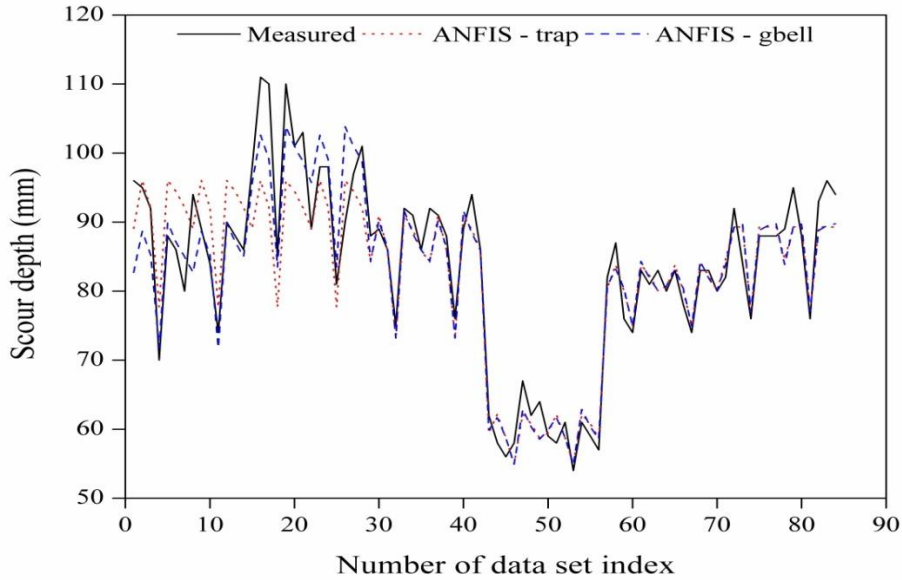


Figure 4.14 Comparison of measured and ANFIS model results in testing phase for round nosed pier in clear water scour condition

The ANFIS model with trapezoidal and gbell MF are used to predict the scour depth around sharp nosed pier. The model predicted results are tabulated in Table 4.2. The positive NMB values from the Table 4.2 indicate that, both the models are performing over prediction. The scatter and comparison plots are draw against measured and predicted values obtained in testing phase as shown in Figure 4.15 and 4.16.

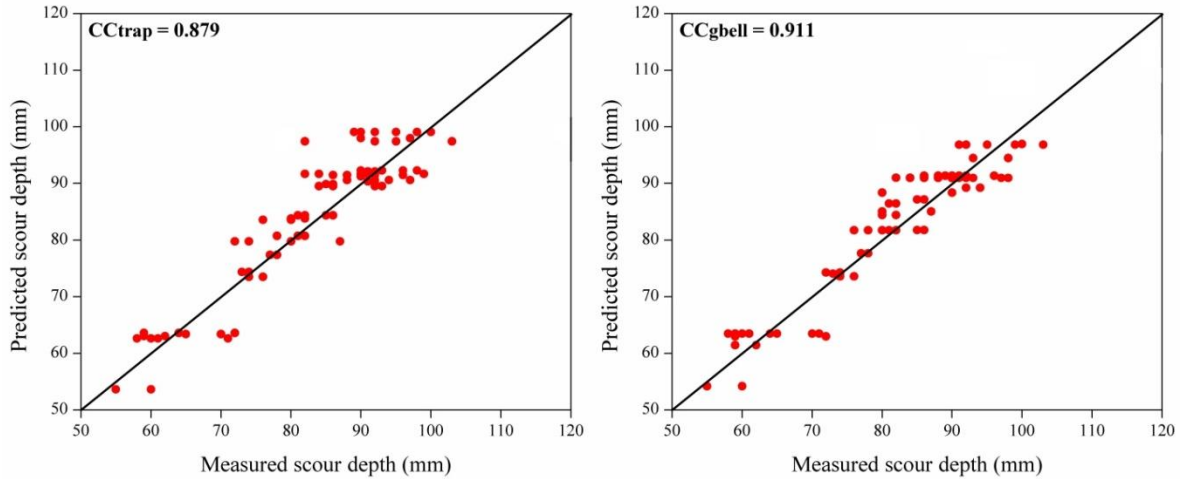


Figure 4.15 Scatter plots of ANFIS models in testing phase for sharp nosed pier in clear water scour condition

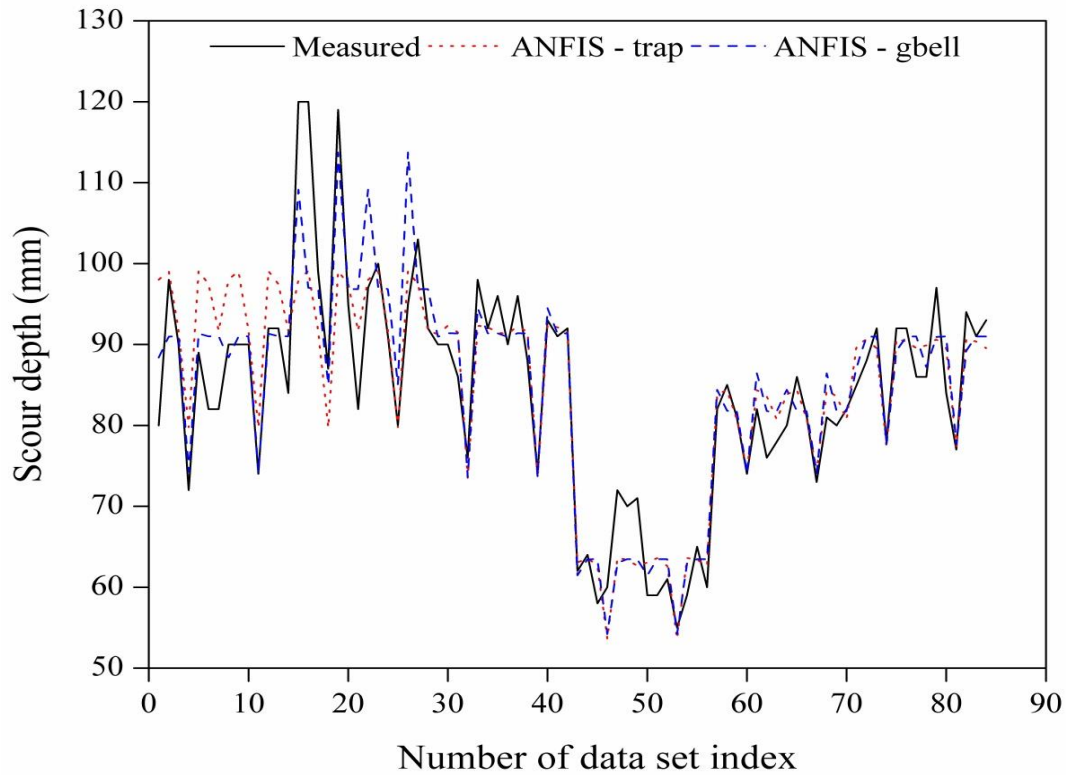


Figure 4.16 Comparison of measured and ANFIS model results in testing phase for sharp nosed pier in clear water scour condition

The scour depth around four different shapes of pier are predicted using ANFIS with trapezoidal and gbell MF. The results obtained from the developed models are tabulated in Table 4.2 in the form of statistical indices. The scatter and comparison plots are presented

against measured and predicted results during testing condition. From the Table 4.2, it is clear that, ANFIS with gbell MF performing well with all the four pier shapes compared to trapezoidal MF. The ANFIS gbell MF shows better prediction with circular pier case among the other three pier shapes.

4.2.3 Performance of a hybrid Particle Swarm Optimized Support Vector Machine (PSO-SVM) in the prediction of scour depth.

The particle swarm technique is used to optimize the kernel parameters of SVM model. The theoretical concept of PSO is explained in section 3.3.4. The model development and flowchart for the PSO-SVM is shown in section 3.4.3. The optimal parameters obtained by optimization process by a hybrid model are tabulated in Table 3.5. Statistical measures computed using the predicted and measured scour depth of training and testing data for the hybrid PSO-SVM models are listed in Table.4.3. The PSO-SVM models with linear, polynomial and RBF kernel functions are used in the prediction. The results of PSO-SVM with linear and polynomial kernel functions are tabulated in Table 4.3. The predicted results are compared with experimental values.

Table 4.3 Results of PSO-SVM model for clear water scour condition

Pier shape	Statistical indices	PSO-SVM Model			
		Linear		Polynomial	
		Train	Test	Train	Test
Circular	CC	0.882	0.881	0.953	0.950
	NRMSE	10.64	11.10	6.84	7.47
	NSE	0.776	0.773	0.907	0.897
	NMB	0.006	-0.003	0.0003	-0.009
Rectangular	CC	0.819	0.810	0.919	0.915
	NRMSE	13.03	13.001	8.96	9.01
	NSE	0.661	0.653	0.840	0.834
	NMB	0.016	0.003	0.007	0.002
Round nosed	CC	0.863	0.878	0.945	0.950

	NRMSE	11.24	11.25	7.14	7.31
	NSE	0.733	0.765	0.890	0.901
	NMB	0.015	-0.012	0.004	-0.01
Sharp nosed	CC	0.823	0.815	0.904	0.922
	NRMSE	11.79	12.09	9.04	8.08
	NSE	0.672	0.653	0.807	0.845
	NMB	-0.008	0.0015	-0.014	0.007

The PSO-SVM with linear and polynomial kernel functions is used to predict the scour depth around circular pier. The model predicted results are tabulated in table 4.3. The scatter and comparison plots are presented against measured and predicted values during testing phase. The statistical measures from the Table 4.3 implies that, PSO-SVM with polynomial kernel function performing well with higher CC=0.950, NSE=0.897 and lower NRMSE=7.47 in testing phase compared to linear kernel function with CC=0.881, NSE=0.773 and NRMSE=11.10. The NMB values from the Table 4.3 indicates that, PSO-SVM model is performing under prediction during testing and over prediction during training for both the kernel functions. The scatter and comparison plots are presented against measured and predicted values during testing phase as shown in Figure 4.17 and 4.18.

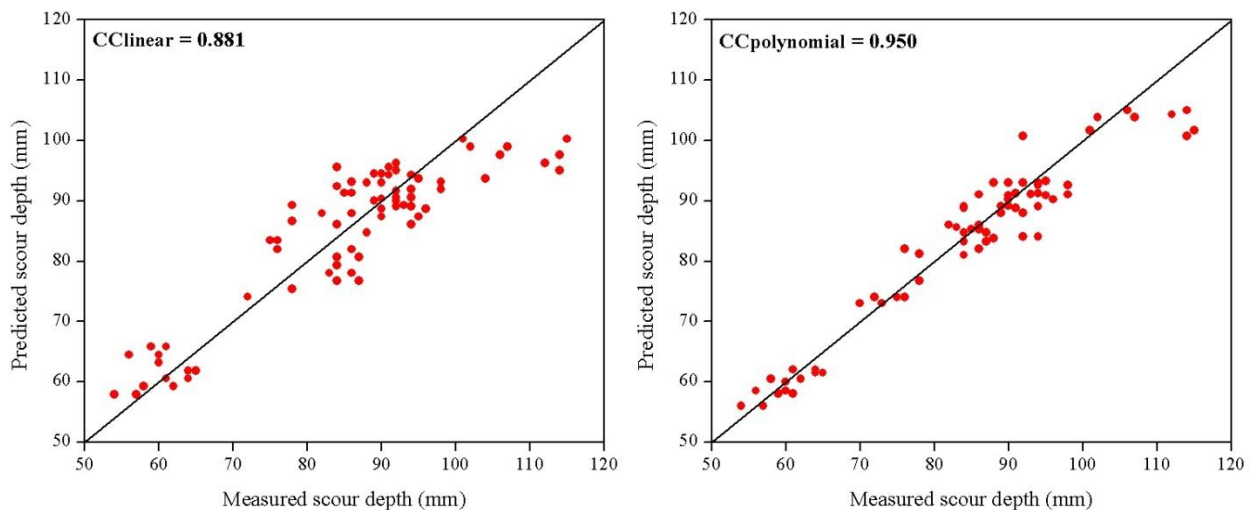


Figure 4.17 Scatter plots of PSO-SVM models in testing phase for circular pier in clear water scour condition

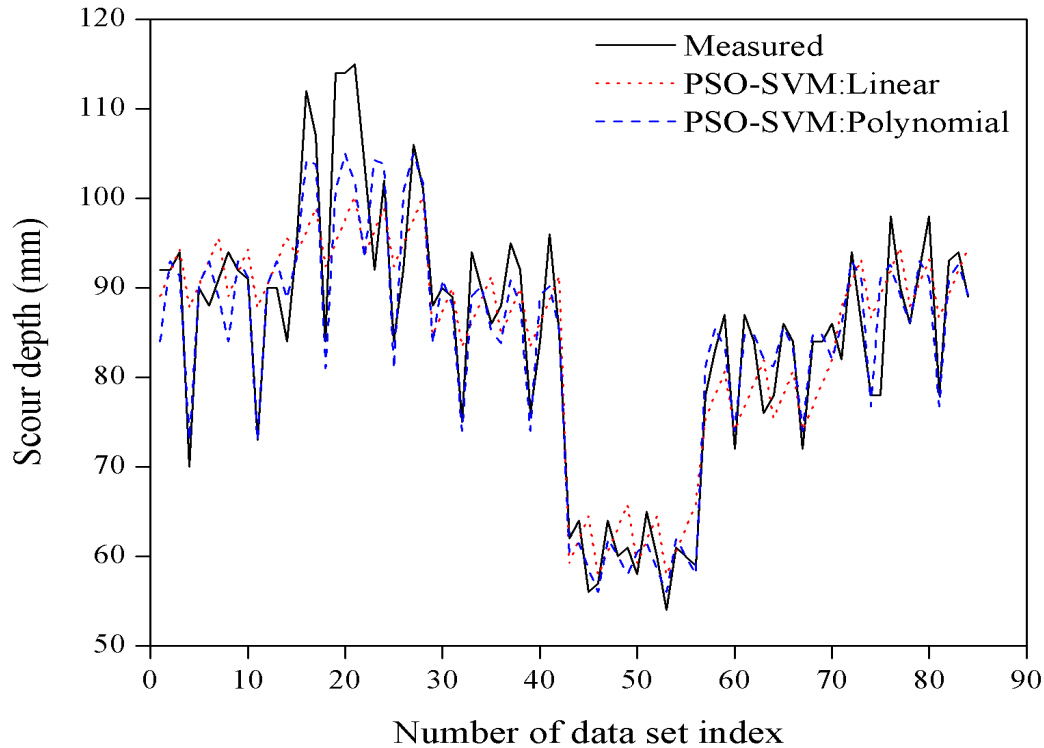


Figure 4.18 Comparison of measured and PSO-SVM model results in testing phase for circular pier in clear water scour condition

The rectangular shaped pier is considered to predict the scour depth around the pier. The PSO-SVM models are developed with linear and polynomial kernel functions and the results are tabulated in Table 4.3. From the Figure 4.19, it is clear that, polynomial kernel function shows good correlation with $CC=0.915$ compared to linear kernel function with $CC=0.810$. The comparison plots of measured and predicted values are drawn in figure 4.20. The positive NMB values from the Table 4.3 indicates that, the models are performing over prediction in both training and testing phase with linear and polynomial kernel functions.

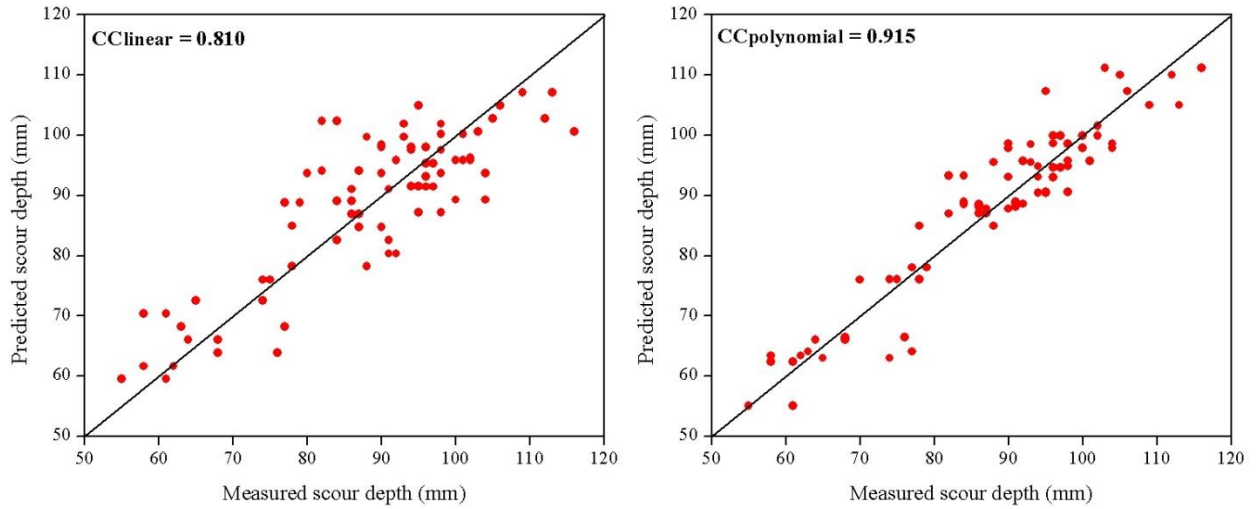


Figure 4.19 Scatter plots of PSO-SVM models in testing phase for rectangular pier in clear water scour condition

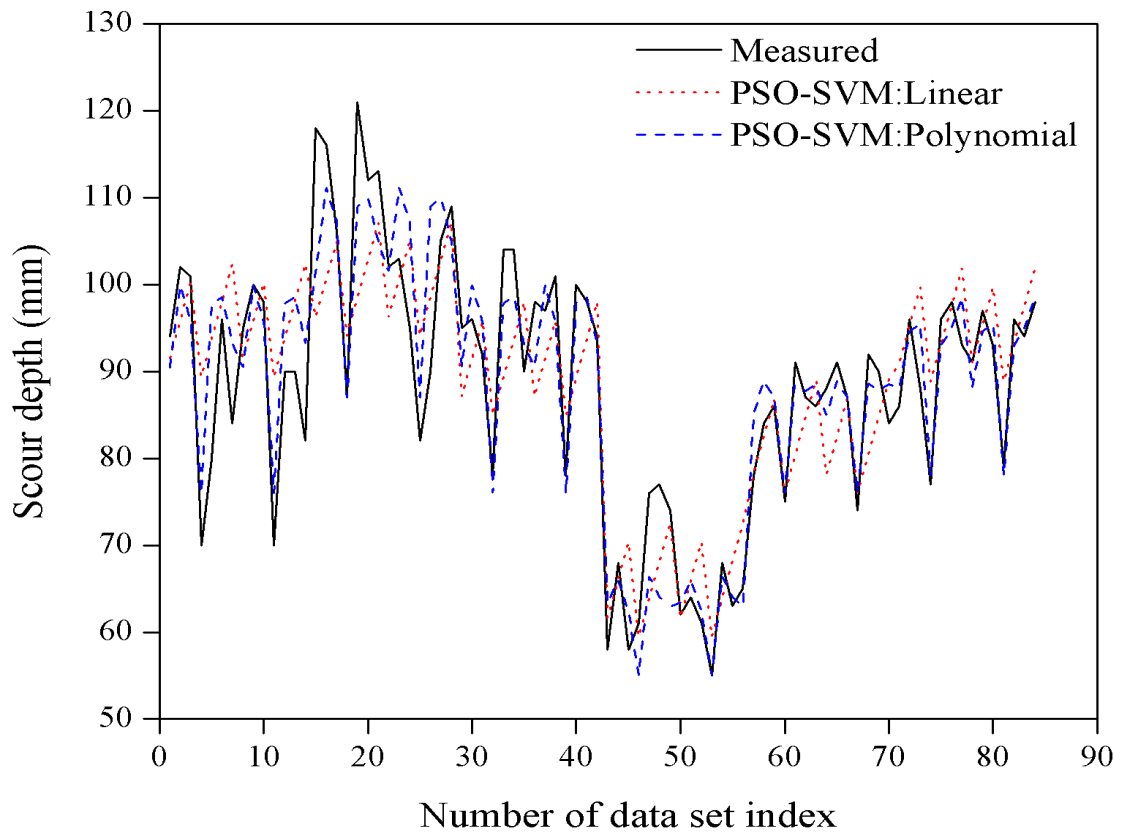


Figure 4.20 Comparison of measured and PSO-SVM model results in testing phase for rectangular pier in clear water scour condition

The PSO-SVM with linear and polynomial kernel functions are used to predict the scour depth around round nosed pier. The model results are tabulated in Table 4.3 in terms of statistical measures. Table 4.3 shows that, the PSO-SVM with polynomial kernel function gives better results with higher NSE=0.890 for training and 0.901 for testing compared to linear kernel function of NSE=0.733 for training and 0.765 for testing. From Figure 4.21, it is clear that, PSO-SVM performs well with polynomial kernel function (CC=0.950) compared to linear kernel function (CC=0.878). The Figure 4.21 shows the comparison of measured and predicted scour depth for testing phase.

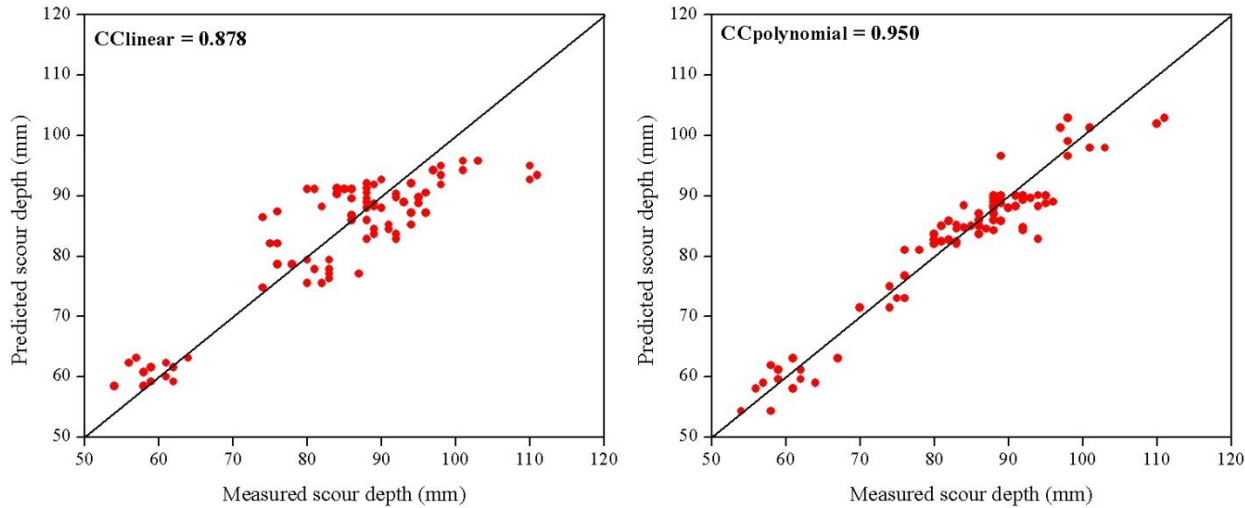


Figure 4.21 Scatter plots of PSO-SVM models in testing phase for round nosed pier in clear water scour condition

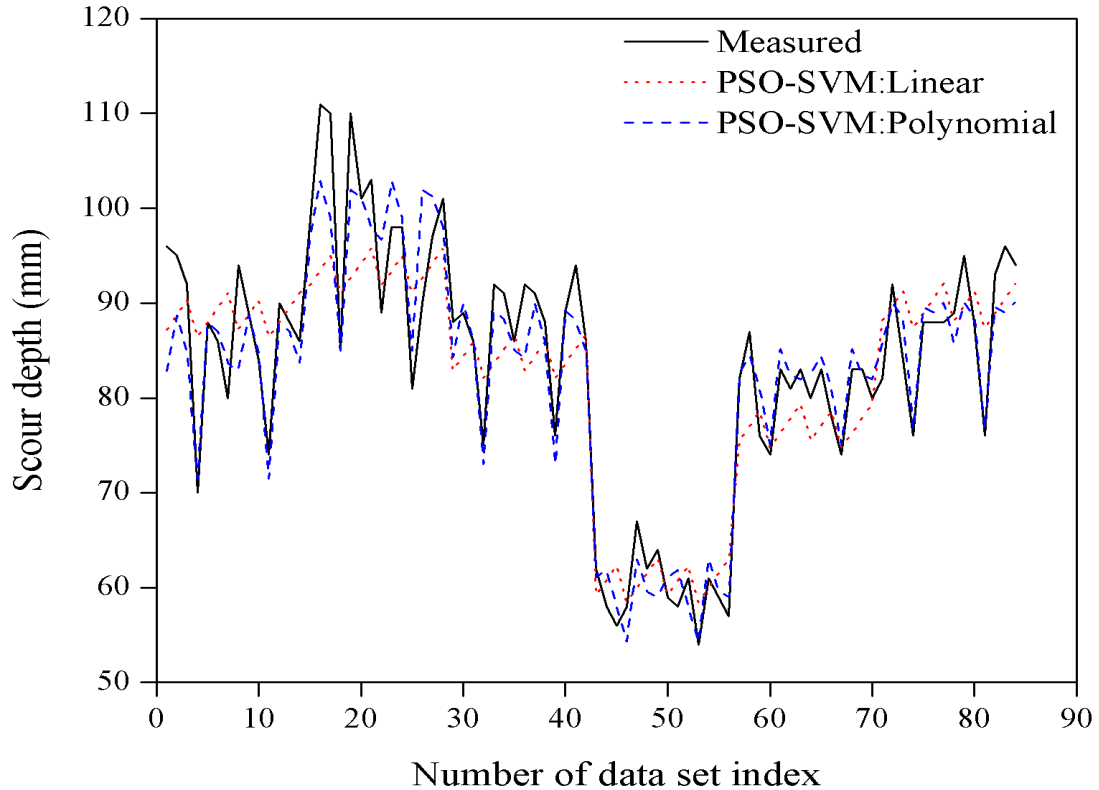


Figure 4.22 Comparison of measured and PSO-SVM model results in testing phase for round nosed pier in clear water scour condition

The scour depth around sharp nosed pier is predicted using PSO-SVM with linear and polynomial kernel functions. The predicted results are plotted against measured values as shown in Figure 4.23 as scatter plots. The Figure 4.24 shows the comparison between model result and experimental values and clears that, the PSO-SVM with polynomial kernel function giving good correlation with the measured values. The statistical results obtained from the models are tabulated in Table 4.3. The results shows that, the PSO-SVM with polynomial kernel function are in good agreement with measured values compared to linear kernel functions. The NMB values from the Table 4.3 indicate that, model is performing under prediction during training and over prediction during testing for both the kernel functions.

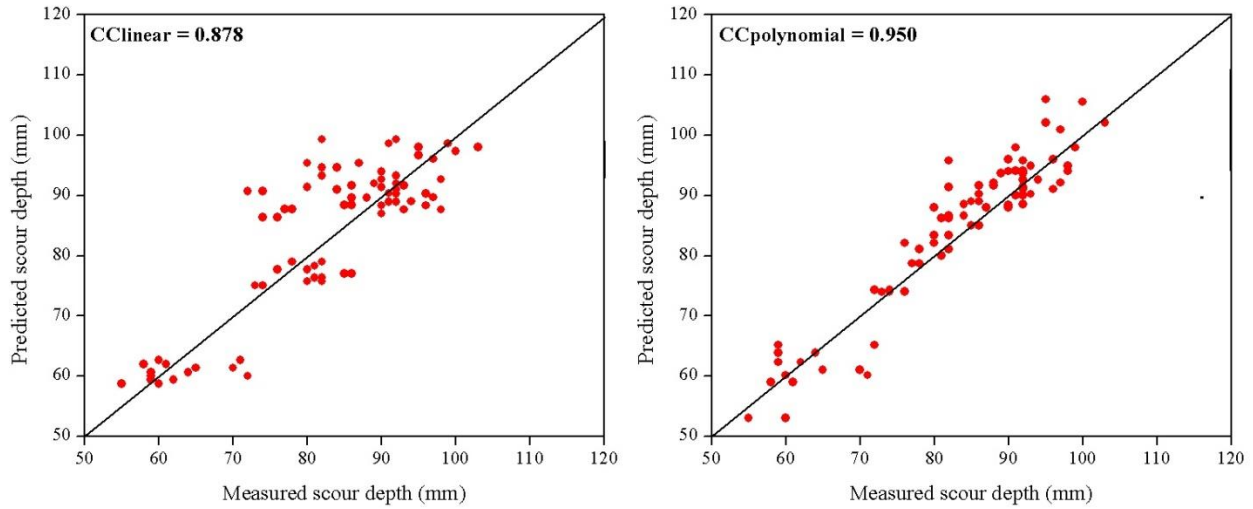


Figure 4.23 Scatter plots of PSO-SVM models in testing phase for sharp nosed pier in clear water scour condition

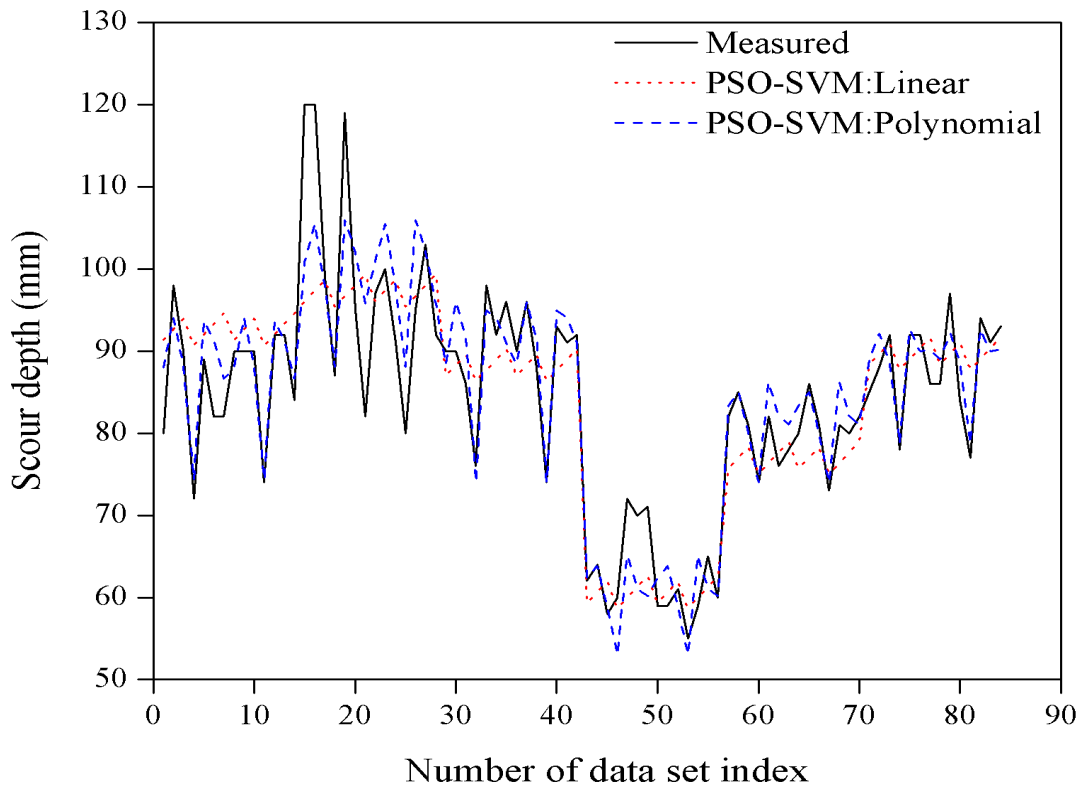


Figure 4.24 Comparison of measured and PSO-SVM model results in testing phase for sharp nosed pier in clear water scour condition

The particle swarm based support vector machine is used to predict the scour depth around different shapes of bridge piers. The PSO-SVM with polynomial and linear kernel functions are used in the study. It is observed from the Table 4.3 that, the PSO-SVM with polynomial kernel functions performs well for all the four pier shapes compared to linear kernel functions. Meanwhile, the PSO-SVM model is shows better prediction for circular pier case among the other pier shapes.

4.2.4 Performance of Artificial Neural Network (ANN) and Particle Swarm Optimized Neural Network (PSO-ANN) model for the prediction of scour depth.

The ANN models are developed using different hidden neurons and the ANN with 2 hidden neuron model shows good agreement and the statistical performance of the same are listed in the Table 4.4. The ANN results are compared with PSO-ANN models. The PSO is combined with neural networks to overcome the drawbacks of an individual ANN model. The FFBP neural network is tuned with particle swarm optimization (PSO-ANN) to predict the scour depth around the pier. The methodology to develop the PSO-ANN model is explained in 3.4.4. The optimal parameters of PSO-ANN model are shown in Table.3.6. The model results are compared with experimental values and same are discussed below. The results of PSO-ANN model in terms of statistical measures are tabulated in Table 4.4 for both training and testing phase. The scatter and comparison plots are presented for testing results of the model developed. The PSO-ANN models are showing good correlation compared to ANN models in terms of statistical parameters and the PSO-ANN results are discussed in this section.

Table 4.4 Results of ANN and PSO-ANN model for clear water scour condition

Pier shape	Statistical indices	ANN Model		PSO-ANN Model	
		Train	Test	Train	Test
Circular	CC	0.915	0.90	0.934	0.925
	NRMSE	12.26	12.93	8.05	8.855
	NSE	0.702	0.69	0.872	0.855
	NMB	-0.034	-0.037	0.0009	-0.002
Rectangular	CC	0.848	0.830	0.890	0.868

	NRMSE	13.04	13.23	10.23	11.023
	NSE	0.66	0.638	0.791	0.751
	NMB	0.01	0.005	-0.001	-0.006
Round nosed	CC	0.906	0.890	0.921	0.932
	NRMSE	11.76	11.96	8.48	8.51
	NSE	0.708	0.734	0.848	0.865
	NMB	0.012	0.002	0.00	-0.009
Sharp nosed	CC	0.865	0.860	0.916	0.890
	NRMSE	12.35	12.46	9.56	9.55
	NSE	0.650	0.643	0.785	0.783
	NMB	0.08	0.095	-0.0005	0.007

The particle swarm optimization tuned neural network model is utilized for the prediction of scour depth around different shapes of bridge pier in clear water scour condition. The obtained model results are analyzed in terms of statistical measures and tabulated in Table 4.4. The Table 4.4 shows that, the PSO-ANN performs well for circular and round nosed pier shapes with higher CC, NSE and lower NRMSE. The PSO-ANN model shows good performance for round nosed pier with higher CC=0.932, NSE=0.865 and lower NRMSE=8.51 compared to that of other pier shapes. The scatter plots and comparison plots are drawn to study the correlation between the measured and predicted values during testing as shown in Figure 4.25- for circular pier, Figure 4.27 for rectangular pier, Figure 4.29 for round nosed pier and Figure 4.31 for sharp nosed pier. The comparison plots, Figure 4.26, 4.28, 4.30 and 4.32 are drawn to study the variation between measured and predicted results.

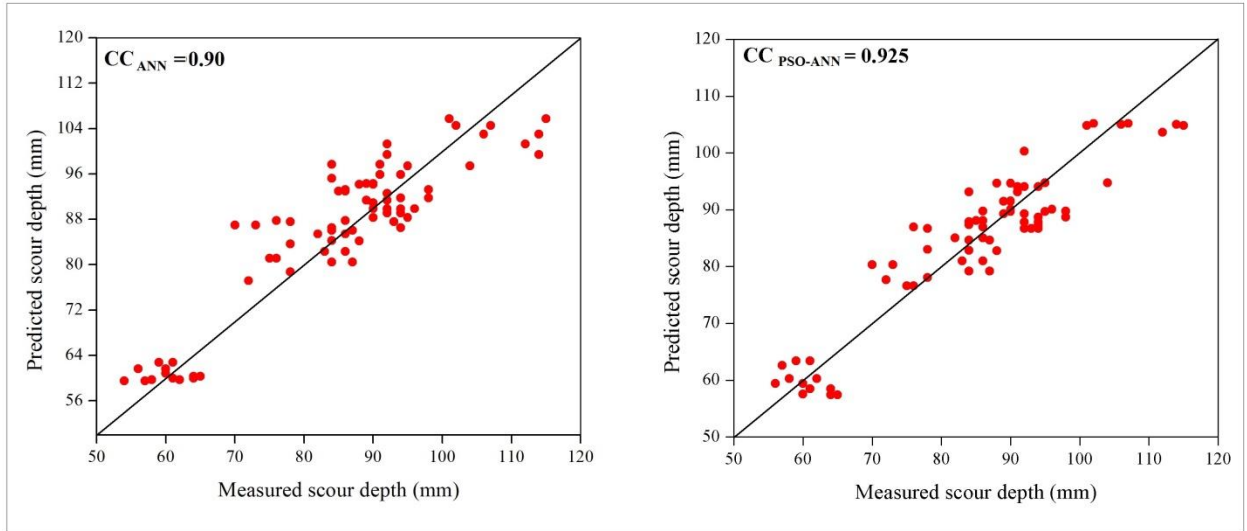


Figure 4.25 Scatter and line plots of ANN and PSO-ANN models in testing phase for circular pier in clear water scour condition

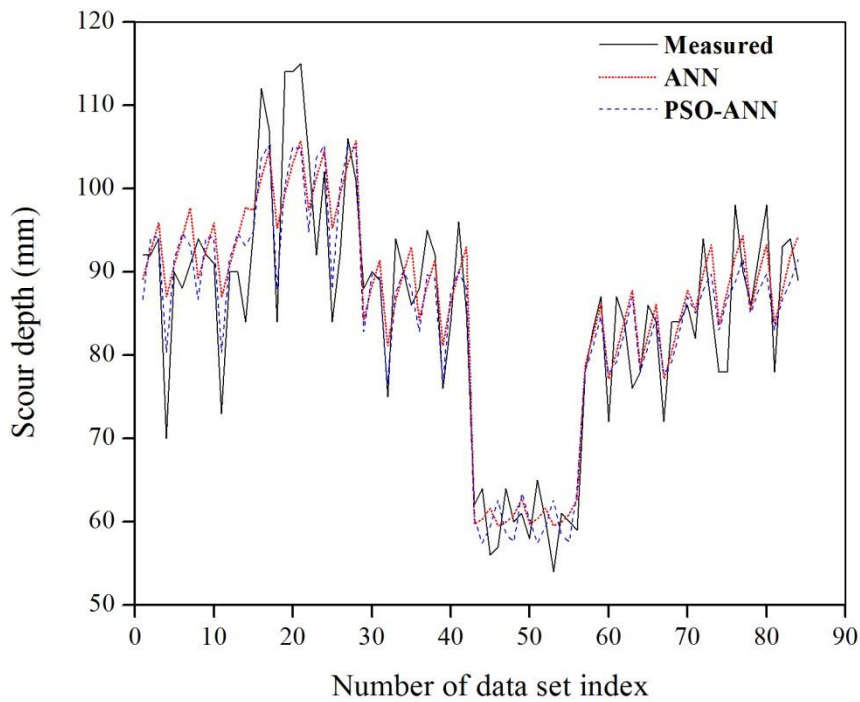


Figure 4.26: Comparison of measured, ANN and PSO-ANN model results in testing phase for circular pier in clear water scour condition

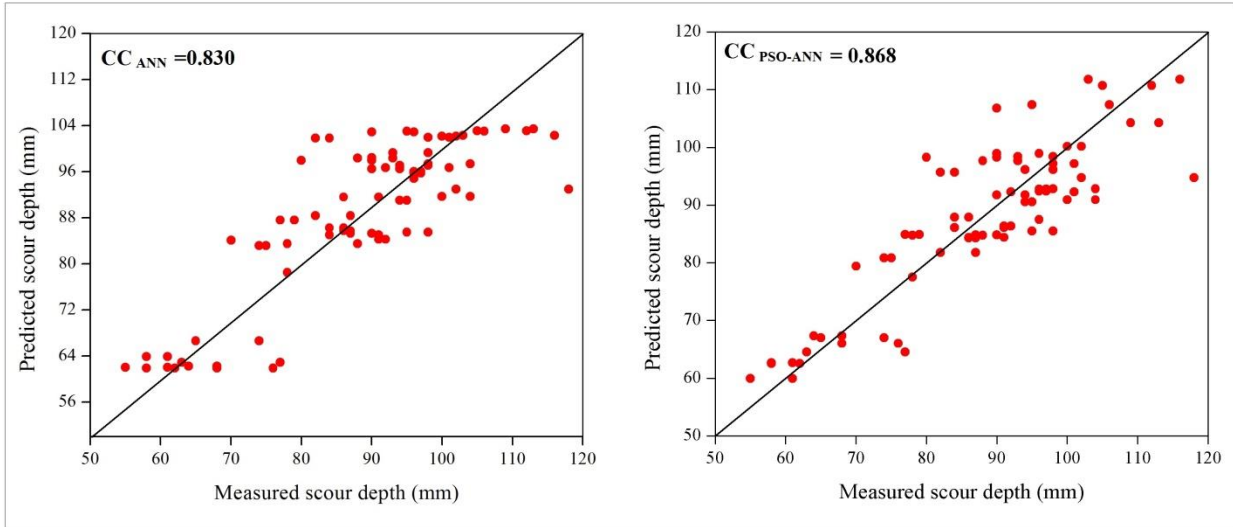


Figure 4.27 Scatter and line plots of ANN and PSO-ANN models in testing phase for rectangular pier in clear water scour condition

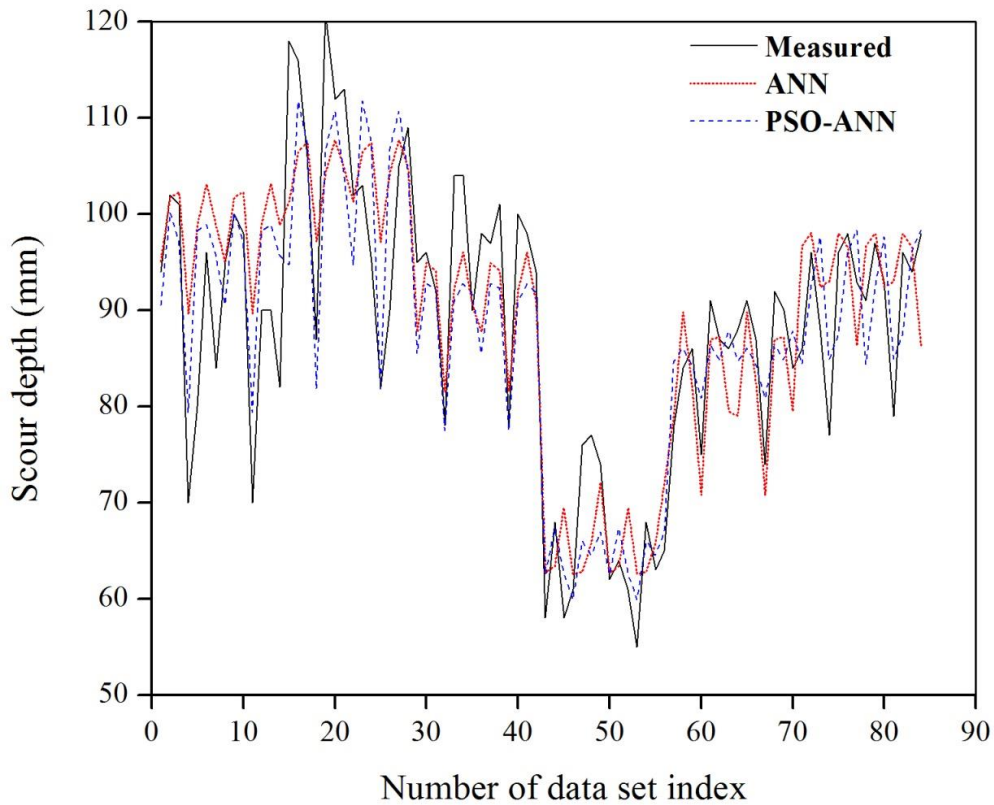


Figure 4.28: Comparison of measured, ANN and PSO-ANN model results in testing phase for rectangular pier in clear water scour condition

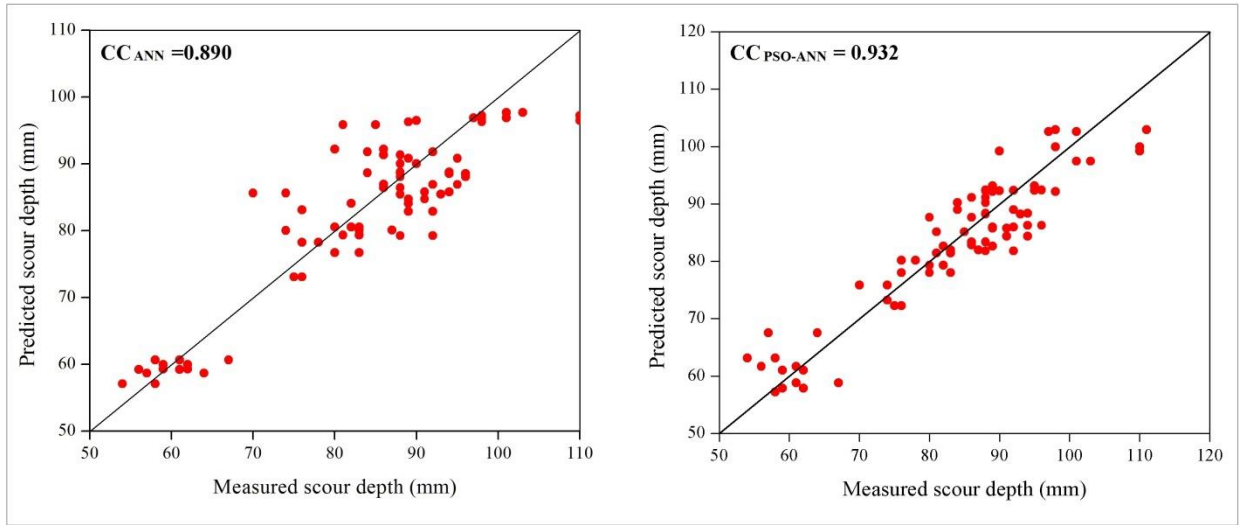


Figure 4.29 Scatter and line plots of ANN and PSO-ANN models in testing phase for round nosed pier in clear water scour condition

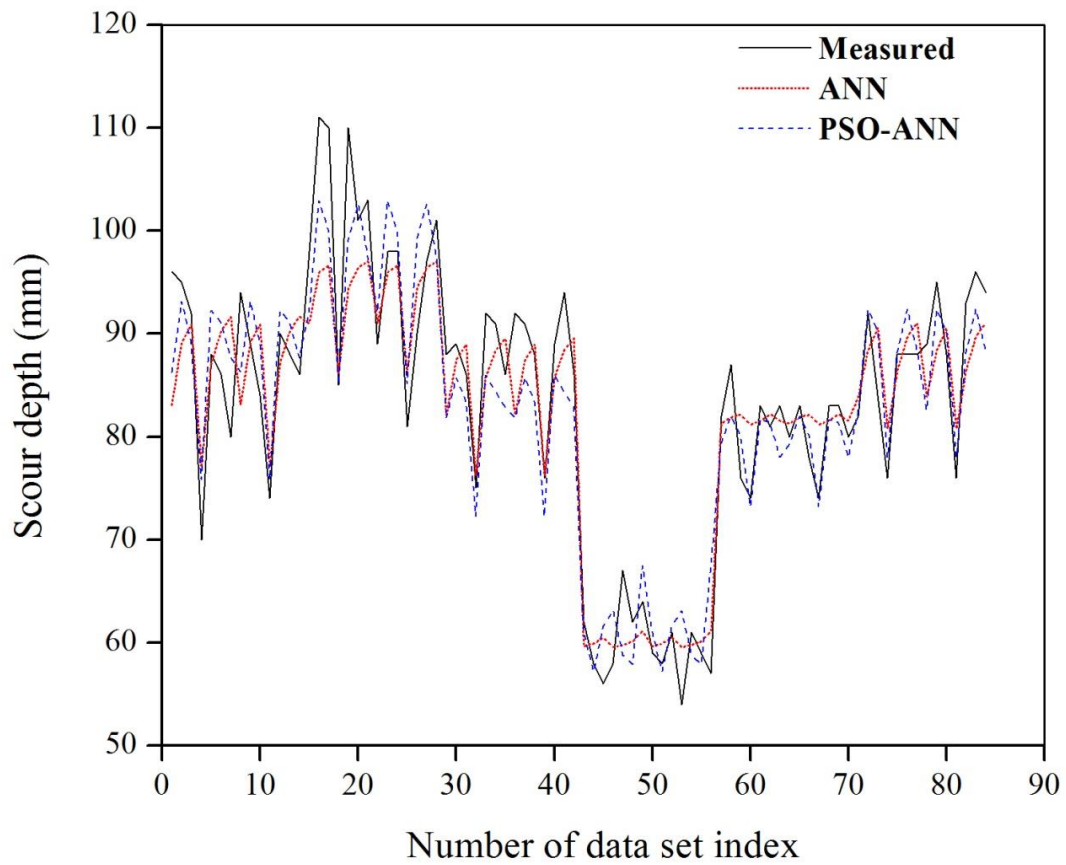


Figure 4.30: Comparison of measured, ANN and PSO-ANN model results in testing phase for round nosed pier in clear water scour condition

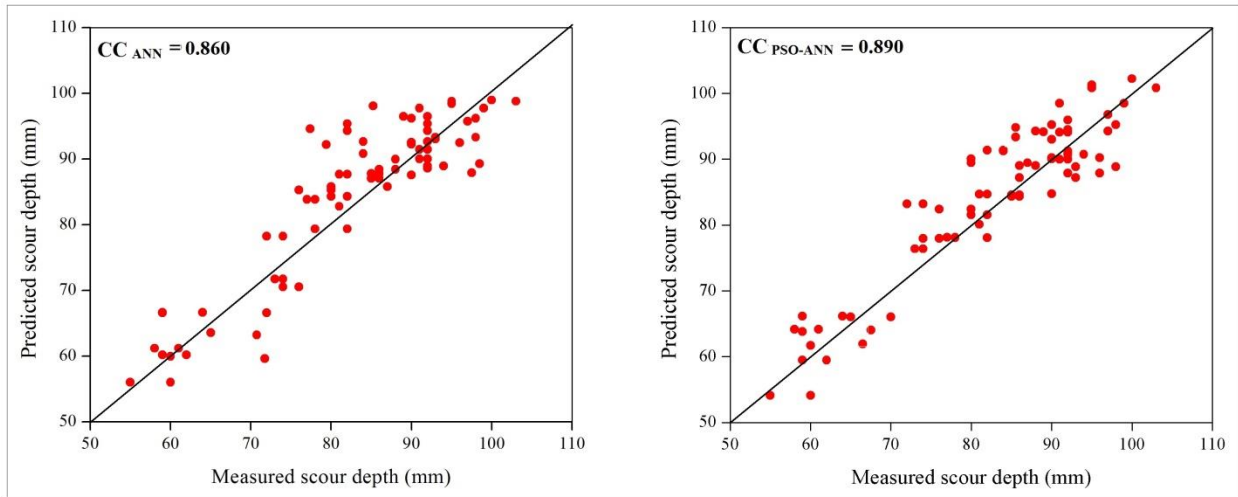


Figure 4.31 Scatter and line plots of PSO-ANN models in testing phase for sharp nosed pier in clear water scour condition

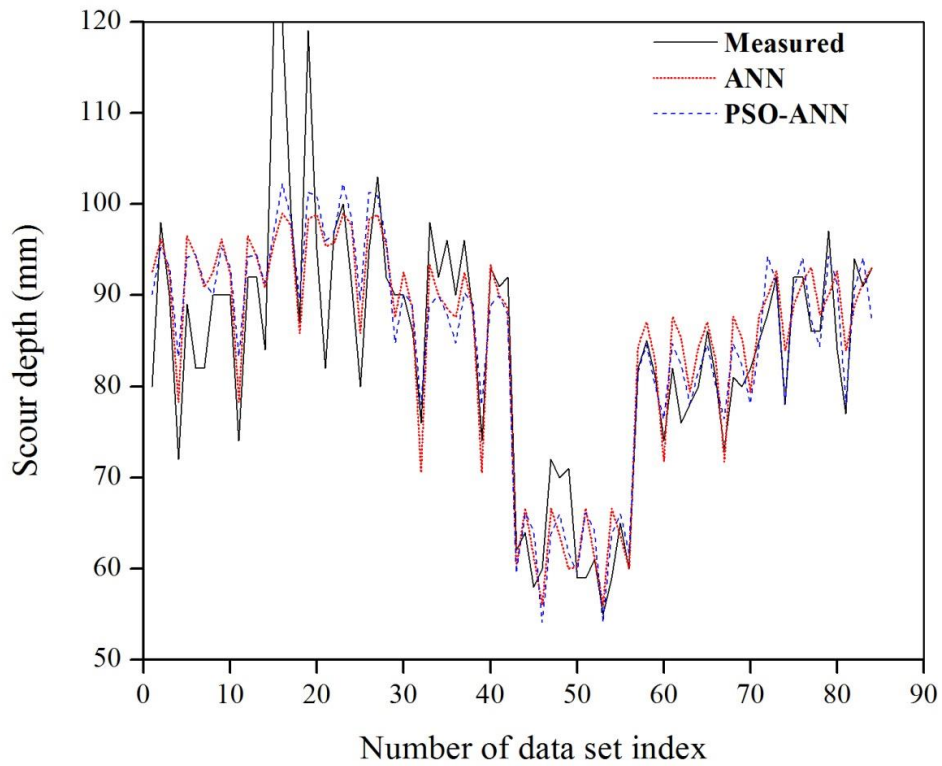


Figure 4.32: Comparison of measured, ANN and PSO-ANN model results in testing phase for sharp nosed pier in clear water scour condition

4.2.5 Comparative study

To select the most accurate model among ANN, SVM, ANFIS, PSO-SVM and PSO-ANN developed for predicting the scour depth around different pier shapes in clear water scour condition. The results obtained from both train and test conditions for all the performance indicators by all the models are listed in Table 4.1, 4.2, 4.3 and 4.4. The performance of the models are evaluated using the different model performance indices such as, correlation coefficient (CC), normalized root-mean-square error (NRMSE), normalized mean bias (NMB) and Nash–Sutcliffe coefficient error (NSE). Figure 4.33 is the comparison plots drawn with measured values and predicted results among the best models during testing phase. From the Figure 4.33, it is clear that, the ANFIS with gbell MF and PSO-SVM with polynomial kernel function are showing good prediction in clear water scour condition compared to other models.

The Box–Whisker plot are plotted to represent the spread of predicted values as shown in Figure 4.34. A skeletal type of box-and-whisker plot with standard error is considered to evaluate the performance of the models by checking distribution of data points. From the box plot it is clear that, the PSO-SVM model shows comparatively similar performance with the measured values.

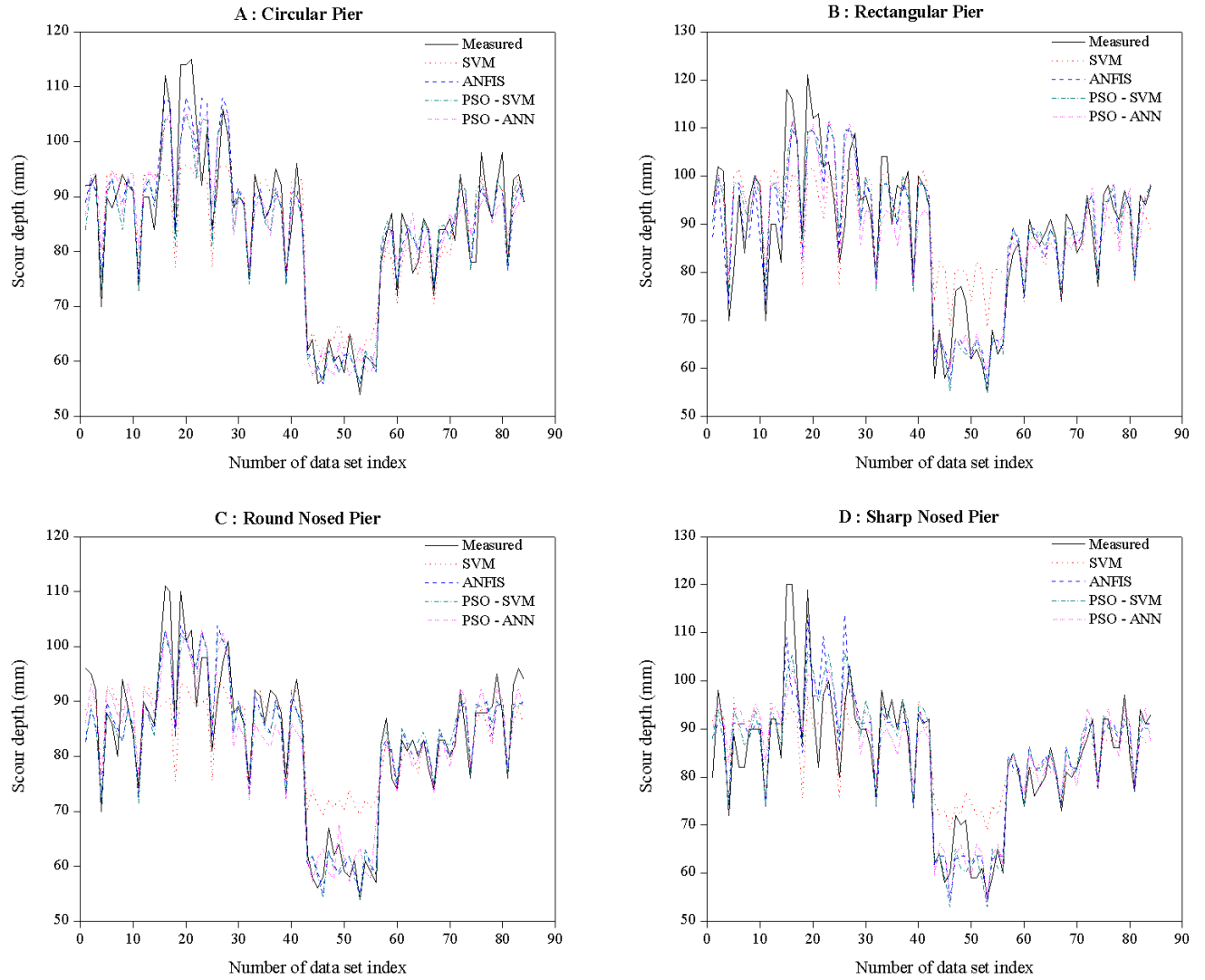


Figure 4.33 Comparison plots in testing phase for clear water scour condition

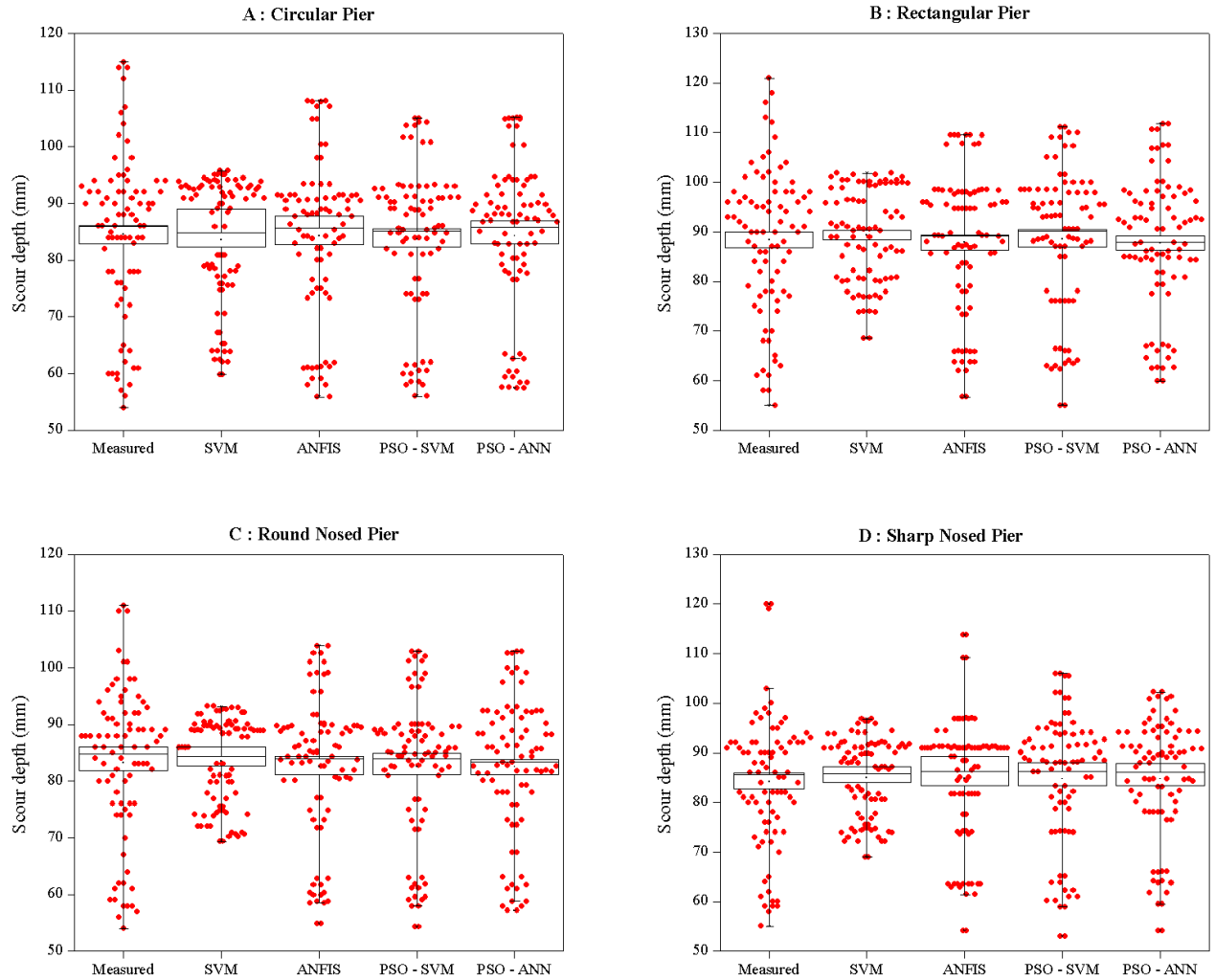


Figure 4.34 Box plots in testing phase for clear water scour condition

The statistical measures such as NRMSE, NSE and NMB are used to analyze the model performance. NRMSE values from the Figure 4.35 shows that, both ANFIS and PSO-SVM predicts well with lower NRMSE for all the four pier shapes. From the NSE value, the PSO-SVM and ANFIS is giving good prediction in testing phase as shown in Figure 4.36. The NMB values from the Figure 4.37 shows that, most of the models are over predicting during training and under predicted during testing phases. The ANFIS model performed comparatively better in terms of NMB as compared with other models in both the training and testing phases.

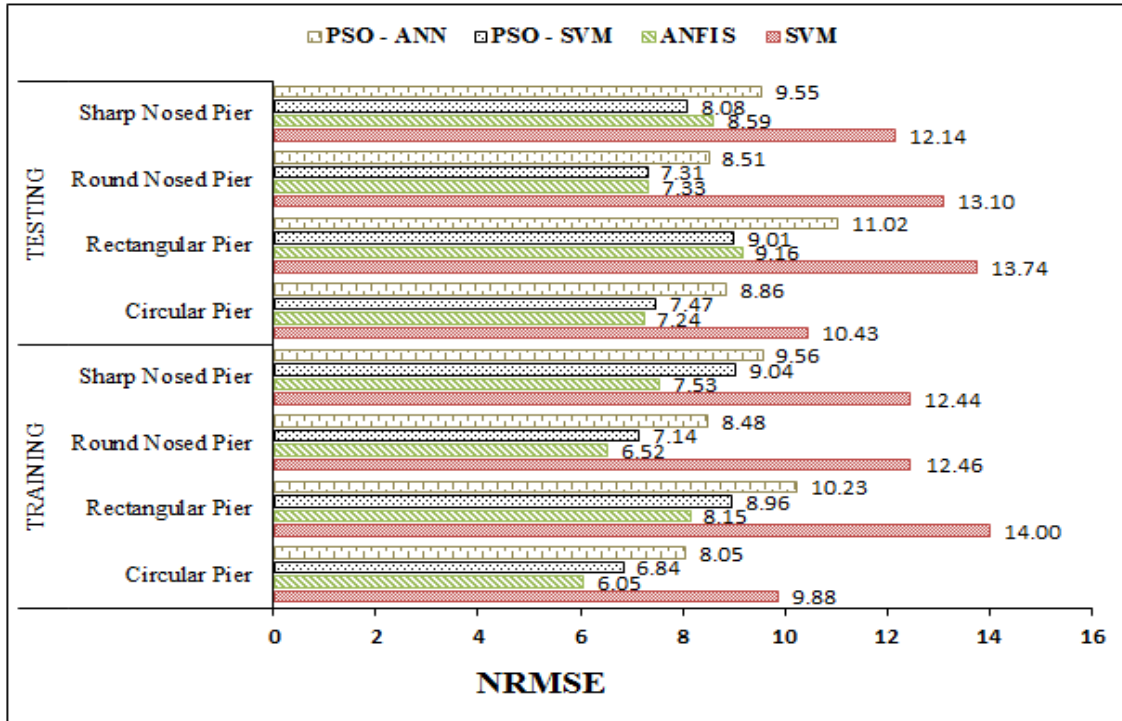


Figure .4.35 NRMSE of all the models for clear water scour condition.

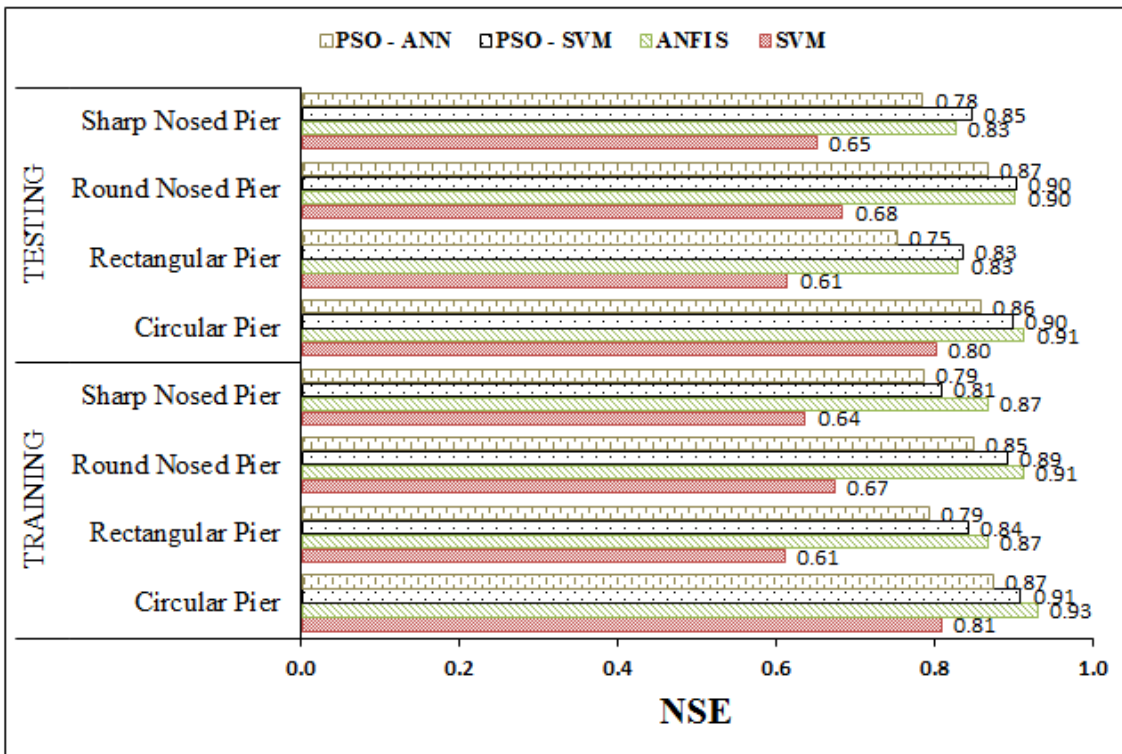


Figure .4.36 NSE of all the models for clear water scour condition.

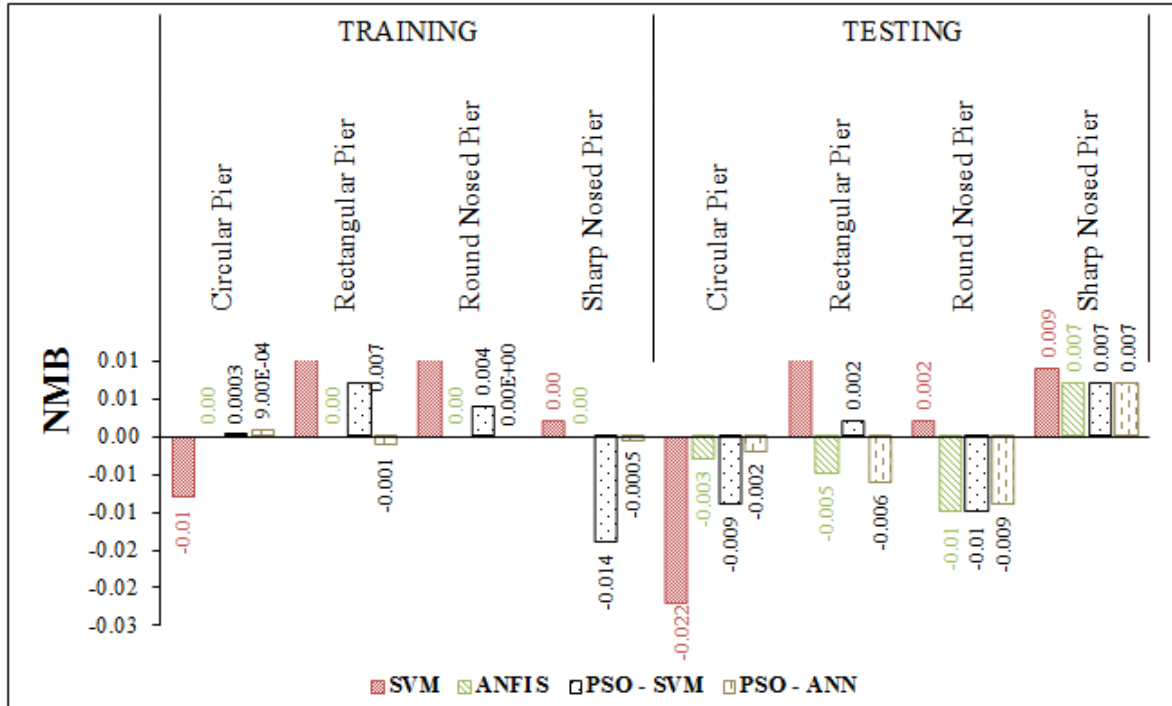


Figure 4.37 NMB of all the models for clear water scour condition.

4.3 Prediction of Scour Depth around Bridge Pier for Live Bed Scour Condition

Live bed scour is another type of scour condition; in this case there is a sediment supply from the upstream flow to the scour hole. The live bed scour condition is normally occurs during the flooding case. The scour depths around different shapes of bridge piers are predicted under live bed scour condition are discussed below. The sediment quantity (ppm), velocity and time are the input parameters used to predict the scour depth as output parameter. The statistical parameters such as max, min, standard deviation and kurtosis of the data set used in the study are tabulated in Table 3.2. The soft computing techniques such as ANN, SVM, ANFIS, PSO-SVM and PSO-ANN are used in the present study. The scour depth around circular, rectangular, round nosed and sharp nosed pier shapes are predicted separately in live bed scour condition and same are discussed in below sections.

4.3.1 Performance of Support Vector Machine (SVM) model in the prediction of scour depth.

The SVM models are developed with linear, RBF and polynomial kernel functions to predict the scour depth in live bed scour condition. The results obtained for the SVM with linear and RBF kernel functions are presented in the Table 4.5 in terms of statistical measures. The predicted results are compared with measured values and discussed in detail for different pier shapes separately in this section. The scatter and comparison plots are presented against measured and predicted results in testing phase.

Table 4.5 Results of SVM models for live bed scour condition

Pier shape	Statistical indices	SVM Model			
		Linear		RBF	
		Train	Test	Train	Test
Circular	CC	0.796	0.789	0.875	0.866
	NRMSE	17.89	17.18	13.844	13.86
	NSE	0.610	0.606	0.764	0.743
	NMB	0.015	0.012	-0.001	-0.004
Rectangular	CC	0.854	0.843	0.928	0.903
	NRMSE	17.07	19.51	10.00	13.04
	NSE	0.59	0.588	0.86	0.816
	NMB	0.04	0.04	0.000	-0.0015
Round nosed	CC	0.810	0.793	0.904	0.853
	NRMSE	17.09	17.62	11.21	13.35
	NSE	0.560	0.522	0.810	0.726
	NMB	-0.004	0.03	-0.004	-0.002
Sharp nosed	CC	0.810	0.839	0.880	0.899
	NRMSE	16.00	16.32	12.660	13.48
	NSE	0.638	0.701	0.77	0.796
	NMB	0.012	0.004	0.003	-0.006

The scour depth is predicted around circular pier using SVM with linear and RBF kernel functions. The results obtained from the models are tabulated in Table 4.5 and shows that, SVM with RBF kernel function model gives good performance with higher efficiency $NSE=0.743$ compared to the linear kernel function of $NSE=0.606$. A comparison using the scatter plots between measured and predicted values as shown in Figure 4.38 and 4.39 respectively. The NMB values from the Table 4.5 shows that, SVM with linear kernel function shows over prediction and SVM with RBF kernel function shows under prediction.

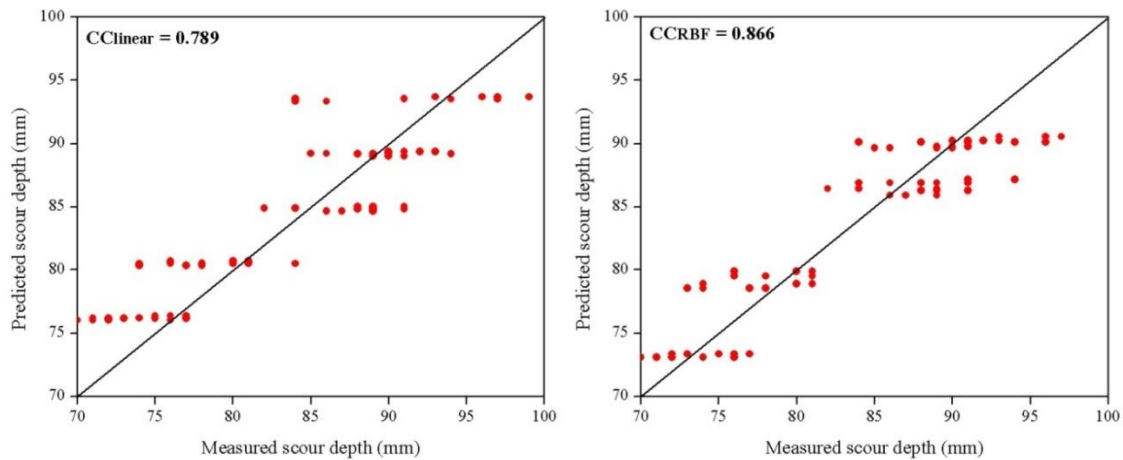


Figure 4.38 Scatter plots of SVM models in testing phase for circular pier in live bed scour condition

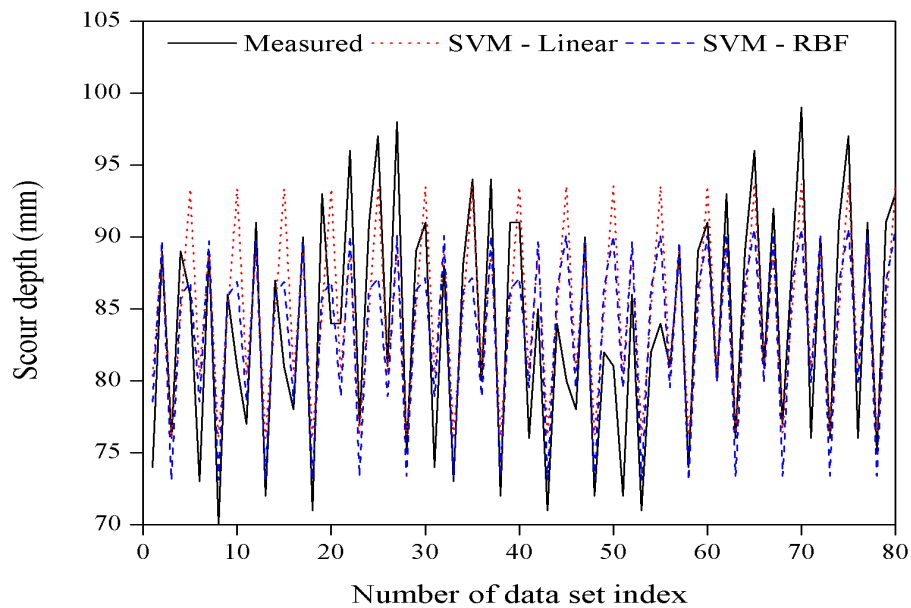


Figure 4.39 Comparison of measured and SVM model results in testing phase for circular pier in live bed scour condition

In case of, the scour depth prediction around the rectangular pier is done by using SVM with linear and RBF kernel functions. The statistical results from the Table 4.5 shows that SVM with RBF kernel function performing better with $NSE=0.816$ compared to linear kernel function with $NSE=0.588$. The scatter plot shows the correlation between measured and predicted results as shown in Figure 4.40. The Figure 4.41 gives the comparison with measured and predicted values.

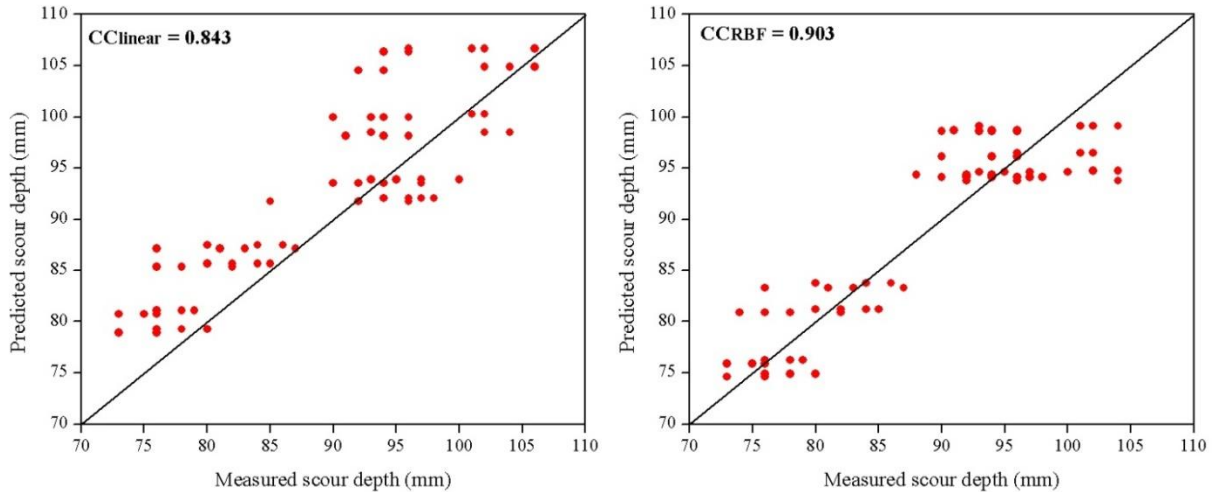


Figure 4.40 Scatter plots of SVM models in testing phase for rectangular pier in live bed scour condition

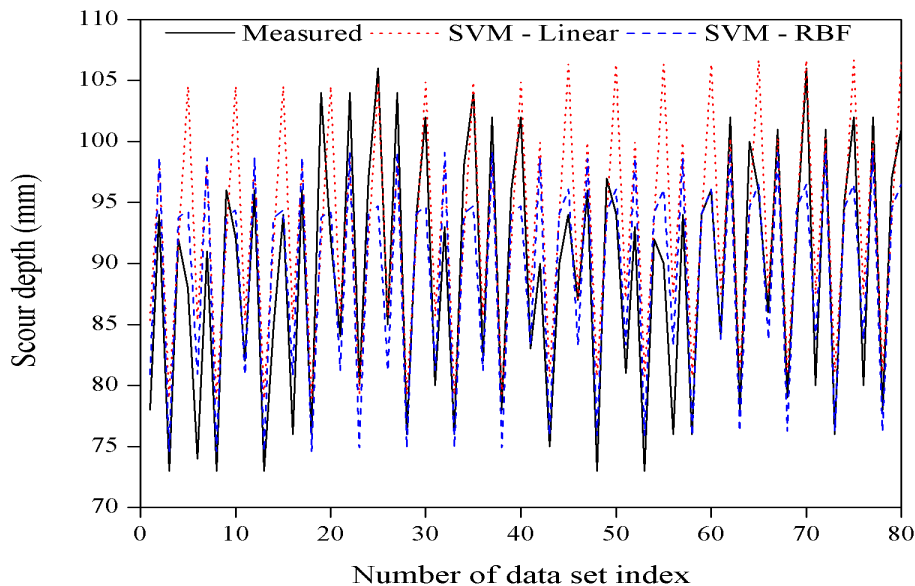


Figure 4.41 Comparison of measured and SVM model results in testing phase for rectangular pier in live bed scour condition

The Figure 4.42 shows the scatter plots of measured and predicted SVM model results for round nosed pier case. It is clear from the figure that, SVM with RBF kernel function performs better than SVM with linear kernel function in terms of CC (CC for linear=0.793 and CC for RBF = 0.853). The measured and predicted results are compared and plotted in Figure 4.43. The results of SVM model in terms of NSE, NRMSE and NMB for both the kernel functions are presented in Table 4.5.

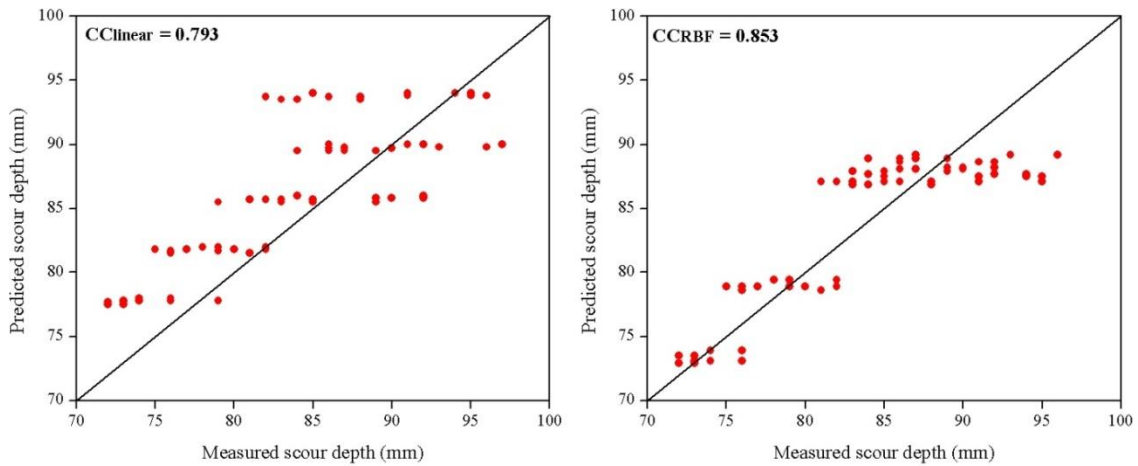


Figure 4.42 Scatter plots of SVM models in testing phase for round nosed pier in live bed scour condition

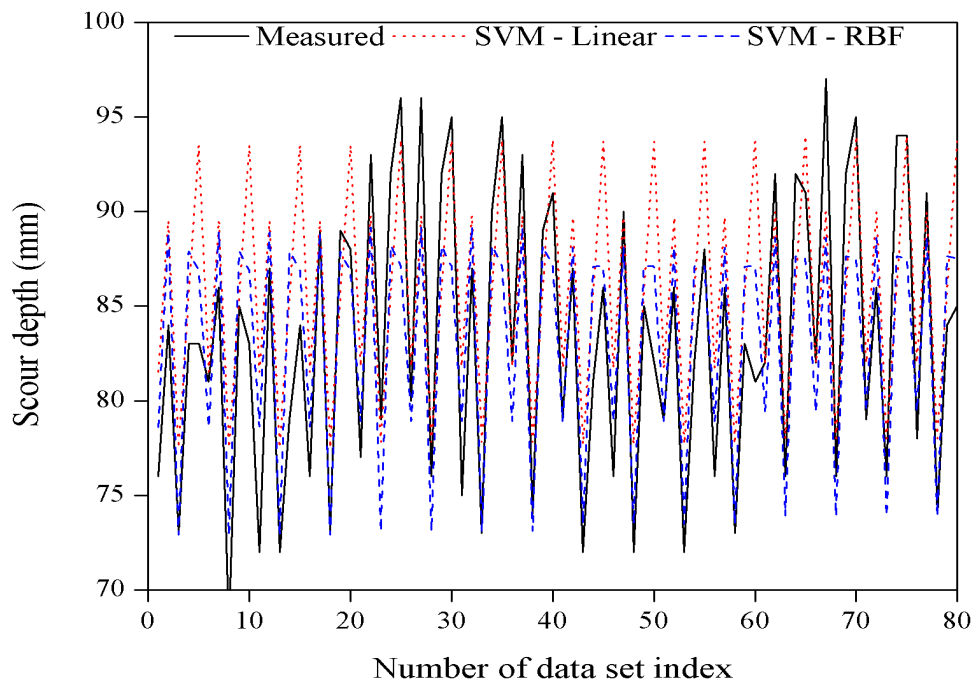


Figure 4.43 Comparison of measured and SVM model results in testing phase for round nosed pier in live bed scour condition

The sharp nosed pier is considered in this case to predict the scour depth using SVM model. The results of SVM model is tabulated in Table 4.5 for both training and testing phase. From the Table 4.5 it is clear that, the SVM with RBF kernel function gives good prediction in terms of lower NRMSE=13.48 compared to linear kernel function of NRMSE=16.32 during testing. The scatter and comparison plots are presented against measured and predicted results in Figure 4.44 and 4.45 respectively.

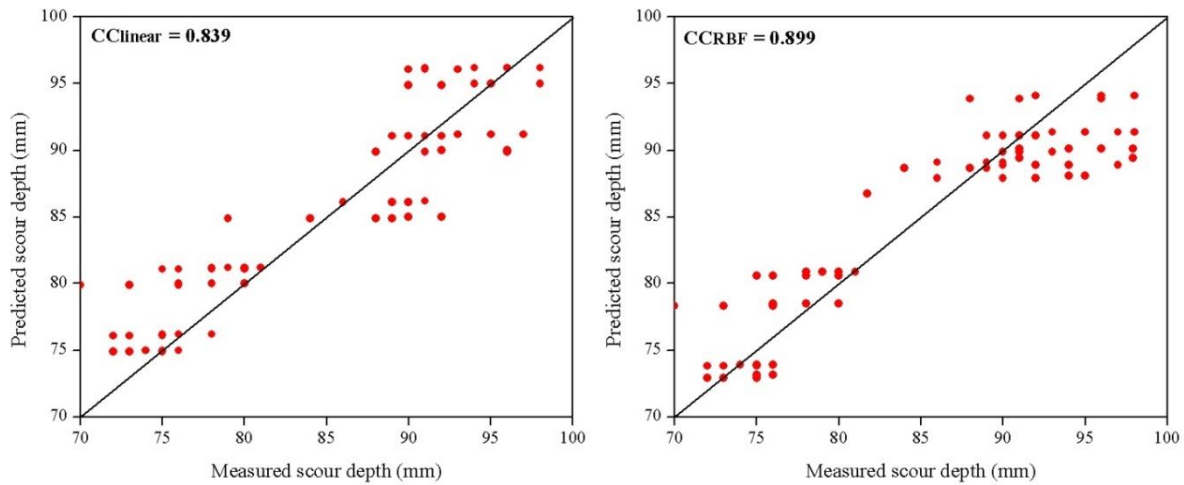


Figure 4.44 Scatter plots of SVM models in testing phase for sharp nosed pier in live bed scour condition

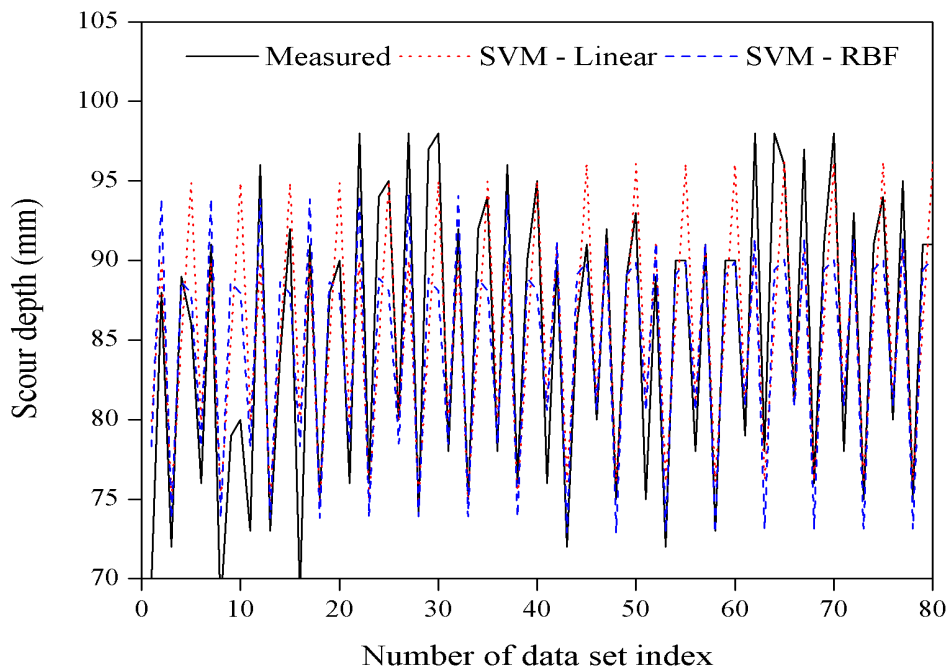


Figure 4.45 Comparison of measured and SVM model results in testing phase for sharp nosed pier in live bed scour condition

The SVM with linear and RBF kernel functions are used to predict the scour depth around different pier shapes in live bed scour condition. The predicted results are compared with measured values. The statistical results of the models are tabulated in Table 4.5. From the Table 4.5 it is observed that, SVM with RBF kernel function performed better in all four shapes compared to linear kernel function. Further, it is clear that, the SVM with RBF kernel function is predicting better particularly for rectangular pier shape in live bed scour condition.

4.3.2 Performance of Adaptive Neuro Fuzzy Inference System (ANFIS) model in the prediction of scour depth.

The ANFIS with trapezoidal and gbell MF is used to predict the scour depth around different pier shapes in live bed scour condition. The architecture of ANFIS for the better prediction is explained in section 3.4.2. The results obtained from the model are tabulated in Table 4.6 for both training and testing phase. The Scatter and comparison plots are presented between measured and predicted results in testing phase.

Table 4.6 Results of ANFIS models for live bed scour condition

Pier shape	Statistical indices	ANFIS Model			
		Trapezoidal		Gbell	
		Train	Test	Train	Test
Circular	CC	0.945	0.908	0.950	0.910
	NRMSE	9.257	11.48	8.997	11.37
	NSE	0.890	0.824	0.900	0.827
	NMB	0.00	-0.003	0.00	-0.003
Rectangular	CC	0.971	0.952	0.975	0.950
	NRMSE	6.37	9.31	5.98	9.72
	NSE	0.943	0.906	0.950	0.898
	NMB	0.00	-0.002	0.00	-0.002
Round nosed	CC	0.948	0.925	0.950	0.923
	NRMSE	8.13	9.67	8.01	9.829
	NSE	0.90	0.856	0.903	0.851

	NMB	0.00	0.002	0.00	0.002
Sharp nosed	CC	0.933	0.940	0.935	0.939
	NRMSE	9.583	10.723	9.397	10.82
	NSE	0.870	0.871	0.875	0.868
	NMB	0.00	-0.009	0.00	-0.009

The ANFIS model with trapezoidal and gbell MF is used to predict the scour depth around circular pier. The results of the model are tabulated in Table 4.6 and shows that, ANFIS with gbell MF shows good correlation (CC=0.910 for testing and CC=0.950 for training) compared to trapezoidal MF (CC=0.908 for testing and CC =0.945 for training). The scatter and comparison plots in Figure 4.46 and 4.47 are drawn against measured and predicted results. The NMB value from the Table 4.6 shows that, the model is performing under prediction during testing and over prediction during training for both the MF.

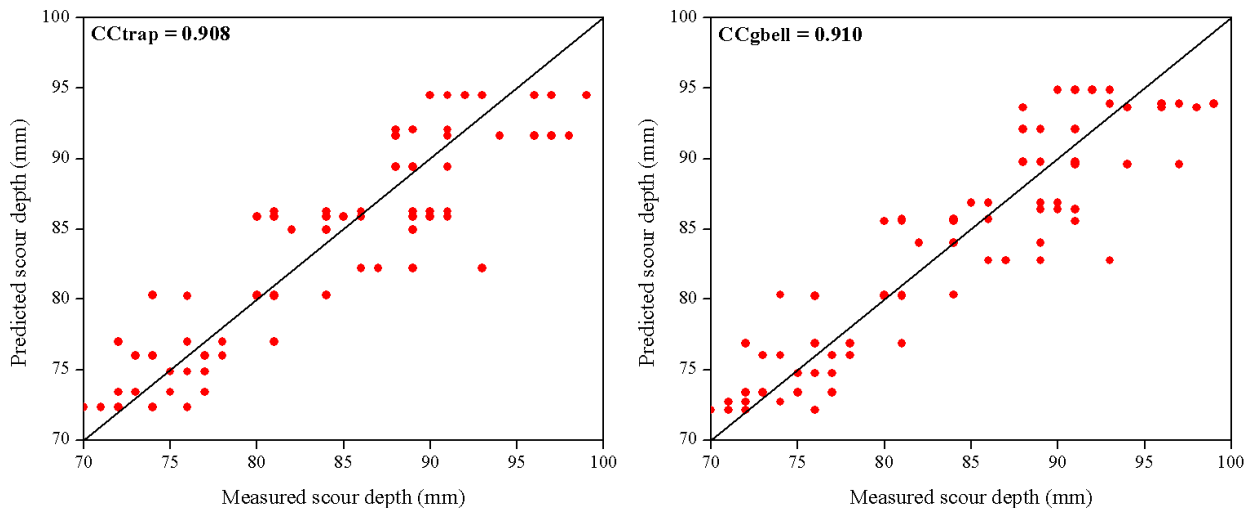


Figure 4.46 Scatter plots of ANFIS models in testing phase for circular pier in live bed scour condition

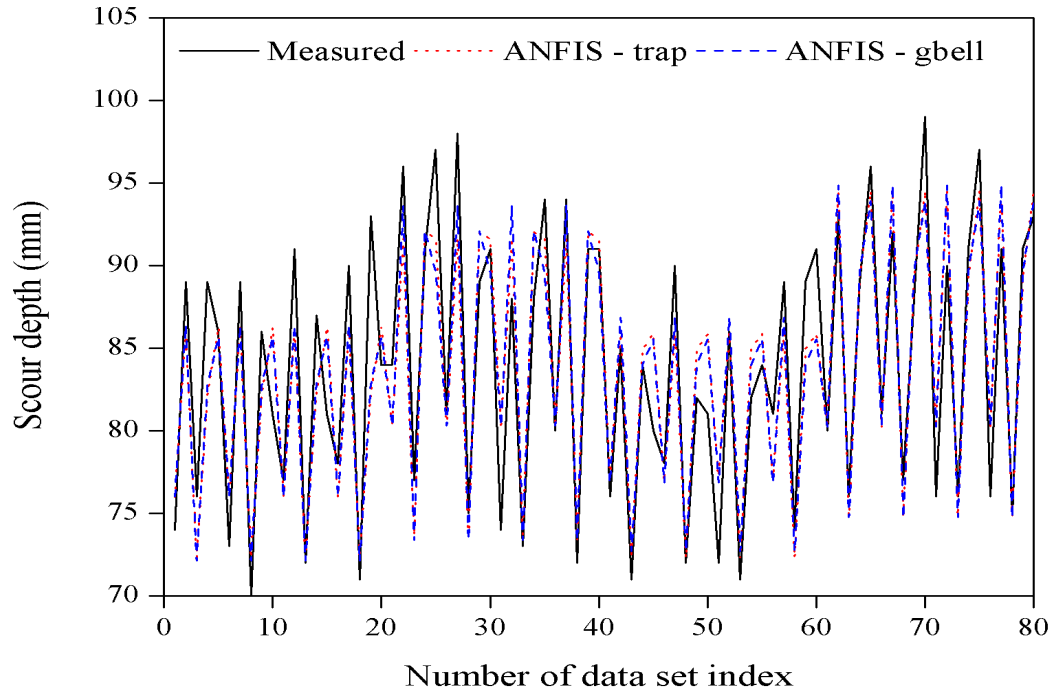


Figure 4.47 Comparison of measured and ANFIS model results in testing phase for circular pier in live bed scour condition

The ANFIS model with trapezoidal and gbell MF is applied to predict the scour depth around rectangular pier and the results are tabulated in the Table 4.6. ANFIS with both MF are performing better with higher $CC=0.952$ for trapezoidal and $CC=0.950$ for gbell MF during testing as shown in Figure 4.48. The comparison plot says that, there is good correlation between ANFIS model and measured values (Figure 4.49). The NMB value from the Table 4.6 shows that, the model is performing under prediction during testing and over prediction during training for both the trapezoidal and gbell MF.

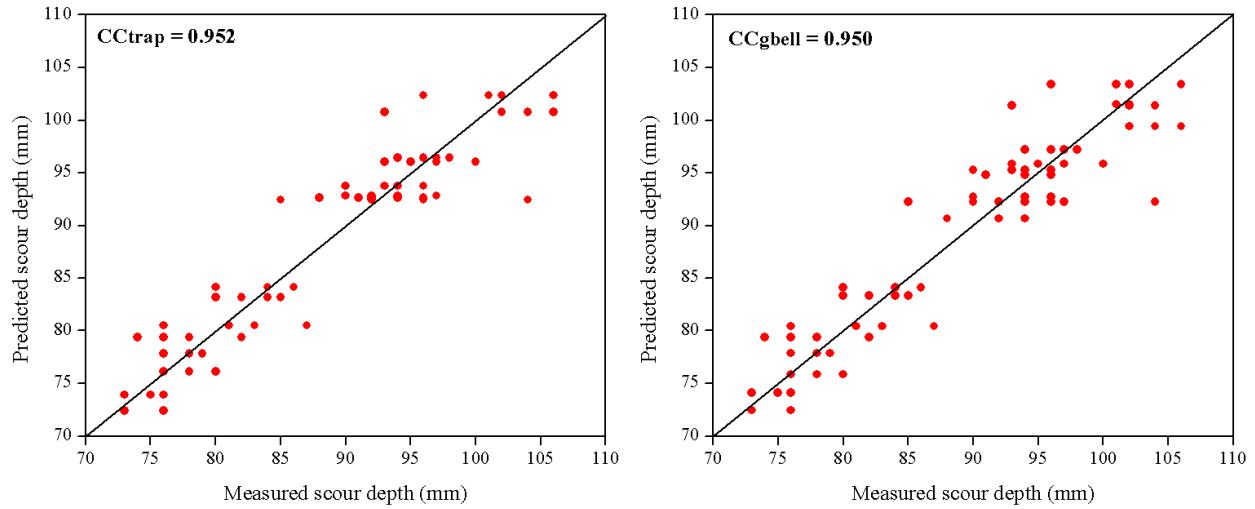


Figure 4.48 Scatter plots of ANFIS models in testing phase for rectangular pier in live bed scour condition

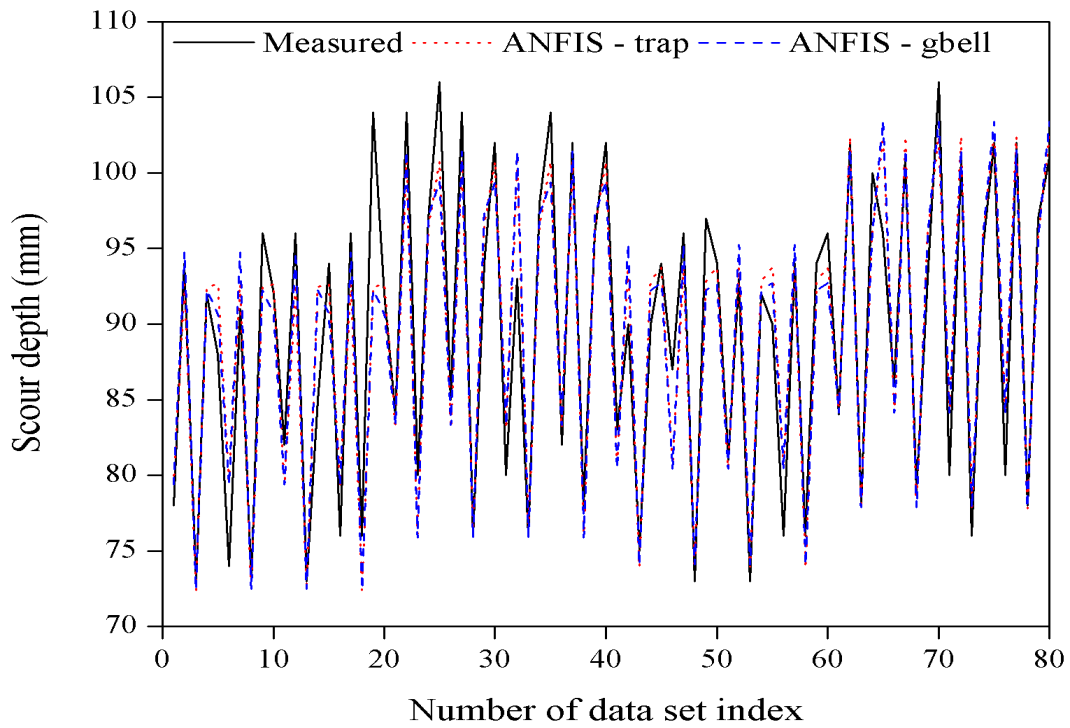


Figure 4.49 Comparison of measured and ANFIS model results in testing phase for rectangular pier in live bed scour condition

The ANFIS model is applied to the prediction of scour depth around round nosed pier. The model results are presented in Table 4.6 in terms of statistical measures and it shows that, ANFIS with both the MFs are performing well. The positive NMB values from the Table 4.6 indicate that, the ANFIS model is performing over prediction for both MFs. Figure 4.50 and 4.51 are the scatter and comparison plots presented against measured and predicted values in testing phase.

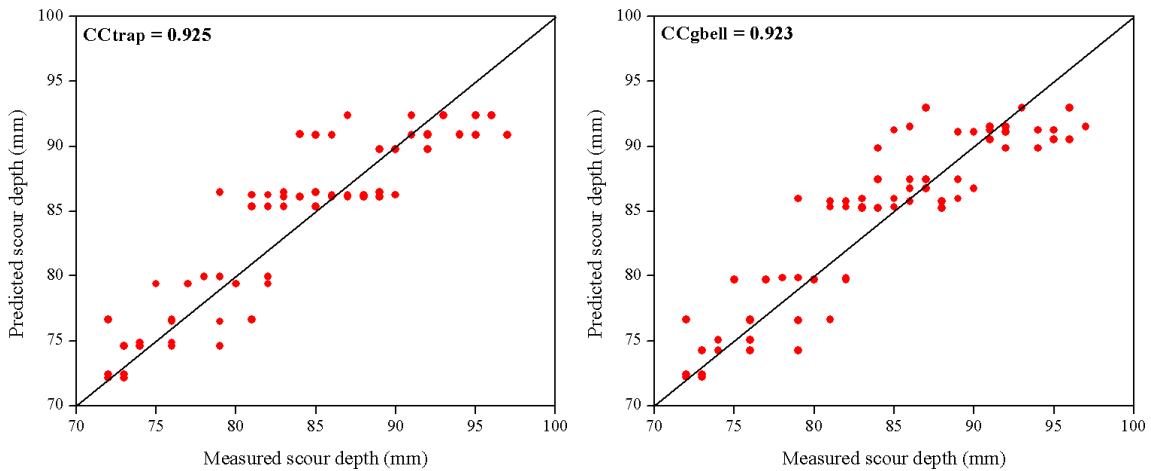


Figure 4.50 Scatter plots of ANFIS models in testing phase for round nosed pier in live bed scour condition

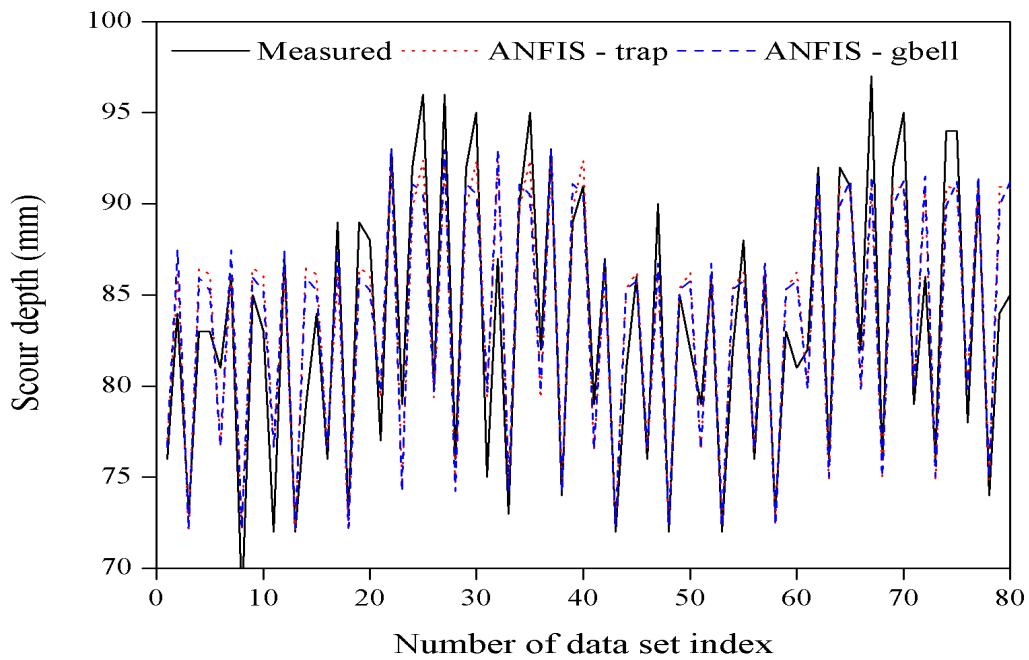


Figure 4.51 Comparison of measured and ANFIS model results in testing phase for round nosed pier in live bed scour condition

In this case, the scour depth is predicted around sharp nose pier using ANFIS model. The obtained results from the model are tabulated in Table 4.6. The ANFIS model is performing better with both the MF in terms of lower NRMSE =10.723 for trapezoidal and 10.82 for gbel in testing phase. From the Figure 4.52 it can be observed that, the ANFIS results are showing good correlation with measured values in terms of $CC= 0.940$ for trapezoidal and $CC=0.939$ for gbell. Figure 4.53 shows the comparison between measured and predicted values.

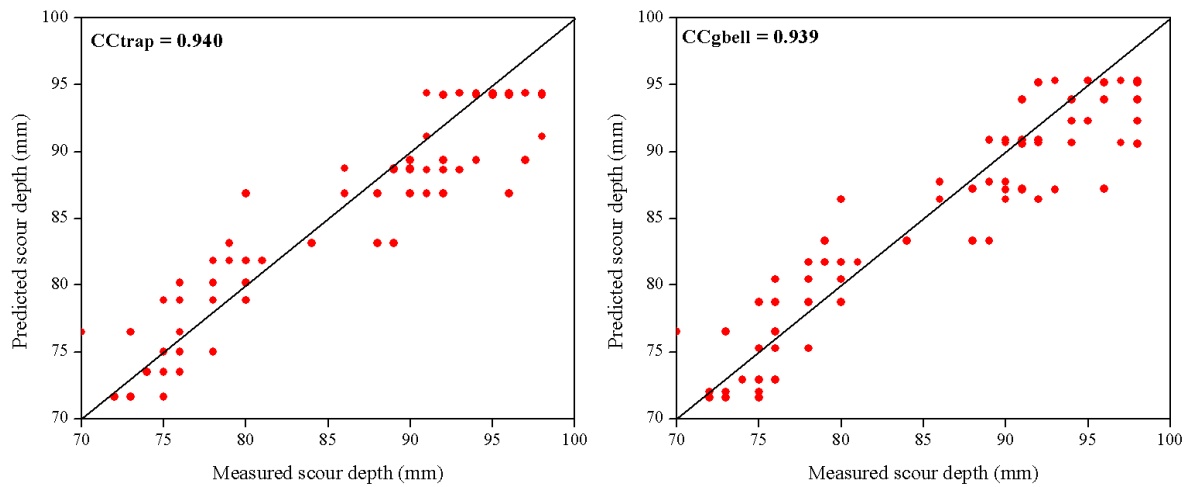


Figure 4.52 Scatter plots of ANFIS models in testing phase for sharp nosed pier in live bed scour condition

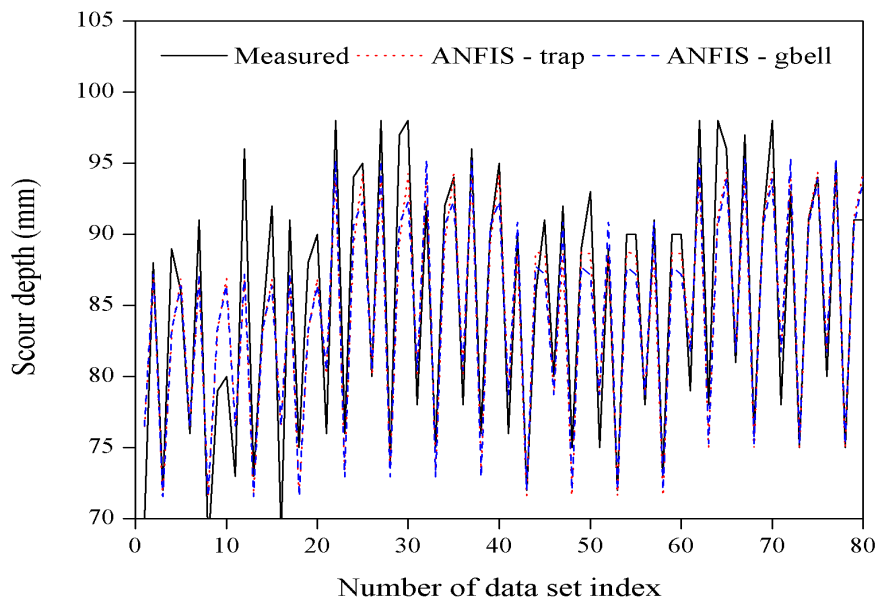


Figure 4.53 Comparison of measured and ANFIS model results in testing phase for sharp nosed pier in live bed scour condition

The ANFIS with trapezoidal and gbell MF are utilized for predicting scour depth around different pier shapes in live bed scour condition. The statistical results from the models are tabulated in Table 4.6 for both training and testing. The scatter and comparison plots are drawn for model testing results. From the Table 4.6 it is clear that, the ANFIS with both MFs performs better for all four pier shapes. Further, the ANFIS model shows good prediction for rectangular pier in live bed scour condition.

4.3.3 Performance of Particle Swarm Optimized Support Vector Machine (PSO-SVM) model in the prediction of scour depth.

The PSO is used as an evolutionary technique to optimize the kernel parameters of SVM (PSO-SVM) in the prediction of scour depth. The PSO based SVM technique is used to predict the scour depth around different shapes of bridge piers under live bed scour condition. The development of PSO-SVM model is explained in section 3.4.3. The optimal kernel parameters of PSO-SVM model are tabulated in Table 3.5. The PSO-SVM with linear and Polynomial kernel functions are used to predict the scour depth. The results of PSO-SVM model with linear and polynomial kernel function are tabulated in Table 4.7 in terms of statistical indices. The predicted results are compared with measured values. The scatter and comparison plots are presented for measured versus predicted results during testing phase.

Table 4.7 Results of PSO-SVM models for live bed scour condition

Pier shape	Statistical indices	PSO-SVM Model			
		Linear		Polynomial	
		Train	Test	Train	Test
Circular	CC	0.856	0.837	0.923	0.920
	NRMSE	15.50	15.23	11.07	10.79
	NSE	0.704	0.690	0.849	0.845
	NMB	0.009	0.01	0.003	0.005
Rectangular	CC	0.893	0.879	0.963	0.932
	NRMSE	12.19	14.66	7.290	11.09
	NSE	0.794	0.767	0.926	0.867

	NMB	0.0004	-0.0066	0.005	0.0007
Round nosed	CC	0.853	0.851	0.919	0.915
	NRMSE	13.712	13.48	10.356	10.33
	NSE	0.716	0.721	0.838	0.836
	NMB	0.00	-0.006	-0.001	0.0016
Sharp nosed	CC	0.851	0.879	0.920	0.938
	NRMSE	14.33	15.37	11.09	10.52
	NSE	0.709	0.734	0.826	0.876
	NMB	0.006	-0.018	0.01	-0.006

The PSO-SVM with polynomial and liner kernel functions is applied to predict the scour depth around circular pier. The model results are tabulated in Table 4.7 and shows that, the PSO-SVM with polynomial kernel function gives good prediction with higher NSE (0.923 for training and 0.920 for testing) compared to linear kernel function (0.856 for training and 0.836 for testing). The Figure 4.54, shows the correlation between the measured and predicted values (CC for, linear=0.837 and polynomial=0.920). The comparison plots are drawn for measured and predicted results in Figure 4.55. The positive NMB values from the Table 4.7 shows that, the PSO-SVM model is performing over prediction in both training and testing.

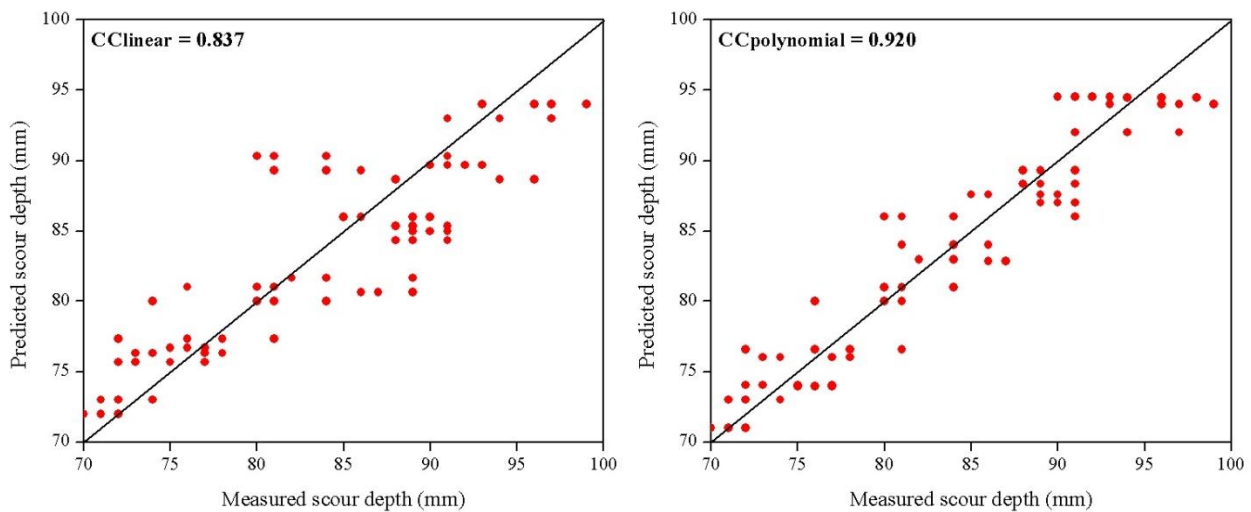


Figure 4.54 Scatter plots of PSO-SVM models in testing phase for circular pier in live bed scour condition

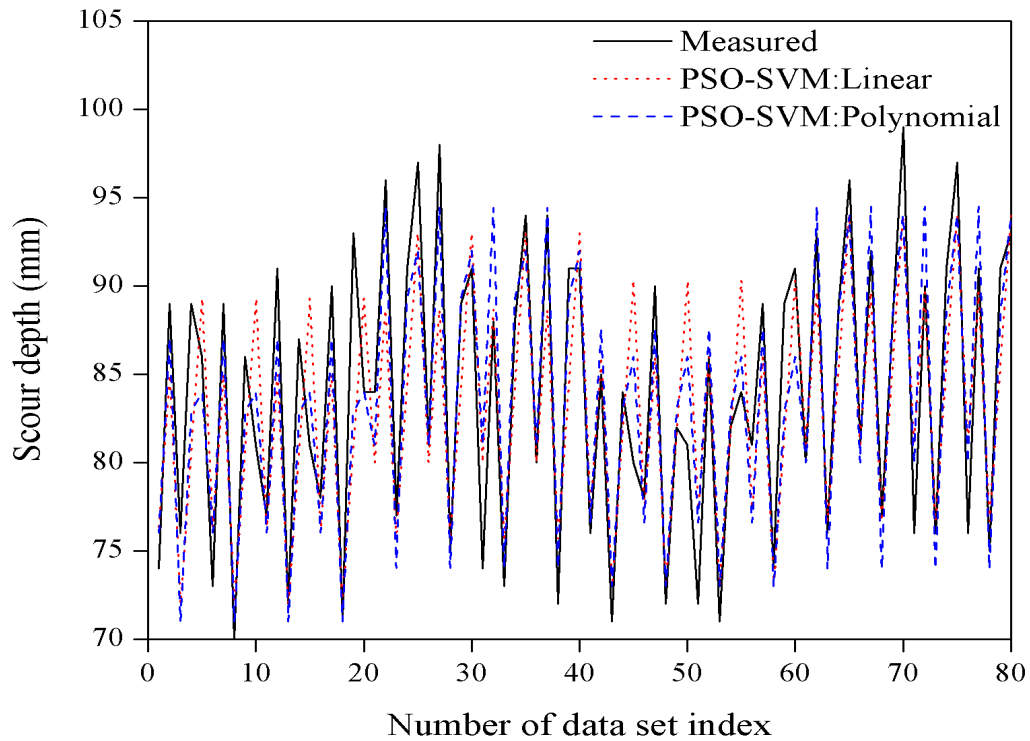


Figure 4.55 Comparison of measured and PSO-SVM model results in testing phase for circular pier in live bed scour condition

In next phase, the PSO-SVM model is used to predict the scour depth around rectangular pier. The model results are presented in Table 4.7 and shows that the PSO-SVM with polynomial kernel function performs well with higher NSE (0.926=training and 0.867=testing) compared to linear kernel function of NSE (0.794=training and 0.767=testing). The scatter and comparison plots are presented with measured and predicted scour depth during testing phase as shown in Figure 4.56 and 4.57 respectively.

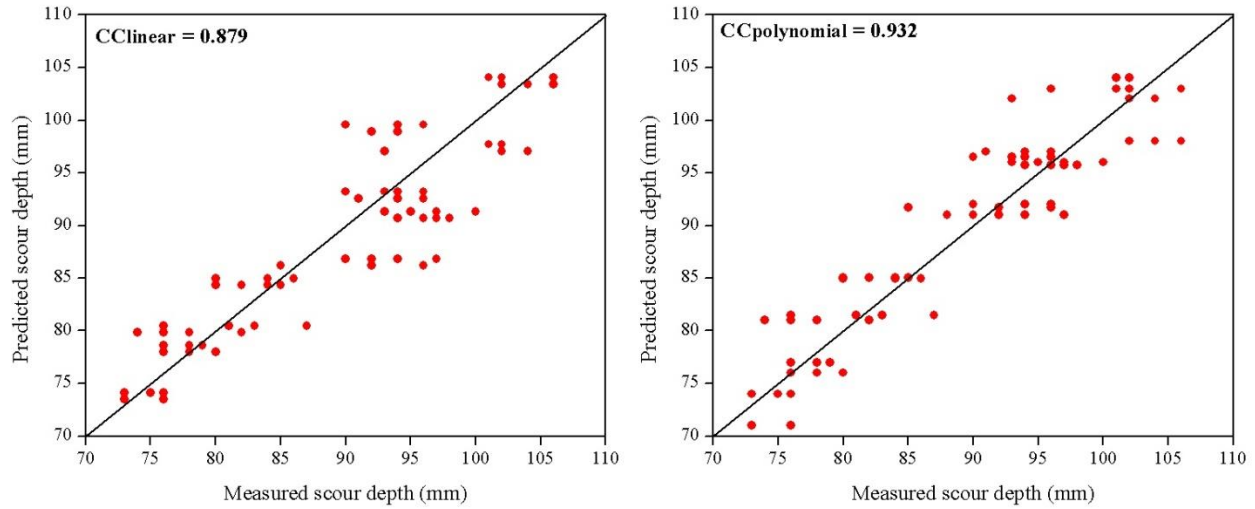


Figure 4.56 Scatter plots of PSO-SVM models in testing phase for rectangular pier in live bed scour condition

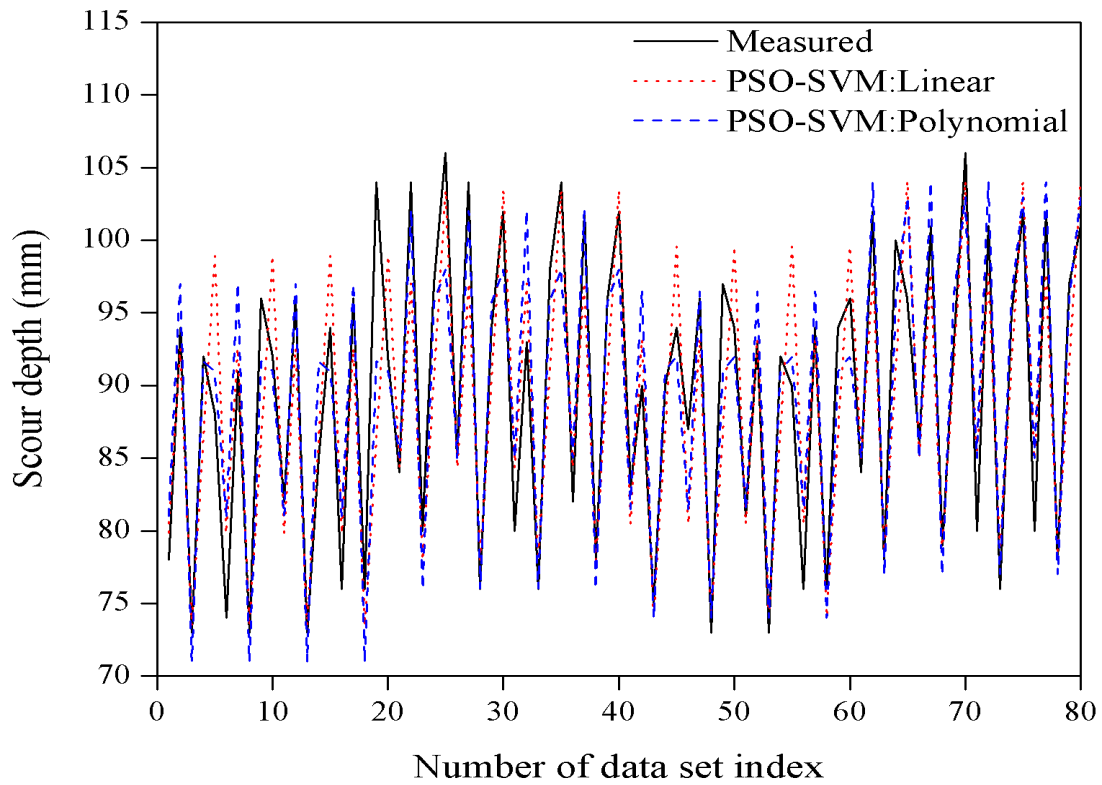


Figure 4.57 Comparison of measured and PSO-SVM model results in testing phase for rectangular pier in live bed scour condition

The scour depth around round nosed pier is predicted using PSO-SVM model and the results are presented in Table 4.7. The results shows that, the PSO-SVM with polynomial kernel function is performing better in terms of lower NRMSE (10.356=training and 10.33=testing) compared to linear kernel function of NRMSE (13.712=training and 13.48=testing). The CC from the Figure 4.58 shows the correlation between the measured and predicted results in testing phase (CC=0.851 for linear and CC=0.915 for polynomial). The comparison plot is shown, against measured and predicted to study the performance of the model are shown in Figure 4.59.

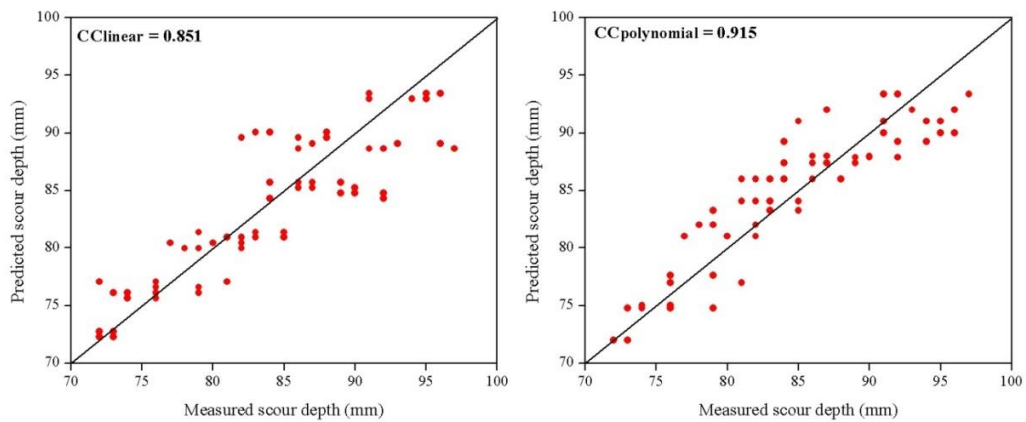


Figure 4.58 Scatter plots of PSO-SVM models in testing phase for round nosed pier in live bed scour condition

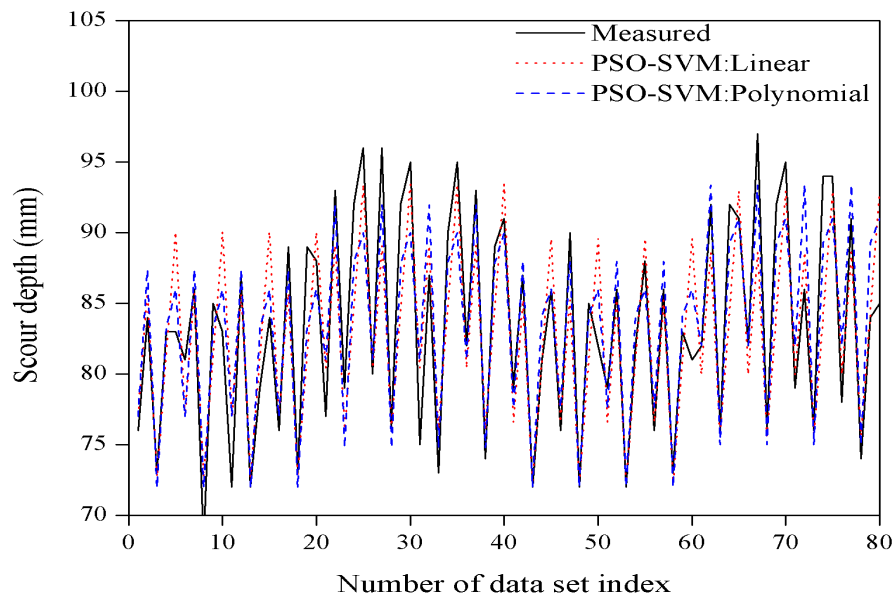


Figure 4.59 Comparison of measured and PSO-SVM model results in testing phase for round nosed pier in live bed scour condition

In this case, the PSO-SVM model is utilized for the prediction of scour depth around sharp nosed pier. The obtained result from the model are tabulated in Table 4.7 and shows that, the polynomial kernel function is performing better than linear kernel function. The NMB values from the Table 4.7 clearly shows that, the PSO-SVM model is performing under prediction during testing and over prediction during training in both the kernel functions. Figure 4.60 and 4.61 are the scatter and comparison plots respectively, which are the plot between the measured and predicted results.

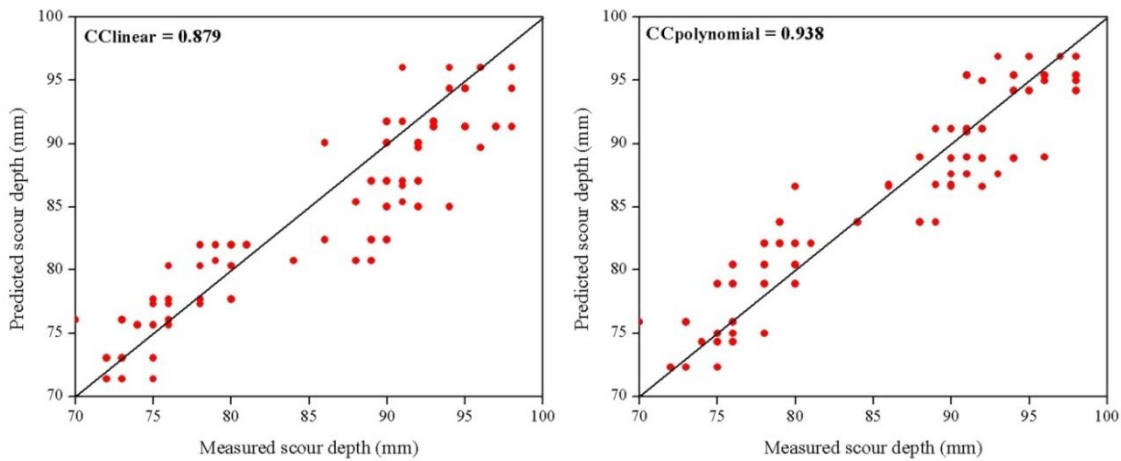


Figure 4.60 Scatter plots of PSO-SVM models in testing phase for sharp nosed pier in live bed scour condition

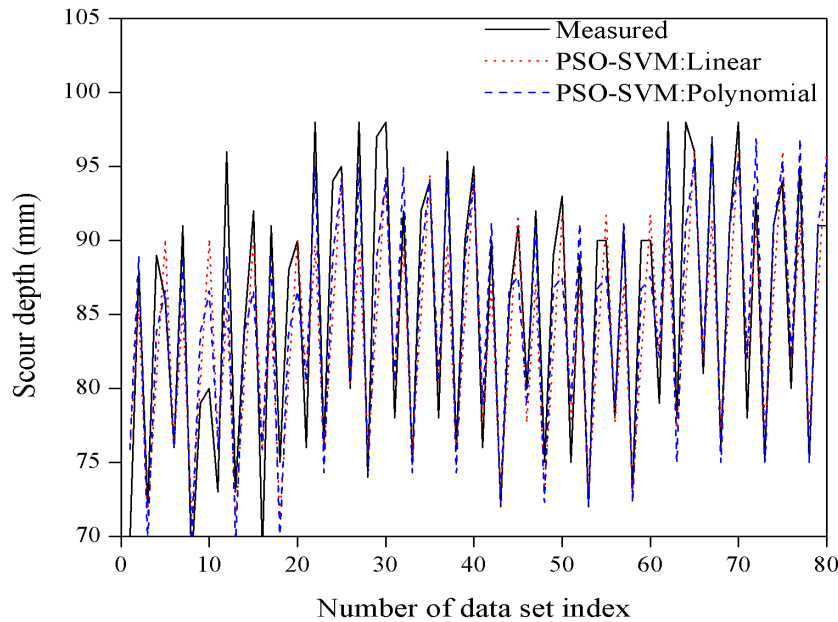


Figure 4.61 Comparison of measured and PSO-SVM model results in testing phase for sharp nosed pier in live bed scour condition

The PSO based SVM model is used for the prediction of scour depth around different pier shapes in live bed scour condition. The model results in terms of statistical indices are presented in Table 4.7. It is clear from the table that, the PSO-SVM with polynomial kernel function shows good correlation in the prediction of scour depth around all four pier shapes. Further, the PSO-SVM with polynomial kernel function performs better particularly for rectangular pier under live bed scour condition compare to other pier shapes and kernel functions.

4.3.4 Performance of Artificial Neural Network (ANN) and Particle Swarm Optimized Neural Network (PSO-ANN) model in the prediction of scour depth.

The ANN models are developed using different hidden neurons and the statistical results of ANN with 2 neurons are tabulated in Table 4.8. The particle swarm optimization is used to overcome the disadvantages and drawbacks of neural network in the prediction of scour depth. The development of PSO-ANN is explained in detail in the section 3.4.4. The PSO based feed forward neural network (PSO-ANN) is used to predict the scour depth around different pier shapes in live bed scour condition. The model results are tabulated in Table 4.8 for both training and testing phases. The PSO-ANN models are showing good correlation compared to ANN models in terms of statistical parameters and the PSO-ANN results are discussed in this section.

Table 4.8 Results of ANN and PSO-ANN models for live bed scour condition

Pier shape	Statistical indices	ANN Model		PSO-ANN Model	
		Train	Test	Train	Test
Circular	CC	0.865	0.840	0.948	0.905
	NRMSE	15.02	16.65	9.11	11.69
	NSE	0.72	0.69	0.898	0.818
	NMB	0.004	0.02	0.0003	-0.003
Rectangular	CC	0.920	0.890	0.942	0.925
	NRMSE	9.93	12.48	7.32	10.81

	NSE	0.86	0.83	0.925	0.873
	NMB	-0.002	-0.003	0.00	-0.002
Round nosed	CC	0.903	0.880	0.935	0.910
	NRMSE	13.35	13.51	8.580	9.830
	NSE	0.730	0.718	0.890	0.851
	NMB	0.0102	0.015	0.00	0.002
Sharp nosed	CC	0.896	0.875	0.945	0.920
	NRMSE	12.1	13.25	9.422	10.610
	NSE	0.801	0.795	0.874	0.873
	NMB	-0.005	-0.01	0.0001	-0.009

The PSO-ANN model predicts the scour depth around different pier shapes (circular, rectangular, round nosed and sharp nosed). The model performances are analyzed in terms of statistical indices and tabulated in Table 4.8. The table shows that, PSO-ANN is performing well for all the four pier shapes. The PSO-ANN model showing better prediction particularly for rectangular pier with higher CC (0.962=training, 0.935=testing), NSE (0.925=training, 0.873=testing) and with lower NRMSE (7.32=training, 10.81=testing) compared to other pier shapes. The scatter and comparison plots are constructed for measured and predicted results for all four pier shapes, Figure 4.62 and 4.63 for circular, 4.64 and 4.65 for rectangular, 4.66 and 4.67 for round nosed and 4.68 and 4.69 for sharp nosed pier.

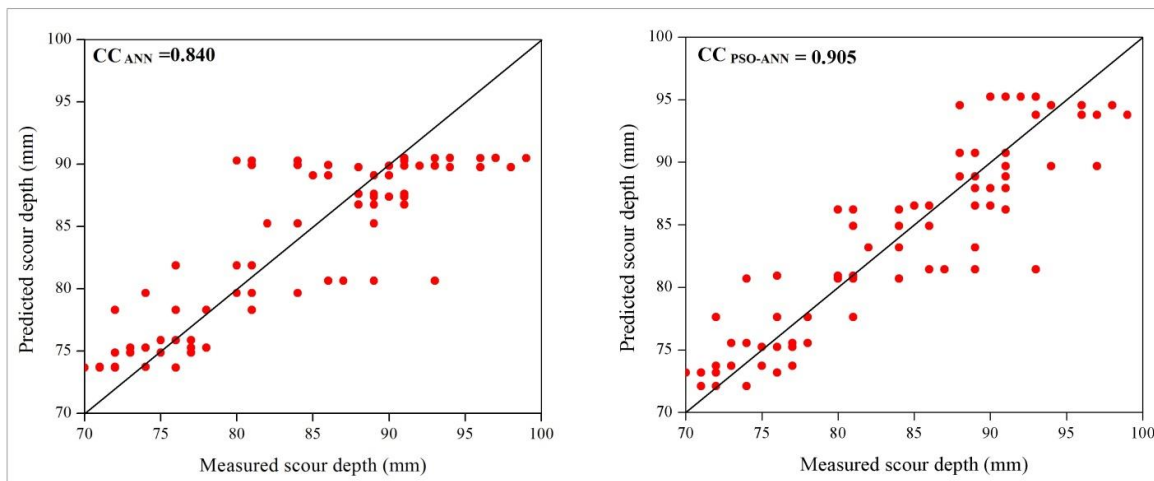


Figure 4.62 Scatter and line plots of ANN and PSO-ANN models in testing phase for circular pier in live bed scour condition

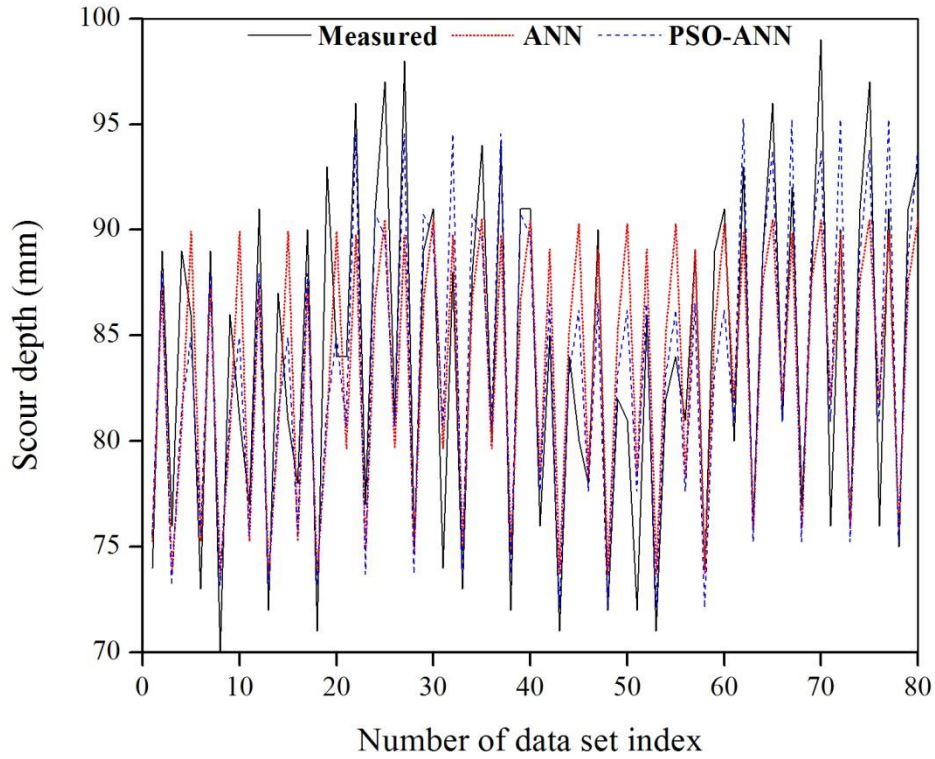


Figure 4.63: Comparison of measured, ANN and PSO-ANN model results in testing phase for circular pier in clear water scour condition

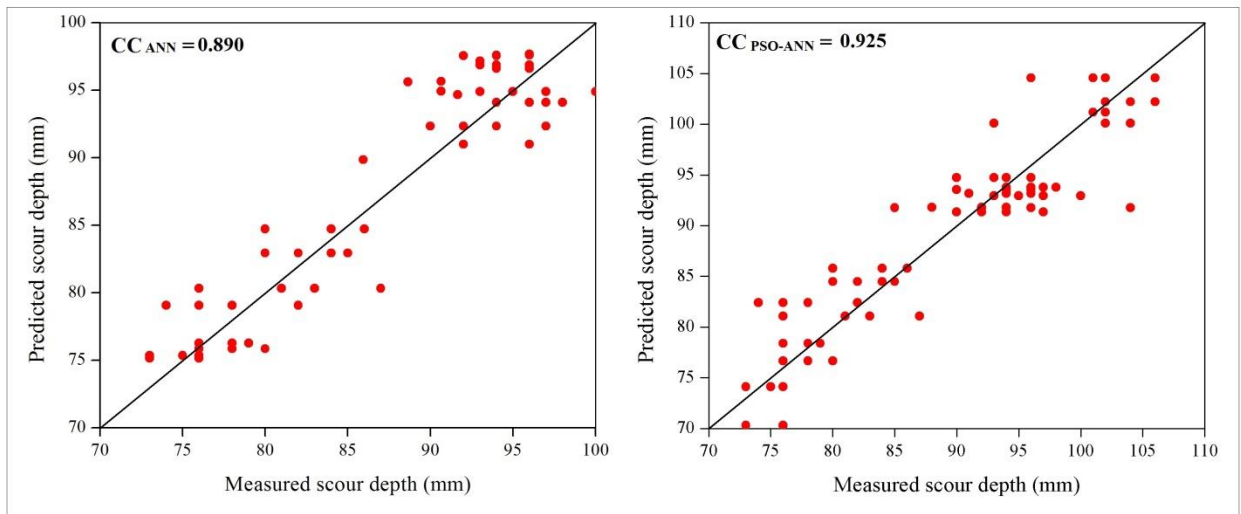


Figure 4.64 Scatter and line plots of ANN and PSO-ANN models in testing phase for rectangular pier in live bed scour condition

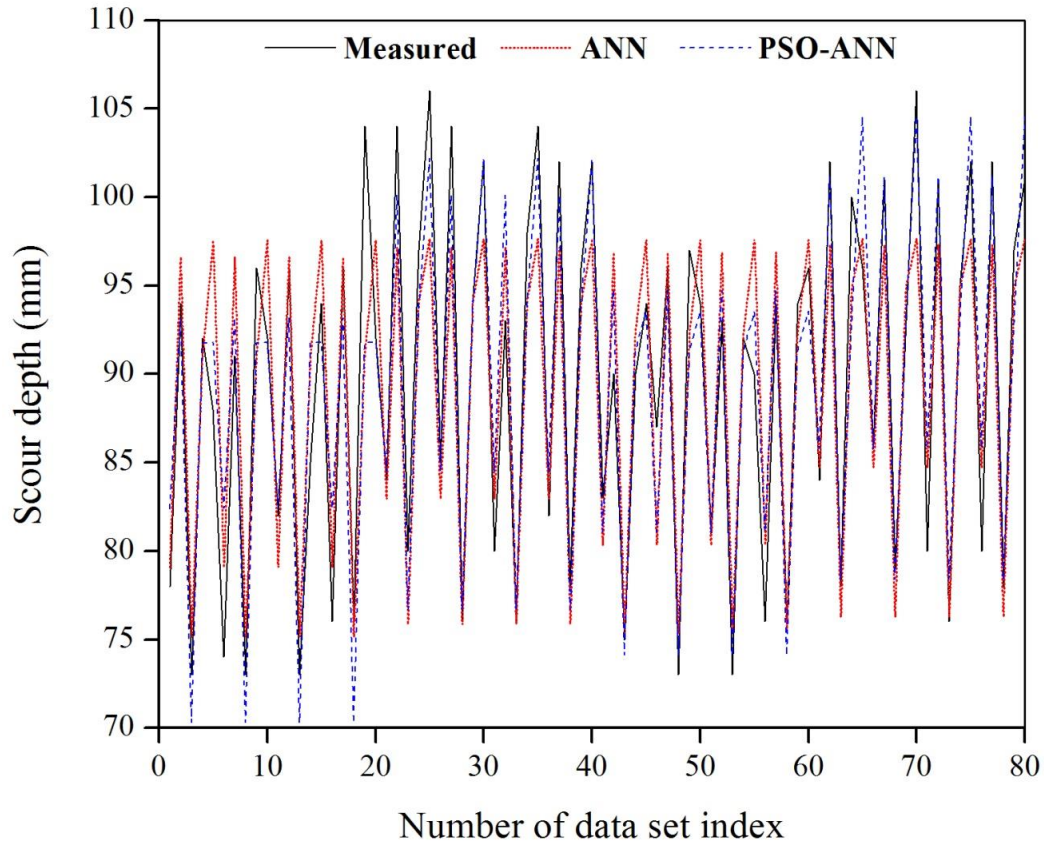


Figure 4.65: Comparison of measured, ANN and PSO-ANN model results in testing phase for rectangular pier in clear water scour condition

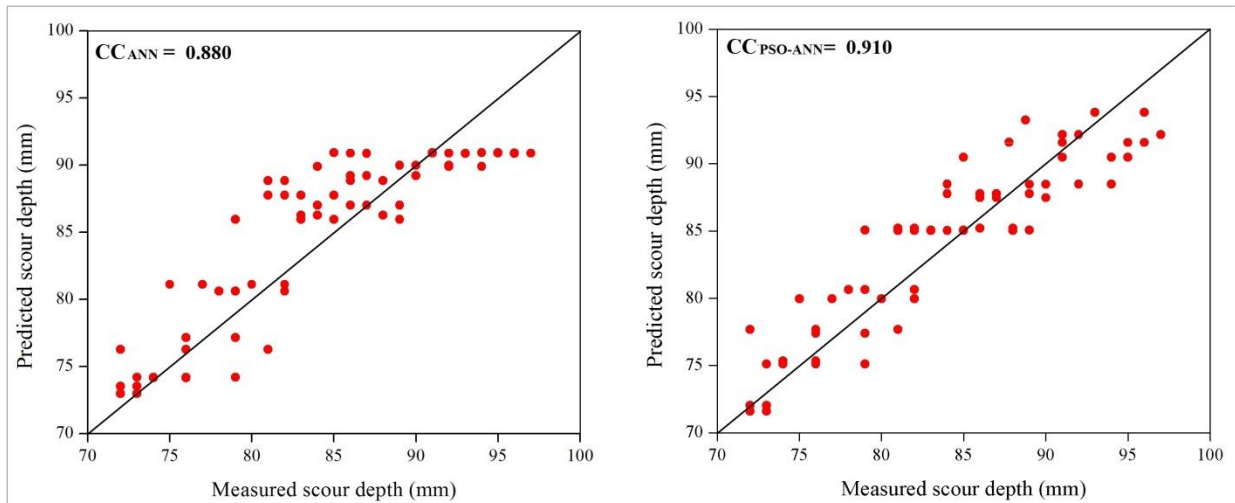


Figure 4.66 Scatter and line plots of ANN and PSO-ANN models in testing phase for round nosed pier in live bed scour condition

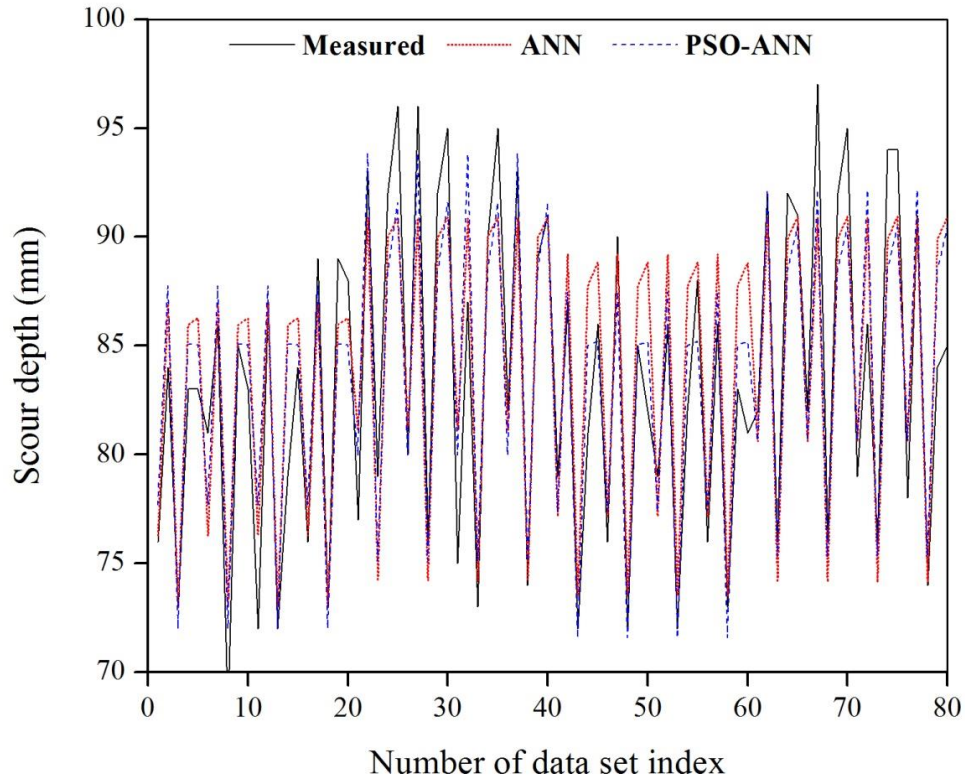


Figure 4.67: Comparison of measured, ANN and PSO-ANN model results in testing phase for round nosed pier in clear water scour condition

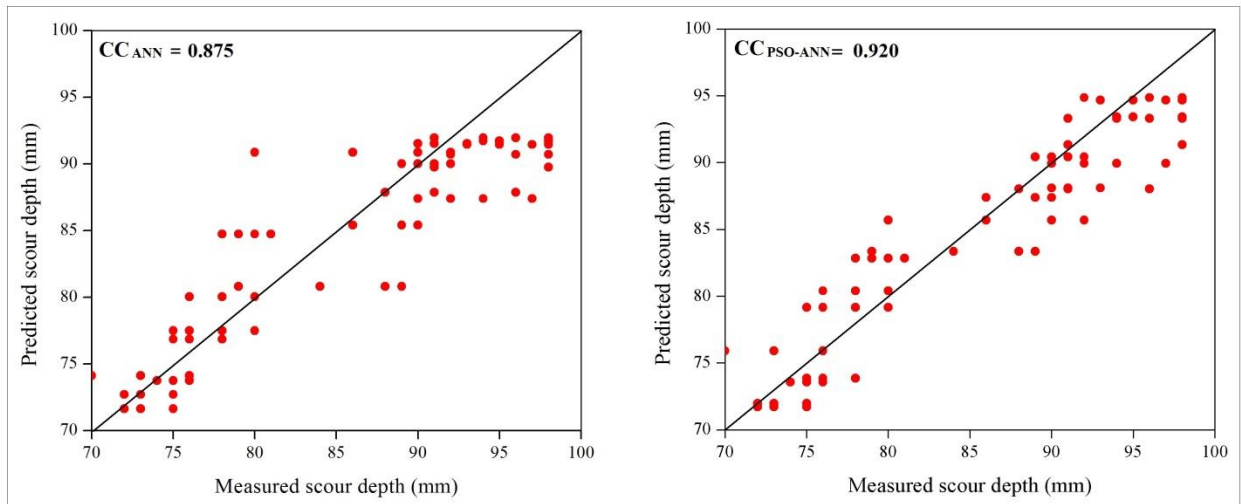


Figure 4.68 Scatter and line plots of ANN and PSO-ANN models in testing phase for sharp nosed pier in live bed scour condition

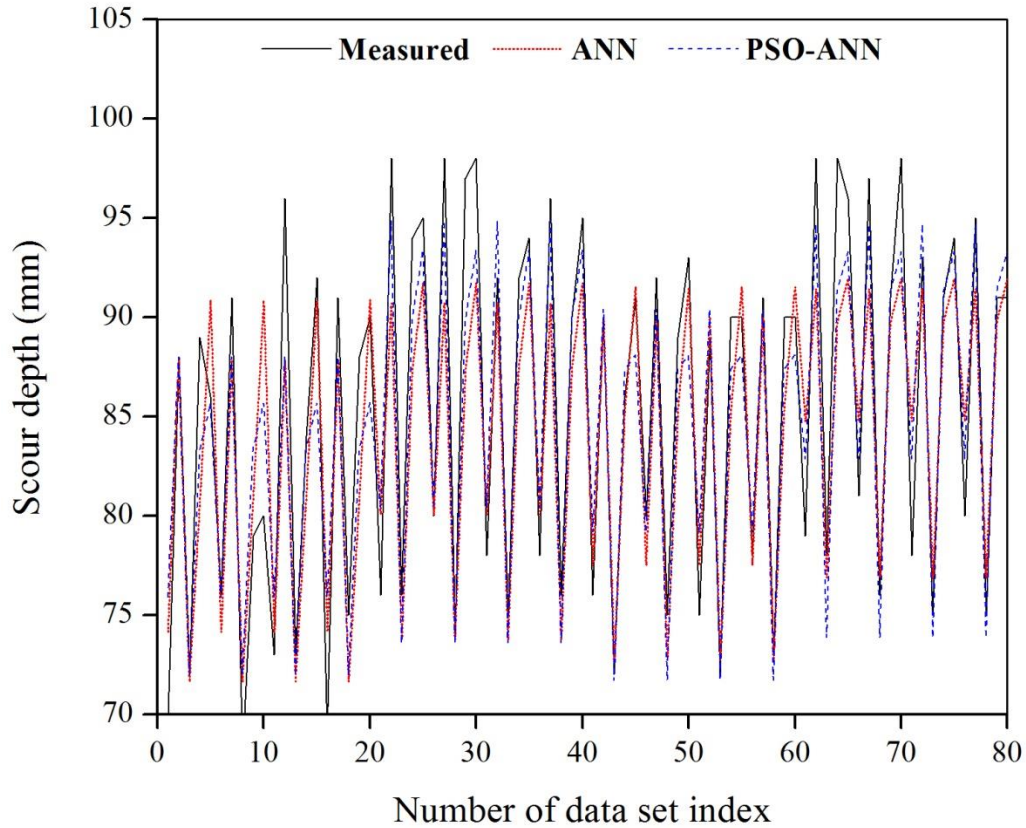


Figure 4.69: Comparison of measured, ANN and PSO-ANN model results in testing phase for sharp nosed pier in clear water scour condition

4.3.5 Comparative study

The SVM, ANFIS, PSO-SVM and PSO-ANN models are developed to fine out the most reliable model for the prediction of scour depth around the pier in live bed scour condition. The results obtained from the models are analyzed using different statistical measures and tabulated in Table 4.5, 4.6, 4.7 and 4.8. The comparison plots are drawn between measured and predicted models as shown in Figure 4.70. It is clear from the Figure 4.70 that, the ANFIS and PSO-SVM models are showing good agreement with the measured results. The box plot from the Figure 4.71 shows that, the PSO-SVM model exhibited a similar type of spread as compared to measured values for all the cases considered in the study.

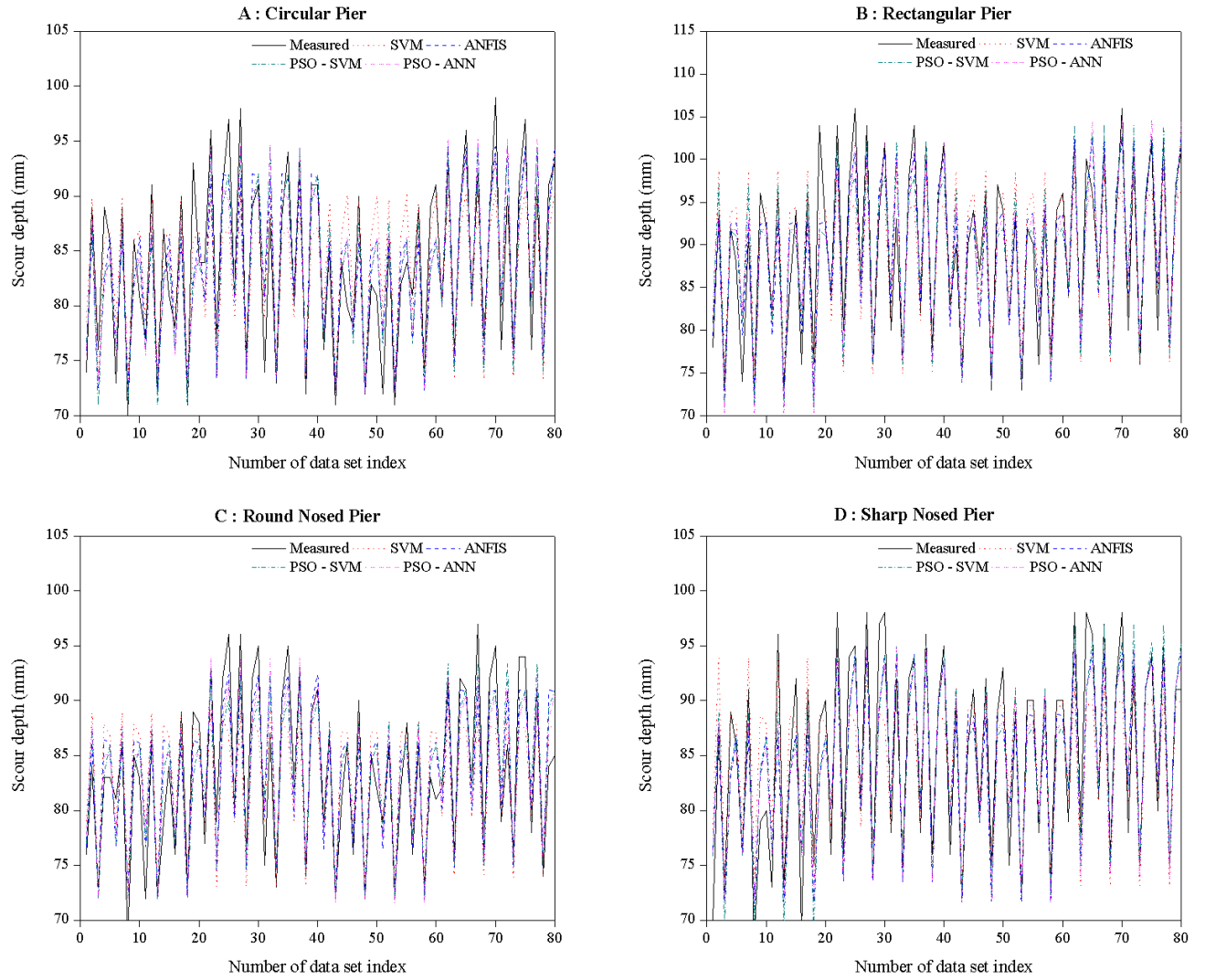


Figure 4.70 Comparison plots in testing phase for live bed scour condition

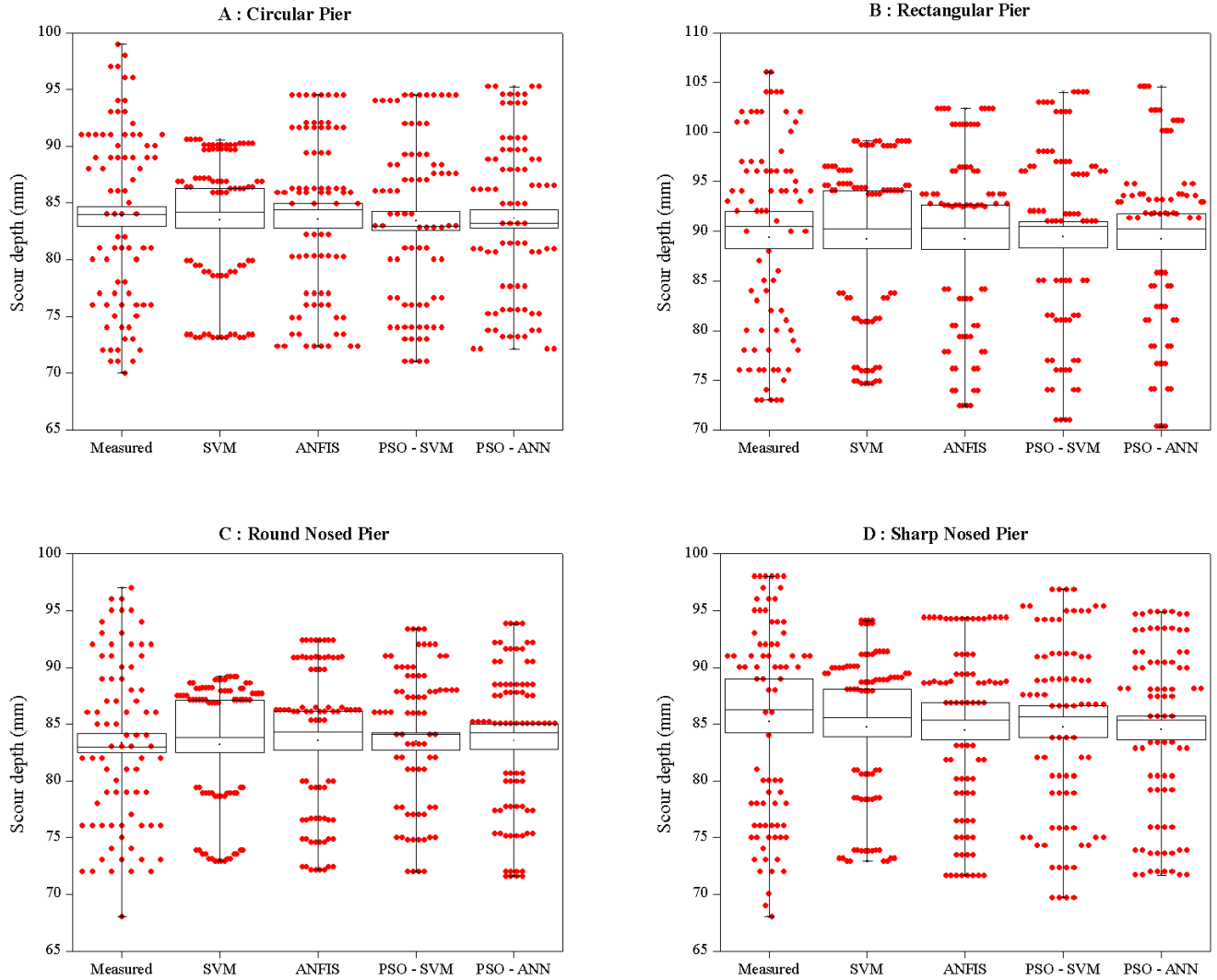


Figure 4.71 Box plots for all the models in testing phase for live bed scour condition

The statistical indices NRMSE, NSE and NMB are considered for the analysis of model performance. Figure 4.72 shows the NRMSE of all the models in both training and testing phase. It is observed that, ANFIS model is performing better in terms of NRMSE for all the models when compared to the other three models. From the Figure 4.73, it is noticed that the ANFIS model has shown good performance for all the four cases in terms of NSE value and also, the PSO-SVM model performing better than SVM model. The NMB values from Figure 4.74 show clearly that, most of the models are performing over prediction during training and under prediction during testing.

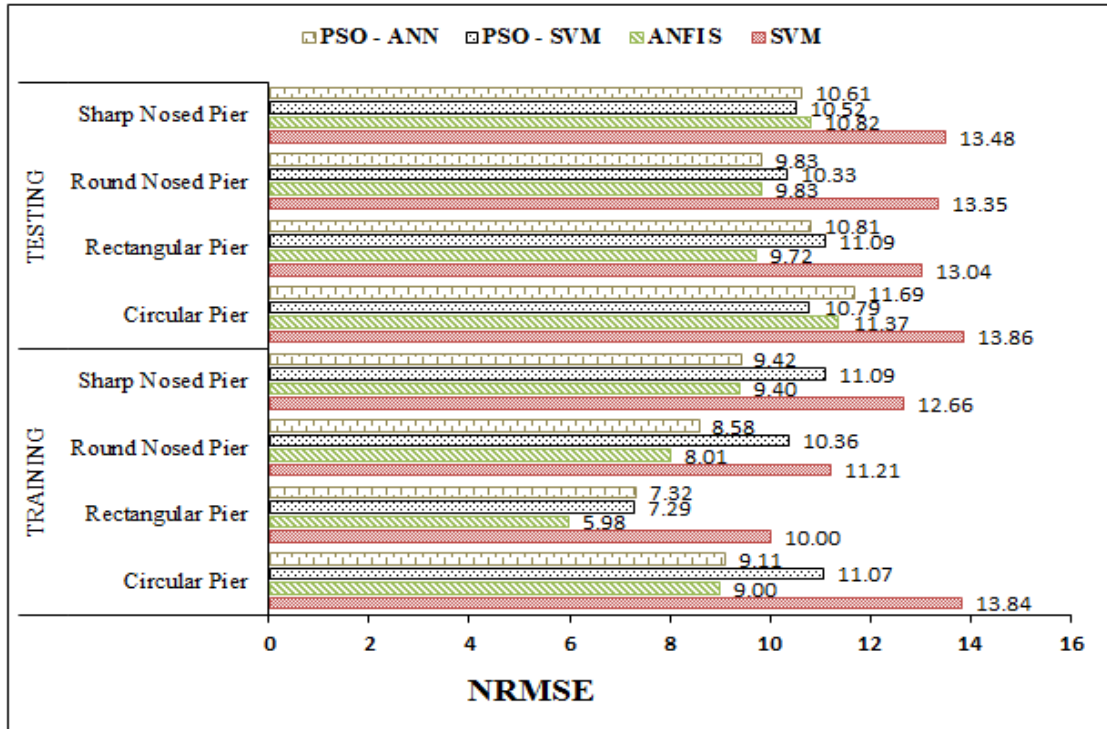


Figure .4.72 NRMSE of all the models for live bed scour condition.

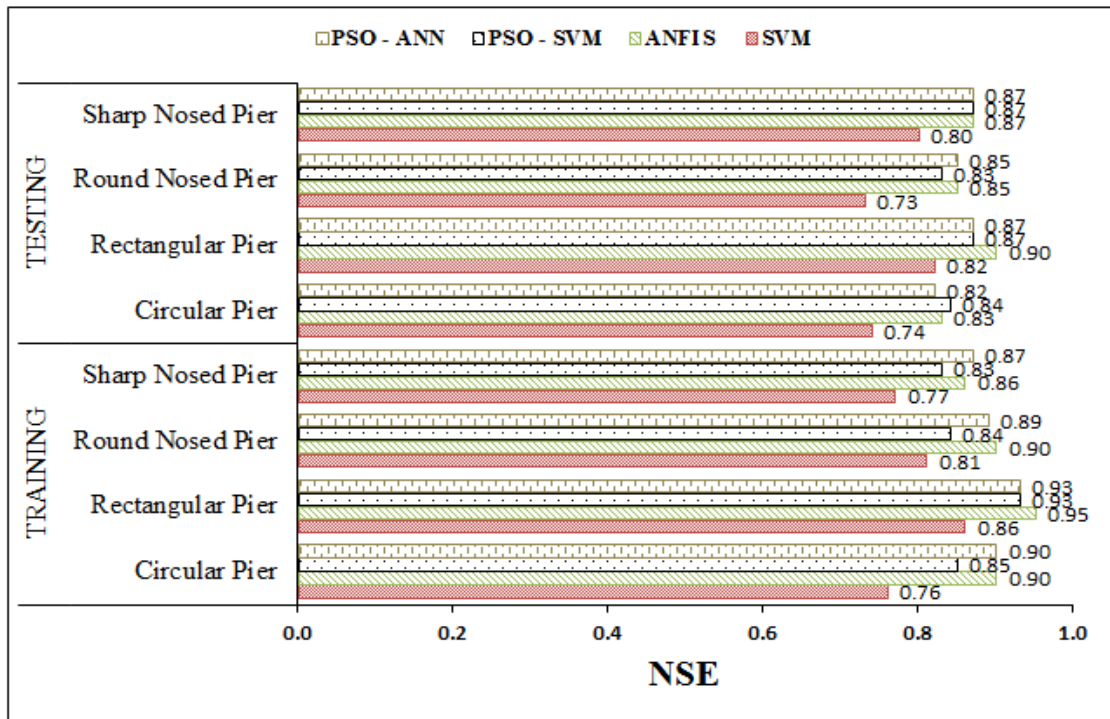


Figure .4.73 NSE of all the models for live bed scour condition.

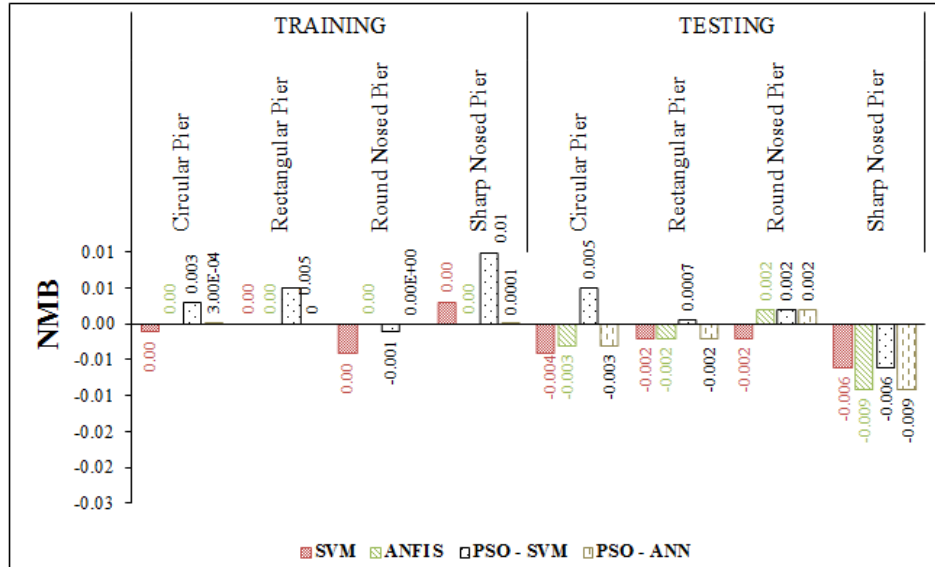


Figure .4.74 NMB of all the models for live bed scour condition.

4.4 Comparison of the Model Results with Standard Empirical Equations

The results of best performing PSO-SVM models are compared with standard empirical equations such as Indian Road Congress (IRC) method, Melville - Coleman method and Kothyari – Garde – Rangaraju method (Mazumder and Kumar, 2006). The results are tabulated in Table 4.9. It is observed that the PSO-SVM has better correlation coefficient (CC) compared to empirical methods. The silt factor, pier shape factor and pier alignment factor considered in the empirical formula are shown in Appendix I.

Table 4.9: Comparison of PSO-SVM results with empirical equations.

Source	Empirical Formula	Correlation coefficient (CC)	
		Empirical method	PSO - SVM
IRC Method (Lacey/Inglis)	$d_{se} = 0.473 \left(\frac{D}{f}\right)^{\frac{1}{3}}$	0.866	0.950
Melville And Coleman Method	$d_{se} = 2.4 K_s K_\theta b$	0.870	
Kothyari – Garde - Rangaraju Method	$\frac{d_{se}}{d_{50}} = 0.88 \left(\frac{b}{d_{50}}\right)^{0.67} \left(\frac{D}{d_{50}}\right)^{0.4} \alpha^{-0.30}$	0.820	

SUMMARY AND CONCLUSIONS

5.1 Summary

This study attempts to develop the different soft computing models such as, ANN, SVM, ANFIS, PSO-SVM and PSO-ANN to predict the scour depth around the bridge pier. In the present study there have been four different shapes (Circular, rectangular, round nosed and sharp nosed) of piers and two scour conditions (clear water and live bed) are used. The sediment size (d_{50}), velocity (u) and time (T) are used as input variables for clear water scour condition and sediment quantity (Sq), velocity (u) and time (T) are used as input parameters for live bed scour condition. The performances of the proposed models are analyzed using various statistical indices such as Correlation Coefficient (CC), Normalized Root Mean Square Error (NRMSE), Nash–Sutcliffe coefficient (NSE) and Normalized Mean Bias (NMB). The model results are compared with measured scour depth. Scatter and comparison plots are used to evaluate the accuracies of the models and box plots are drawn to learn the spread of the data points estimated by the models with respect to measured values.

5.2 Conclusions

Based on the results of the present investigations and discussion thereon, following conclusions are derived:

- The ANN, SVM, ANFIS, PSO-SVM and PSO-ANN models give good results for the range of velocity (0.184 - 0.351) m/sec, sediment size (0.42 - 4.2) mm, Sediment quantity (474.77- 1066.67) ppm.
- SVM with different kernel functions are performed, among them RBF kernel yields higher CC, NSE and lower NRMSE compared to other kernel functions.
- ANFIS and PSO-SVM showed a better as compared to ANN, SVM and PSO-ANN. When the hybrid models are compared, ANFIS model gives higher CC, NSE and lower NRMSE. But considering computational time ANFIS has taken more time than PSO-SVM model. Hence, PSO-SVM is computationally efficient as compared to ANFIS.

- The ANFIS and PSO-SVM models perform better particularly, for circular pier in case of clear water scour condition and rectangular pier under live bed scour condition compared to other cases.
- The PSO-SVM model gives higher CC when compared with that from various empirical equations while estimating scour depth.
- The PSO-SVM model performs better than ANFIS, PSO-ANN, SVM and ANN. Hence, PSO-SVM can be recommended in place of ANFIS, PSO-ANN, SVM and ANN for the prediction of scour depth around the pier in clear water and live bed scour conditions.

5.3 Limitations of the Study

- Soft computing techniques are data driven and will give the best results when sufficient experimental data is available beforehand.
- The models cannot be generalized unless similar field conditions are available. These are site specific models

5.4 Scope for Future Work

There is a scope for carrying out further research. The following suggestion may be considered for further study:

- The study can be extended to other evolutionary optimization techniques such as Ant Colony Optimization (ACO) and any improvement in the efficiency of predictions can be checked.
- The scour is a complex phenomenon and there are various factors affecting on the scour depth need to be considered in addition to the three input parameters which are used in the study.

REFERENCES

- Abraham, A. (2005). "Adaptation of fuzzy inference system using neural learning". *Fuzzy systems engineering*, 53-83.
- Akib, S., Mohammadhassani, M., & Jahangirzadeh, A. (2014). "Application of ANFIS and LR in prediction of scour depth in bridges". *Computers & Fluids*, 91, 77-86.
- Ansari, S. A., Kothiyari, U. C., & Ranga Raju, K. G. (2002). "Influence of cohesion on scour around bridge piers". *Journal of Hydraulic Research*, 40(6), 717-729.
- Azamathulla, H. M., Deo, M. C., & Deolalikar, P. B. (2008). "Alternative neural networks to estimate the scour below spillways". *Advances in Engineering Software*, 39(8), 689-698.
- Azamathulla, H. M., & Ghani, A. A. (2010). "ANFIS-based approach for predicting the scour depth at culvert outlets". *Journal of pipeline systems engineering and practice*, 2(1), 35-40.
- Barbhuiya, A. K., & Mazumder, M. H. (2014). "Live-bed local scour around vertical-wall abutments". *ISH Journal of Hydraulic Engineering*, 20(3), 339-351.
- Basser, H., Karami, H., Shamshirband, S., Akib, S., Amirmojahedi, M., Ahmad, R., & Javidnia, H. (2015). "Hybrid ANFIS-PSO approach for predicting optimum parameters of a protective spur dike". *Applied Soft Computing*, 30, 642-649.
- Bateni, S. M., Borghei, S. M., & Jeng, D. S. (2007). "Neural Network and Neuro-Fuzzy assessments for scour depth around bridge piers". *Engineering Applications of Artificial Intelligence*, 20(3), 401-414.
- Begum, S. A., Fujail, A. M., & Barbhuiya, A. K. (2012). "Artificial Neural Network to predict equilibrium local scour depth around semicircular bridge abutments". 6th SASTech, Malaysia, Kuala Lumpur.
- Bonakdari, H., & Ebtehaj, I. (2017). "Scour Depth Prediction around Bridge Piers Using Neuro-Fuzzy and Neural Network Approaches". *International Journal of Civil, Environmental, Structural, Construction and Architectural Engineering*, 11(6), 835-839.

- Breusers, H. N. C., Nicollet, G., & Shen, H. W. (1977). "Local scour around cylindrical piers". *Journal of Hydraulic Research*, 15(3), 211-252.
- Catto, J. W., Linkens, D. A., Abbod, M. F., Chen, M., Burton, J. L., Feeley, K. M., & Hamdy, F. C. (2003). "Artificial intelligence in predicting bladder cancer outcome: a comparison of Neuro-Fuzzy modeling and Artificial Neural Networks". *Clinical Cancer Research*, 9(11), 4172-4177.
- Choi, S. U., Choi, B., & Lee, S. (2017). "Prediction of local scour around bridge piers using the ANFIS method". *Neural Computing and Applications*, 28(2), 335-344.
- Chou, J. S., & Pham, A. D. (2014). "Hybrid computational model for predicting bridge scour depth near piers and abutments". *Automation in Construction*, 48, 88-96.
- Coleman, S. E., Lauchlan, C. S., & Melville, B. W. (2003). "Clear-water scour development at bridge abutments". *Journal of Hydraulic Research*, 41(5), 521-531.
- Cortes, C., & Vapnik, V. (1995). "Machine learning". *Support vector networks*, 20, 273-297.
- Debnath, K., & Chaudhuri, S. (2010). "Laboratory experiments on local scour around cylinder for clay and clay-sand mixed beds". *Engineering Geology*, 111(1-4), 51-61.
- Firat, M., & Gungor, M. (2009). "Generalized regression neural networks and feed forward neural networks for prediction of scour depth around bridge piers". *Advances in Engineering Software*, 40(8), 731-737.
- Ghani, A. A., & Mohammadpour, R. (2016). "Temporal variation of clear-water scour at compound Abutments". *Ain Shams Engineering Journal*, 7(4), 1045-1052.
- Ghasemi, H., Kolahdoozan, M., Pena, E., Ferreras, J., & Figuero, A. (2017). "A new hybrid ANN model for evaluating the efficiency of π -type floating breakwater". *Coastal Engineering Proceedings*, 1(35), 25.
- Ghazanfari H, S., Etemad S, A., Kazeminezhad, M. H., & Mansoori, A. R. (2011). "Prediction of pile group scour in waves using support vector machines and ANN". *Journal of Hydroinformatics*, 13(4), 609-620.

- Goel, A. (2008). "Estimation of scour downstream of spillways using SVM modeling". *Proceedings of the World Congress on Engineering and Computer Science WCECS*, 22-24.
- Goel, A. (2015). "Predicting bridge pier scour depth with SVM". *World Academy of Science, Engineering and Technology, International Journal of Civil, Environmental, Structural, Construction and Architectural Engineering*, 9(2), 211-216.
- Goswami P (2013). "Evaluation of scour depth around bridge piers". PhD thesis, Guwahati University, Guwahati, India.
- Harish, N., Mandal, S., Rao, S., & Patil, S. G. (2015). "Particle Swarm Optimization based Support Vector Machine for damage level prediction of non-reshaped berm breakwater". *Applied Soft Computing*, 27, 313-321.
- Hasanipanah, M., Noorian B, M., Armaghani, D. J., & Khamesi, H. (2016). "Feasibility of PSO-ANN model for predicting surface settlement caused by tunneling". *Engineering with Computers*, 32(4), 705-715.
- Hong, J. H., Goyal, M. K., Chiew, Y. M., & Chua, L. H. (2012). "Predicting time-dependent pier scour depth with Support Vector Regression". *Journal of hydrology*, 468, 241-248.
- Jang, J. S. (1992). "Self-learning fuzzy controllers based on temporal back propagation". *IEEE Transactions on neural networks*, 3(5), 714-723.
- Jang, J. S., & Sun, C. T. (1995). "Neuro-Fuzzy modeling and control". *Proceedings of the IEEE*, 83(3), 378-406.
- Jannaty, M. H., Eghbalzadeh, A., & Hosseini, S. A. (2015). "Hybrid ANFIS model for predicting scour depth using Particle Swarm Optimization". *Indian Journal of Science and Technology*, 8(22).
- Katukam R. (2014). "Engineering Optimization using Artificial Neural Network". *International Journal of Innovations in Engineering and technology*, 4(3), 50-63.

- Kaya, A. (2010). "Artificial Neural Network study of observed pattern of scour depth around bridge piers". *Computers and Geotechnics*, 37(3), 413-418.
- Kennedy, J., & Eberhart, R. (1995). "Particle Swarm Optimization". *Proceedings of IEEE International Conference on neural networks (ICNN'95)*.
- Kızıloz, B., Çevik, E., & Aydoğan, B. (2015). "Estimation of scour around submarine pipelines with Artificial Neural Network". *Applied Ocean Research*, 51, 241-251.
- Kothyari, U. C. (2007). "Indian practice on estimation of scour around bridge piers—A comment". *Sadhana*, 32(3), 187-197.
- Kuntoji, G., Rao, M., & Rao, S. (2018). "Prediction of wave transmission over submerged reef of tandem breakwater using PSO-SVM and PSO-ANN techniques". *ISH Journal of Hydraulic Engineering*, 1-8.
- Lança, R., Fael, C., Maia, R., Pêgo, J. P., & Cardoso, A. H. (2013). "Clear-water scour at pile groups". *Journal of Hydraulic Engineering*, 139(10), 1089-1098.
- Laursen, E. M., & Toch, A. (1956). "Scour around bridge piers and abutments". *Ames, IA: Iowa Highway Research Board*, 4.
- Lawrence, S., Tsoi, A. C., & Giles, C. L. (1996, June). "Local minima and generalization in Neural Networks". *IEEE International Conference*, 1, 371-376.
- Lawrence, S., & Giles, C. L. (2000, July). "Overfitting and neural networks: conjugate gradient and backpropagation". *Proceedings of the IEEE-INNS-ENNS International Joint Conference on Neural Networks*, 1114.
- Ludermir, T. B., Yamazaki, A., & Zanchettin, C. (2006). "An optimization methodology for neural network weights and architectures". *IEEE Transactions on Neural Networks*, 17(6), 1452-1459.
- Mahabir, C., Hicks, F., & Fayek, A. R. (2006). "Neuro-Fuzzy river ice breakup forecasting system". *Cold regions science and technology*, 46(2), 100-112.

- Mazumder, S. K., & Kumar, Y. K. (2006). Estimation of scour in bridge piers on alluvial non-cohesive soil by different methods. *IRC Highway Research Bulletin*. 67th IRC Congress, Panchkula.
- Melville, B. W. (1975). "Local scour at bridge sites". *PhD Thesis*, Research Space, Auckland.
- Mohamed, Y. A., Nasr-Allah, T. H., Abdel-Aal, G. M., & Awad, A. S. (2015). "Investigating the effect of curved shape of bridge abutment provided with collar on local scour, experimentally and numerically". *Ain Shams Engineering Journal*, 6(2), 403-411.
- Mohamed, Y. A., Abdel-Aal, G. M., Nasr-Allah, T. H., & Shawky, A. A. (2016). "Experimental and theoretical investigations of scour at bridge abutment". *Journal of King Saud University-Engineering Sciences*, 28(1), 32-40.
- Najafzadeh, M. (2015). "Neuro-fuzzy GMDH based particle swarm optimization for prediction of scour depth at downstream of grade control structures". *Engineering Science and Technology, an International Journal*, 18(1), 42-51.
- Najafzadeh, M., & Barani, G. A. (2011). "Comparison of group method of data handling based Genetic Programming and back propagation systems to predict scour depth around bridge piers". *Scientia Iranica*, 18(6), 1207-1213.
- Najafzadeh, M., Etemad S, A, & Lim, S. Y. (2016). "Scour prediction in long contractions using ANFIS and SVM". *Ocean Engineering*, 111, 128-135.
- Oben N, K., & Ettema, R. (2011). "Pier and abutment scour interaction". *Journal of Hydraulic Engineering*, 137(12), 1598-1605.
- Pal, M., Singh, N. K., & Tiwari, N. K. (2011). "Support Vector Regression based modeling of pier scour using field data". *Engineering Applications of Artificial Intelligence*, 24(5), 911-916.
- Qi, W. G., & Gao, F. P. (2014). "Physical modeling of local scour development around a large-diameter monopile in combined waves and current". *Coastal Engineering*, 83, 72-81.

- Raikar, R. V., Wang, C. Y., Shih, H. P., & Hong, J. H. (2016). "Prediction of contraction scour using ANN and GA". *Flow Measurement and Instrumentation*, 50, 26-34.
- Raudkivi, A. J., & Ettema, R. (1983). "Clear-water scour at cylindrical piers". *Journal of Hydraulic Engineering*, 109(3), 338-350.
- Richardson, E. V., Harrison, L. J., Richardson, J. R., & Davis, S. R. (1993). "Evaluating scour at bridges" (No. HEC 18 (2nd edition)).
- Soliman, M. (2007). "Artificial neural network prediction of maximum scour hole downstream hydraulic structures". In *Eleventh International Water Technology Conference, IWTC11* (pp. 769-777).
- Sturm, T. W., & Janjua, N. S. (1994). "Clear-water scour around abutments in floodplains". *Journal of Hydraulic Engineering*, 120(8), 956-972.
- Vapnik, V. N. (1999). "An overview of statistical learning theory". *IEEE transactions on neural networks*, 10(5), 988-999.
- Varaki, M. E., Kanani, A., & Jamali, A. "Prediction of Scour Depth Scour around Inclined Bridge Piers Using Optimized ANFIS with GA". *Journal of Hydrosiences and Environment*, 1(2).
- Wang, Y. M., & Elhag, T. M. (2008). "An Adaptive Neuro-Fuzzy Inference System for bridge risk assessment". *Expert Systems with Applications*, 34(4), 3099-3106.
- Zhao, F. (2016). Optimized algorithm for Particle Swarm Optimization. *World Acad. Sc., Eng. Technol*, 10, 96-100.

PUBLICATIONS BASED ON PRESENT RESEARCH WORK

International Journals

1. **Sreedhara, B. M.**, Rao, M., & Mandal, S (2018). Application of an evolutionary technique (PSO–SVM) and ANFIS in clear-water scour depth prediction around bridge piers. *Neural Computing and Applications*, 1-15. (Springer) (<https://doi.org/10.1007/s00521-018-3570-6>).
2. **Sreedhara, B. M.**, Manu & Mandal, S. (2018). Estimation of live bed scour depth around different shapes of bridge piers using ANFIS and SVMR approach. *International Journal of Ecology & Development™*, 33 (3), 30-46. (Ceser Publication) ([ISSN 0972-9984 \(Print\); ISSN 0973-7308 \(Online\)](https://doi.org/10.1007/s00521-018-3570-6)).
3. **Sreedhara, B. M.**, Geetha Kuntoji, Manu & Mandal, S. “Application of evolutionary artificial intelligence to predict scour depth of the bridge pier”. *International Journal of Intelligent Systems and Applications*. (Under review).

Scopus Indexed Book Chapters

1. **Sreedhara B M**, Manu and S Mandal (2018), “Swarm intelligence based Support Vector Machine (PSO-SVM) approach in the prediction of scour depth around the Bridge pier”. In *Advances in Intelligent Systems and Computing* with ISSN: 2194-5357, (Springer) (https://doi.org/10.1007/978-981-13-1595-4_36).
2. **Sreedhara B. M.**, Geetha Kuntoji, Manu and S Mandal (2018), “PSO-SVM approach in the prediction of scour depth around different shapes of bridge pier in live bed scour condition”, In *Advances in Intelligent Systems and Computing* 741, (Springer) (https://doi.org/10.1007/978-981-13-0761-4_37).

International Conferences

1. **Sreedhara B. M.**, Geetha Kuntoji, Manu and S Mandal (2018), “PSO-SVM approach in the prediction of scour depth around different shapes of bridge pier in live bed

scour condition”, *4th International Conference on Harmony search, Soft computing and Applications* held at BML Munjal University, Haryana, India, during 7-9th February.

2. **Sreedhara B M**, Manu, S Mandal (2017), “ Swarm intelligence based Support Vector Machine (PSO-SVM) approach in the prediction of scour depth around the Bridge pier”, *7th International Conference on Soft Computing for Problem Solving - SocProS 2017*, during December 23-24, 2017 held at Indian Institute of Technology Bhubaneswar, Bhubaneswar.
3. **Sreedhara B M**, Manu and Pruthviraj U (2015) “ Comparative Study on different Bridge Scour Monitoring Techniques: A Review”, *20th International Conference on Hydraulics, Water Resources and River Engineering- HYDRO 2015*, organized by Civil Engineering Department, IIT Roorkee, India, 17-19th December.

APPENDIX I

1. PROGRAM TO DEVELOP ANN MODEL

```
% Code for predicting D using ANN
% Loading train data
xlsread('scour.xlsx')
d_train=xlsread('scour.xlsx','A2:A85');
u_train=xlsread('scour.xlsx','B2:B85');
t_train=xlsread('scour.xlsx','C2:C85');
D_train=xlsread('scour.xlsx','D2:D85');
% Loading test data
d_test=xlsread('scour.xlsx','A86:A169');
u_test=xlsread('scour.xlsx','B86:B169');
t_test=xlsread('scour.xlsx','C86:C169');
D_test=xlsread('scour.xlsx','D86:D169');
% Loading the ranges for train and test data
% Train input vector
TRAIN_INPUT = [d_train'; u_train'; t_train'];
% Train output vector
% TRAIN_OUTPUT = [D_train'];
TRAIN_OUTPUT = [D_train'];
% Test input vector
TEST_INPUT = [d_test'; u_test'; t_test'; D_test'];
% Test output vector
% TEST_OUTPUT = [D_test'];
TEST_OUTPUT = [D_test'];
% Creating a feedforward network
% Network parameters
NET.trainparam.show = 5;
NET.trainparam.epochs = 200;
% due to undefined function error %NET.trainparam.min_grd = 1.0e-3;
NET.trainparam.goal = 1.0e-3;
% Training of network
NET = train (NET, TRAIN_INPUT, TRAIN_OUTPUT);
% Simulate the network with train data
SIMULATED_TRAINED_OUTPUT = sim(NET, TRAIN_INPUT);
% Simulate the network with test data
SIMULATED_TEST_OUTPUT = sim(NET, TEST_INPUT);
cTRAIN = ctrain (1,2)
% Coefficient of correlation for testing
ctest = corrcoef (SIMULATED_TEST_OUTPUT', TEST_OUTPUT)
cTEST = ctest (1,2)
clear all
clc
```

2. PROGRAM TO DEVELOP SVM MODEL

```
% TRAINING DATASET
SPECTR = csvread('train.csv'); % read a csv file
trainlabels = SPECTR(:, 1); % labels from the 1st column
trainfeatures = SPECTR(:, 2:end);
trainfeatures_sparse = sparse(trainfeatures); % features must be in a sparse matrix
libsvmwrite('SPECTRlibsvm.train', trainlabels, trainfeatures_sparse);
% TESTING DATASET
SPECTE = csvread('test.csv'); % read a csv file
testlabels = SPECTE(:, 1); % labels from the 1st column
testfeatures_sparse = sparse(testfeatures); % features must be in a sparse matrix
libsvmwrite('SPECTElibsvm.test', testlabels, testfeatures_sparse);
% PARAMETER SELECTION USING 4-FOLD CROSS VALIDATION
bestcv = 0;
for c = 1:500,
    for g = 1:10,
        cmd = ['-v 4 -c ', num2str(c), ' -g ', num2str(g)];
        bestcv = cv; bestc = c; bestg = g;
    end
    fprintf('%g %g %g (best c=%g, g=%g, rate=%g)\n', c, g, cv, bestc, bestg, bestcv);
end
end
options = ['-s 3 -t 2 -c ', num2str(bestc), ' -g ', num2str(bestg), '-p' 0.1, '-h' 0];
[predicted_trainlabel, accuracy_train, decision_values] = svmpredict(trainlabels,
trainfeatures, model);
[predicted_testlabel, accuracy
```

3. PROGRAM TO DEVELOP PSO-SVM MODEL

```
clc;
clear all;
%SVM Support Vector Machine
filename = 'total.xlsx';
P = xlsread(filename,'A:D');
X1= P([1:80],[1:3]);
Y1= P([1:80],[4]);
X2= P([81:160],[1:3]);
Y2= P([81:160],[4]);
nvars = 2;
x = particleswarm(@(x)svmexp(x,X1,Y1,X2,Y2),nvars,[0.0001,500],[0.0001,1000]);
mdl =
fitsvm(X1,Y1,'KernelFunction','rbf','Standardize',true,'Epsilon',x(1),'BoxConstraint',x(2));
yfit = predict(mdl,X2);
n=80;
%mape = (1/n)*sum(e);
```

```

%rmse = sqrt((1/(n))*sum((e.^2)));
% mre = (1/(n))*sum(abs(e./yfit));
den = sqrt(sum((Y2-yf).^2).*sum((yfit-yf).^2));
cc = num/den;
%SI = rmse./(mean(Y2));
function [mape] = svmexp(Epsi,X1,Y1,X2,Y2)
mdl = fitcsvm(X1,Y1,'KernelFunction','rbf','KernelScale','auto','Standardize',true);
yfit = predict(mdl,X2);
Epsi = mdl.Epsilon;
e = abs(yfit-Y2);
mape = (1/100)*sum(e./Y2) * 100;
end

```

4. PROGRAM TO DEVELOP PSO-ANN MODEL

```

clc
tic
close all
clear all
rng default
filename = 'datafile1.xlsx';
sheetname1 = 'Sheet1';
sheetname2 = 'Sheet2';
input = xlsread(filename,sheetname1,'A1:Z1000');
target = xlsread(filename,sheetname2,'A1:Z1000');
inputs=input';
targets=target';
n=6;
net=feedforwardnet(n);
net=configure(net,inputs,targets);
for j=1:kk
LB(1,j)=-1.5;
UB(1,j)=1.5;
end
pop=25;
for i=1:pop
for j=1:kk
xx(i,j)=LB(1,j)+rand*(UB(1,j)-LB(1,j));
end
end
fun=@(x) myfunc(x,n,m,o,net,inputs,targets);
x0=xx;

% pso initialization-----start
x=x0; % initial population
v=0.01*x0; % initial velocity

```

```

for i=1:pop
f0(i,1)=fun(x0(i,:));
end
pbest=x0; % initial pbest
gbest=x0(index0,:); % initial gbest
% pso initialization-----end

% pso algorithm-----start
c1=0.8; c2=3.2;
ite=1; maxite=1000; tolerance=1;
while ite<=maxite && tolerance>10^-8

w=0.1+rand*0.4;
% pso velocity updates
v(i,j)=w*v(i,j)+c1*rand*(pbest(i,j)-x(i,j))...
+c2*rand*(gbest(1,j)-x(i,j));
end
end
% pso position update
for i=1:pop
for j=1:kk
x(i,j)=x(i,j)+v(i,j);
end
end
% handling boundary violations
for i=1:pop
for j=1:kk
x(i,j)=LB(j);
elseif x(i,j)>UB(j)
x(i,j)=UB(j);
end
end
end
% evaluating fitness
for i=1:pop
end
% updating pbest and fitness
for i=1:pop
pbest(i,:)=x(i,:);
f0(i,1)=f(i,1);
end
end
[fmin,index]=min(f0); % finding out the best particle
ffmin(ite,run)=fmin; % storing best fitness
ffite(run)=ite; % storing iteration count
% updating gbest and best fitness

```

```

if fmin<fmin0
fmin0=fmin;
end

% calculating tolerance
if ite>100;
tolerance=abs(ffmin(ite-100,run)-fmin0);
end
% displaying iterative results
if ite==1
disp(sprintf('Iteration Best particle Objective fun'));
end
disp(sprintf('%8g %8g %8.4f',ite,index,fmin0));
ite=ite+1;
end
% pso algorithm-----end

xo=gbest;
fval=fun(xo);
ybest(run,1)=fun(xo);
disp(sprintf('*****'));
disp(sprintf(' RUN fval ObFuVa'));
disp(sprintf('%6g %6g %8.4f %8.4f',run,fval,ybest(run,1)));
end
toc

% Final neural network model
disp('Final nn model is net_f')
net_f = feedforwardnet(n);
net_f=configure(net_f,inputs,targets);
[a b]=min(ybest);
xo=xbest(b,:);
k=0;
for i=1:n
for j=1:m
k=k+1;
end
end
for i=1:n
k=k+1;
xb1(i,1)=xo(k+n);
end
k=k+n
for i=1:o
k=k+1;
xb2(i,1)=xo(k);

```



```

end
net_f.iw{1,1}=xi;
net_f.b{1,1}=xb1;
net_f.b{2,1}=xb2;

%Calculation of MSE
err=sum((net_f(inputs)-targets).^2)/length(net_f(inputs))
%Regression plot
plotregression(targets,net_(inputs))
disp('Trained ANN net_f is ready for the use');

```

5. IRC Method (Lacey’s method): (IRC 78-2014)

$$d_{se} = 0.473 \left(\frac{D}{f} \right)^{\frac{1}{3}}$$

Where, d_{se} = effective scour depth

D = flow depth

f = silt factor and it is given by $1.76\sqrt{d_m}$

d_m = mean diameter of bed material in millimeter.

The values of ‘ f ’ for various grades of bed materials are shown in table.

Types of bed material	d_m (mm)	f
Coarse silt	0.04	0.35
Silt/fine sand	0.081 to 0.158	0.5 to 0.7
Medium sand	0.223 to 0.505	0.85 to 1.25
Coarse sand	0.725	1.5
Fine bajri and sand	0.988	1.75
Heavy sand	1.29 to 2.00	2.0 to 2.42

6. Melville and Coleman Method:

$$d_{se} = 2.4 K_s K_\theta b$$

Where, d_{se} = effective scour depth

K_s = Pier shape factor

K_θ = Pier alignment factor

b = Pier thickness

The pier shape factor (K_s) for various shapes are shown below.

Pier Shape	K_s
Circular	1.0
Round Nosed	1.0
Rectangular/Square Nosed	1.1
Sharp Nosed	0.9

The pier alignment factor (K_θ) for various pier alignments is listed below.

θ (°)	30	45	60	90	120	135	150
K_θ	0.90	0.95	0.98	1.0	1.05	1.07	1.08

7. Kothyari – Garde – Rangaraju Method:

$$\frac{d_{se}}{d_{50}} = 0.88 \left(\frac{b}{d_{50}} \right)^{0.67} \left(\frac{D}{d_{50}} \right)^{0.4} \alpha^{-0.30}$$

Where, d_{se} = effective scour depth

d_{50} = Sediment size

b = Pier thickness

D = Flow depth

α = Center to center spacing of the pier

CURRICULUM VITAE



Name:	SREEDHARA B M
Permanent Address:	S/O MARULASIDDAPPA B V, BASOOR AT POST, KADUR TALUK, CHIKKAMAGALURU DISTRICT, KARNATAKA - 577116
EDUCATION:	MASTER OF TECHNOLOGY (2011-13) Discipline: Computer Aided Design of Structures University B D T College of Engineering, Davanagere
	BACHELOR OF ENGINEERING (2007-11) Discipline: Civil Engineering Adichunchanagiri Institute of Technology, Chikkamagaluru. Affiliated to: Visvesvaraya Technological University, Belgaum.
Contact No.:	+91-9945498010
Email ID:	bmsreedhar@gmail.com
ORCID:	0000-0001-8400-2369
